Realizability of Tropical Plane Curves and Tropical Incidence Geometry

vorgelegt von
M. Sc.
Ayush Kumar Tewari

an der Fakultät II – Mathematik und Naturwissenschaften
der Technischen Universität Berlin
zur Erlangung des akademischen Grades

Doktor der Naturwissenschaften
Dr.rer.nat.

genehmigte Dissertation

Promotionsausschuss:

Vorsitzender: Prof. Dr. Peter K. Friz
Gutachter: Prof. Dr. Michael Joswig
Gutachterin: Prof. Dr. Hannah Markwig
Gutachter: Dr. Dhruv Ranganathan

Tag der wissenschaftlichen Aussprache: 07.12.2020

Berlin 2021

to my mother, my first teacher

Acknowledgements

This research work could not have been completed by help and guidance from many people, whom I would like to acknowledge. Firstly, I would like to thank my supervisors Hannah Markwig and Michael Joswig, for having regular discussions with me and helping me in trying to start with the right questions and to make my way forward with the solutions. I am also thankful to the respective institutes, i.e. Eberhard Karls Universität Tübingen and Technische Universität Berlin, both of which hosted me as a doctoral student during the duration of this work. I would also like to thank my various colleagues, management staff at both these institutes for making my stay easy and fruitful.

I would like to thank the members of the Geometry group at Eberhard Karls Universität Tübingen, for helping me with getting accustomed to the new city and the university. I am also thankful to colleagues in the Discrete Mathematics/Geometry group at TU Berlin, especially Marta, Lars, Paco, Benjamin and Antje for her help with the logistics and for helping me at various stages of my research work.

I would like to thank my parents, my sister and my friends Arka, Bikash and Soham Saha for their constant support which immensely helped me while working on this project.

Abstract

Tropical plane curves are one of the building blocks in the study of tropical algebraic geometry. A lot of work has been done to understand and establish connections between tropical and classical algebraic geometry. The first step in this direction is to consider the case of smooth tropical curves. This in turn comes with a nice connection to lattice polytopes and their unimodular triangulations. This highly combinatorial setting helps to explore the algebro-geometric aspects of tropical curves by trying to find when a smooth tropical curve is realizable. This leads us to study the skeleton of a tropical curve, which is a metric graph that encodes the combinatorial information regarding the curve. Our main goal here is to understand the combinatorial nature of these skeletons and to try to find which graphs can occur as skeletons of smooth tropical plane curves, and in this way, we come up with certain obstructions which prevent a graph from being a skeleton of a tropical curve. We encounter a special class of lattice polytopes, namely panoptigons, which help us in identifying a new criterion for non-realizability of a graph as a skeleton.

Having studied about smooth tropical planar curves, in the latter section we move on to the study of incidence of points and lines in the tropical plane and arrangements of tropical lines. In the light of recent results exploring tropical point-line incidence, we establish a tropical De-Bruijn Erdős theorem. We also study stable tropical lines and using projective duality in the tropical plane, we find dual results concerning stable intersections. Utilizing duality of tropical curves with subdivisions of Newton polytopes we also establish connections between point-line geometry and the faces of subdivisions of Newton polytopes. With tropical Sylvester-Gallai theorem and tropical De-Bruijn Erdős theorem, we discuss other results which have been obtained about point-line geometry in the tropical plane and beyond.

Zusammenfassung

Tropische ebene Kurven bilden einen Teil des Fundaments der tropischen algebraischen Geometrie. Die Verbindung zwischen klassischer und tropischer Geometrie zu untersuchen und zu vertiefen ist Thema vieler aktueller Arbeiten. Der erste Schritt ist die Untersuchung glatter tropischer Kurven mittels ihrer Verbindung mit unimodularen Triangulierungen von Gitterpolytopen. In diesem kombinatorischen Rahmen lässt sich die Frage nach der Realisierbarkeit tropischer Kurven stellen. Dies führt uns zum Studium des Skeletts tropischer Kurven, einem metrischen Graphen, der die kombinatorische Information der Kurve kodiert. Wir wollen verstehen, welche Graphen als Skelett glatter tropischer Kurven auftreten können. Dadurch gelangen wir zu Bedingungen an einen Graphen, die ihn davon abhalten, Skelett einer tropischen Kurve zu sein. Eine besondere Klasse von Gitterpolytopen, "panoptigons", hilft uns neue Kriterien für Nichtrealisierbarkeit eines Graphen als Skelett zu finden.

Nach den glatten tropischen Kurven beschäftigen wir uns mit der Inzidenz von Punkten und Geraden in der tropischen Ebene, sowie Arrangements von tropischen Geraden. Basierend auf jüngsten Ergebnissen über tropische Punkt-Geraden Inzidenz, leiten wir eine tropische Version des De-Bruijn Erdős Theorems her. Außerdem untersuchen wir stabile tropische Geraden und, vermöge projektiver Dualität, bekommen wir duale Ergebnisse für stabile Schnitte. Durch die Dualität tropischer Kurven mit Unterteilungen von Newtonpolytopen können wir Verbindungen zwischen der Punkt-Geraden-Geometrie und den Seiten in der Unterteilung des Newonpolytops herstellen. Unter dem Gesichtspunkt des tropischen Sylvester-Gallai Theorems und des tropischen De-Bruijn Erdős Theorems erläutern wir andere Ergebnisse zur Punkt-Geraden Geometrie in der tropischen Ebene und darüber hinaus.

Contents

List of Figures

Chapter 1

Introduction

Tropical geometry started gaining immense traction as a new sphere for research starting from the early years of the current century. Although, research had been conducted regarding max plus algebras in the preceding century, the impact of the topic was realized only some decades later with immensely strong results like the fundamental theorem of tropical geometry, tropical convexity, etc [38]. This was also enhanced with various applications found in economics [5], optimization [33], string theory [25] etc. which has brought the study of this subject at the cross hair of researchers from various fields of interest. It even offers something of interest to the star wars aficionado (cf. *TIE-fighter graph* [16]). In this thesis we would be considering the connections between discrete geometry and the study of tropical curves, relating lattice polytopes, regular subdivisions and tropical curves. Tropical geometry thrives on the connections between tropical curves and their dual Newton subdivisions. Hence, let us get acquainted with what is a subdivision and the combinatorics related to it. In [20], a *polyhedral subdivision* is defined as follows,

Definition 1.0.1. Let J be a set of labels for the point configuration $V \subset \mathbb{R}^d$. A collection Δ of subsets of J is a *polyhedral subdivision* of V if it satisfies the following conditions

1. If $C \in \Delta$ and $F \leq C$, then $F \in \Delta$ as well. (Closure property)
2. $\cup_{C \in \Delta} \text{conv}_V(C) \supseteq \text{conv}_V(J)$. (Union Property)
3. If $C \neq C'$ are two cells in Δ, then $\text{relint}_V(C) \cap \text{relint}_V(C) = \Phi$. (Intersection Property)

A *triangulation* of V is a polyhedral subdivision all of whose cells are simplices. If that subdivision is induced by a height function on V, it is called *regular*.

Tropical geometry is briefly the study of polynomials and the hypersurfaces defined by them, over the tropical semiring $(\mathbb{R} \cup \infty, \oplus, \odot)$, where the binary operations act on the elements in the following way

$$x \oplus y = \max(\text{x,y}) \qquad \text{and} \qquad x \odot y = x + y$$

The tropical semiring can also be considered with a min-plus operation, however we would be considering the max-plus operation in our case. A *tropical polynomial* is a tropical analogue of a polynomial with the binary operations between monomials replaced with tropical operations. The usual notion of vanishing which is studied in classical algebraic geometry is replaced in the realm of tropical geometry with the notion of maxima (or minima) being achieved at least twice. The corresponding vanishing sets are referred as *tropical hypersurfaces*. These hypersurfaces imbibe a metric graph structure, with each vertex satisfying a *balancing* condition. In this thesis we would be studying tropical planar curves which are hypersurfaces corresponding to bi-variate tropical polynomials.

We now define the setup for smooth tropical planar curves, which we would be studying in this work. Let P be a (convex) *lattice polygon*, i.e., P is the convex hull of finitely many points in $\mathbb{Z}^2$, and $V = P \cap \mathbb{Z}^2$ is the set of lattice points in P. We refer to the convex hull of the interior points of P as the *interior polygon of* P, denoted P_{int}. If $\dim(P_{\text{int}}) = 2$, we call P *non-hyperelliptic*; if $\dim(P_{\text{int}}) \leq 1$, we call P *hyperelliptic*. Any function $h : V \to \mathbb{R}$ can be identified with a tropical polynomial as follows [10],

$$p(x, y) = \bigoplus_{(i,j) \in V} h_{(i,j)} \odot x^i \odot y^j$$

The tropical curve C corresponding to this tropical polynomial is dual to a regular subdivision of V, which can be obtained by raising the lattice points in V to corresponding heights in $\mathbb{R}^3$, the heights being specified by the function h. We consider the upper convex hull of the points in V and their corresponding heights and obtain the subdivision by projecting back to $\mathbb{R}^2$. The maximal cells are obtained as images of facets of the upper convex hull under projection [10]. In the planar case, such a regular subdivision is a triangulation if all maximal cells are triangles. A triangulation Δ of V is *unimodular* if each triangle in Δ has normalized area one, i.e., Euclidean area $\frac{1}{2}$. This is the case if and only if Δ uses all points in V (by Pick's Theorem [44]) . We refer a tropical planar curve dual to a unimodular triangulation as a *smooth* tropical planar curve.

Any tropical plane curve C contains a trivalent, planar, minor G which has exactly g distinct cycles, and it is the smallest space to which the curve admits a deformation retract. We refer to this graph as the *skeleton* of genus g of the tropical curve. Each skeleton has $2g - 2$ vertices and $3g - 3$ edges [10]. We also notice that skeleta of unimodular regular triangulations of lattice polygons are termed as *tropically planar* or "troplanar" graphs in [16], and we refer the tropical curves corresponding to a tropically planar skeleton as *realizable*

smooth tropical planar curve. We explain in Chapter 2.1 how this minor is obtained from a tropical curve and how it relates to the dual unimodular triangulations.

Tropical curves have been studied previously since they occur as the simplest examples of tropical hypersurfaces. Additionally, the moduli spaces associated with planar tropical curves, $\mathbb{M}_g^{\text{planar}}$ enjoys intricate and important connections to moduli spaces in classical algebraic geometry. An important aspect of study has been to analyze the cohomology of classical spaces in algebraic geometry by using the connections with the moduli space of tropical curves, as explored in [15]. In 2015, Brodsky et al [10] studied the moduli space of tropical curves, for lower genera $g = 3, 4$ and 5. This boiled down to studying the underlying *skeletons* of all possible smooth tropical planar curves of a given genus. In there study, with the help of a computational setup, they were able to find which trivalent planar graphs could occur as skeletons for lower genera. There study showed that not all graphs can occur and one can try to come up with combinatorial criteria to specify graphs which are forbidden from occurring as skeletons. This approach was pushed to genus 7 in Coles et al [16], along with new criteria for forbidden skeletons. However, these studies could not provide a complete classification and as they involve computational enumeration of triangulations, therefore the results are bounded by computational complexity, which increases rapidly as the genus increases. In this thesis, we try to find answers to the questions which arose from [10] and [16] and in the first chapter we provide two new criteria for graphs which are forbidden from occurring as skeletons. This also leads us to studying highly symmetrical triangulations which we refer to as *anti-honeycomb*. Also, with our results we are able to provide a full classification of all curves for genus $g \leq 5$, independent of the previous computational setup, i.e., by eliminating all graphs which fall under known criteria.

In the third chapter of this thesis, we study *lattice visibility*, which can be understood as the search for lattice points inside polytopes which can be connected to all other lattice points via a straight line, without any intermediate lattice point. Visible points inside lattice polytopes have been studied previously based on applications relating to optimization and even in theoretical physics [28]. In this thesis, we define a new class of lattice polygons *panoptigons*, which have a lattice point which is visible to all other lattice points. We first show that there are only finitely many panoptigons and enumerate all possible nonhyperelliptic panoptigons, via a constructive proof and a computational enumeration. This study regarding lattice polytopes was however inspired by questions concerning tropical curves, and we elaborate this connection by establishing a new criteria namely *big face graphs*, which is based on the enumeration of panoptigons. This provided us with a new criteria for skeletons apart from *crowded* criterion, which does not involve a cut edge.

In the last chapter, we move on to the arrangement of the simplest example of tropical curves, namely *tropical line arrangements*. We provide a definition for a *stable* tropical line and establish the equivalence between previously known notions of stable tropical lines, and using this definition we state and prove the tropical analogue of the classical De Beuijn Erdős theorem, which establishes a lower bound on the number of lines determined by a set of points. This is inspired by recent point-line incidence results proved in [8]. Hyperplane arrangements have been studied previously in tropical geometry, entailing to connections with tropical convexity [21], hence tropical line arrangements turn out to be the base case in this scenario. Also, hyperplane arrangements have been studied in order to explore there connections with subdivisions of dilated simplex and a notion of a tropical oriented matroid is established in [2] in connection to hyperplane arrangements. In the light of all these results, we establish the lower bound on the number of stable tropical lines determined by a set of n points in the tropical plane, hence a tropical De Bruijn Erdős theorem. With projective duality, the result also translates to tropical line arrangements and stable intersections. The proof of this result brings out the deep connections between faces of dual Newton subdivision and corresponding stable intersections. We also state the connections of our result with the study of tropical oriented matroids as specified in [2].

In summary, in this thesis we study which graphs can occur as skeletons of smooth tropical planar curves; this classification provides us insights about the moduli space of tropical curves and with our results we are able to provide a complete classification for lower genera. In this process, we also discover a new class of lattice polygons, which helps us understand lattice visibility in greater details, and in turn relates back to our study of tropical curves by helping us to establish a new criteria for forbidden skeletons. Subsequently, we study an active example of curves in the forms of tropical line arrangements and study point-line incidence in the tropical plane.

Chapter 2

Forbidden patterns in tropical plane curves

2.1 Lattice polygons and tropical plane curves

We start with a finite set of points $V \subset \mathbb{R}^d$ and recall that *polyhedral subdivision* of V is a polyhedral complex which covers the convex hull $\operatorname{conv} V$ and uses (a subset of) the given point set V as its vertices. Let P be a (convex) *lattice polygon*, and $V = P \cap \mathbb{Z}^2$ is the set of lattice points in P.

Let Δ be a (not necessarily unimodular) triangulation of V. The *dual graph* $\Gamma = \Gamma(\Delta)$ is the abstract graph whose nodes are the triangles of Δ; they form an edge in Γ if two triangles share an edge in Δ. The dual graph is necessarily connected and planar, and each node has degree at most three.

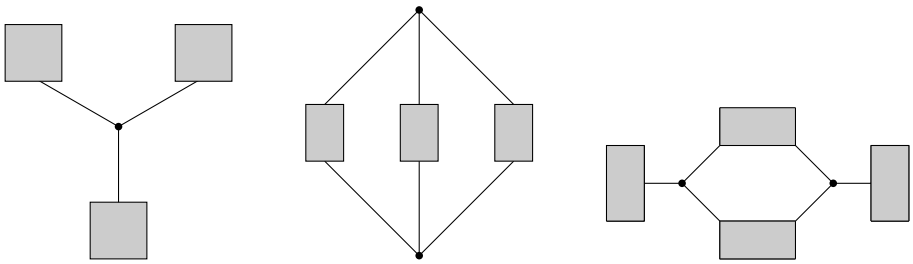

Figure 2.1: Graph with a sprawling node (left), a crowded graph (center), and a TIE-fighter graph (right). Each box represents some subgraph of positive genus.

Next we describe a procedure to obtain the *skeleton* G from Γ. First, if there is a node of degree one, we delete it together with the unique incident edge. We repeat this step until no nodes of degree one are left. The remaining edges are *nonredundant*. Second, if there is a node of degree two, we delete the node and join its neighbors by an edge. Again we repeat until there are no more nodes of degree two. The resulting graph is the skeleton. By

construction the skeleton is a trivalent planar graph, and it does not depend on the ordering in which the edge deletions and contractions are performed [24, Section 3.1.2]. In this way each edge of G arises as an edge path in Γ. This yields a surjective map, which we denote η, from the nonredundant edges of Γ onto the edges of G. Note that this *contraction map* η is undefined for any edge which is redundant. This elementary description of the skeleton is algorithmic in nature and serves our purposes.

A *split* is a subdivision of V with exactly two maximal cells; it is necessarily regular [27, Lemma 3.5]. If U and W are the two maximal cells of a split, then the intersection $U \cap W$ is a common edge of the two convex polygons U and W. It spans the corresponding *split line*. A set of splits of V is *weakly compatible* if there is a triangulation which simultaneously refines them all. Moreover, a set of splits is *(strongly) compatible* if any two split lines do not meet in the interior of P. Compatibility implies weak compatibility. The split lines of two weakly compatible splits which are not strongly compatible must meet in a point in V, i.e., an interior lattice point of P. An edge e of the connected graph G is a *cut edge* if deleting e creates two connected components. Otherwise e lies in some cycle of G.

The following three technical results are extracted from the proof of [16, Theorem 3.4], where cut edges are called "bridges".

Lemma 2.1.1. *Let e be a cut edge of G. Then $\eta^{-1}(e)$ comprises a single cut edge of Γ, which is dual to an edge, s, of Δ. Moreover, the vertices of s lie on the boundary ∂P, and s spans a split line of V.*

Here the "vertices" are the two endpoints of the edge s. In the unimodular case these are also the only lattice points contained in s. Our arguments below do not rely on the uniqueness of the cut edge in $\eta^{-1}(e)$. It suffices to know that such edge (and its dual edge s) exist.

Lemma 2.1.2. *Let e be an edge between v_1 and v_2 in a cycle, C of G. Furthermore, let T_1 and T_2 be triangles in Δ which correspond to v_1 and v_2 on the path $\eta^{-1}(e)$. Then T_1 and T_2 share an interior lattice point of P, and this is dual to C.*

Lemma 2.1.3. *Let $z \in V$ be some lattice point in P with two incident triangles $T_1 = \operatorname{conv}\{z, a_1, b_1\}$ and $T_2 = \operatorname{conv}\{z, a_2, b_2\}$ both of which are in Δ. Further, let L_i be the line spanned by a_i and b_i, for $i = 1, 2$. Suppose that L_1 and L_2 meet in some point, say w, such that a_i is closer to w than b_i, for $i = 1, 2$. Then the interior of the quadrangle $\operatorname{conv}\{z, a_1, w, a_2\}$ does not contain a point in V, unless $a_1 = a_2 = w$.*

With this we can take a small first step to our main results. Recall that Lemma 2.1.1 associates a split of V to each cut edge of G.

Lemma 2.1.4. *Splits corresponding to distinct cut edges are compatible.*

Proof. It suffices to consider pairs of splits. From Lemma 2.1.1 the cut edges e_1 and e_2 yields two split lines, S_1 and S_2, which may not be unique. Unless S_1 and S_2 are compatible, they must meet in a point of the point configuration V, which does not lie on ∂P, i.e., an interior lattice point of P. Yet, by Lemma 2.1.1 the line S_1 (and similarly S_2) contains precisely two points of V, and neither lies in the interior. □

We now recall the duality between unimodular triangulations of lattice polygons and smooth tropical planar curves as discusssed in Chapter 1. We illustrate this duality with the following example,

Example 2.1.5. We consider the *anti-honeycomb* triangle

$$A_{(-2,4;\,-2,4;\,-2,4)} \;=\; \mathrm{conv}\{(2,2),(-2,0),(0,-2)\}\ , \tag{2.1.1}$$

which occurs as $Q_3^{(4)}$ in [10]. The genus is $g(A_{(-2,4;-2,4;-2,4)}) = 4$. We call the unimodular triangulation $\Delta_{(-2,4;-2,4;-2,4)}$, shown in Figure 2.2 (left), the *anti-honeycomb triangulation* of $A_{(-2,4;-2,4;-2,4)}$. Its skeleton, shown in Figure 2.2 (right) and called (303) in [10], features three cut edges which correspond to three compatible splits of $A_{(-2,4;-2,4;-2,4)}$. The triangulation $\Delta_{(-2,4;-2,4;-2,4)}$ is regular, whence it defines a moduli cone of tropical plane curves. That cone is 7-dimensional, while the entire moduli space $\mathbb{M}_4^{\mathrm{planar}}$ has dimension nine; see [10, Table 4]. See Section 2.4 for a more comprehensive discussion of anti-honeycomb polygons, their triangulations and the notation (2.1.1).

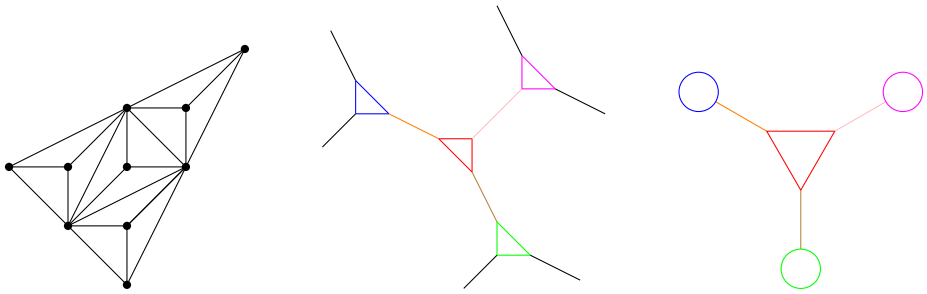

Figure 2.2: Anti-honeycomb triangulation $\Delta_{(-2,4;-2,4;-2,4)}$ of genus 4 (left), its dual graph (center), and the corresponding skeleton (right)

We now sketch the forbidden patterns which are known already. A node in G is *sprawling* if its deletion leaves three connected components; cf. Figure 2.1 (left). This obstruction to tropical planarity was identified in [12, Proposition 4.1] and [10, Proposition 8.3]. Note that graphs with a sprawling node were called "sprawling" in [10] and [16]. A planar embedding

of a graph G is called *crowded* if either: there exist two bounded regions sharing at least two edges; or, there exists a bounded region sharing an edge with itself. If all planar embeddings of G are crowded, then G itself is said to be *crowded*. In [40, Lemma 3.5], it is shown that crowded graphs can never be tropically planar. Additionally, [40, Corollary 3.7] describes a family of crowded graphs, and this is depicted in Figure 2.1 (center). A graph is a *TIE-fighter* if it looks like the one in Figure 2.1 (right). TIE-fighter graphs can never be tropically planar; this was shown in [16, Theorem 3.4].

2.2 Heavy Cycles and Sprawling Triangles

Let P be a lattice polygon with precisely g interior lattice points. Moreover, let Δ be a unimodular triangulation of P with dual graph $\Gamma = \Gamma(\Delta)$ and skeleton $G(\Delta) = G$. The contraction map η sends nonredundant edges of Γ to edges of G. The g interior lattice points of P bijectively correspond to the bounded regions of the planar graph G. By Euler's formula we have $g = m - n + 1$, where m and n are the numbers of edges and nodes of G, respectively. Our arguments in this section do not require Δ to be regular. That is, our results extend to a class of planar graphs, which is slightly more general than tropical plane curves.

Two lattice polygons, P and Q, are *unimodularly equivalent* if there is a lattice vector $\alpha \in \mathbb{Z}^2$ and an integer linear transformation $\tau \in \mathrm{SL}(2, \mathbb{Z})$ such that $P = \alpha + \tau(Q)$; cf. [20, Section 9.3]. In that case, we have $P \cap \mathbb{Z}^2 = \alpha + \tau(Q \cap \mathbb{Z}^2)$, i.e., the lattice points are transformed alike. The map $x \mapsto \alpha + \tau(x)$ is a *unimodular transformation*.

Lemma 2.2.1. *Assume that P contains a unimodular triangle with vertices a, b, z such that neither a nor b is a vertex of P, and z is an interior lattice point. If a and b lie on ∂P then either a and b lie on a common edge of P or the lattice point $a + b - z$ is contained in P.*

Proof. Up to unimodular equivalence we may assume $a = (1, 0)$, $b = (0, 1)$ and $z = (0, 0)$. Let L and M be the lines spanned by the edges of P containing a and b, respectively. Suppose that $(1, 1)$ is not contained in P. Since P is a lattice polygon, then the intersection of P with the positive orthant agrees with the unit triangle abz. This entails that L and M agree, which means that $L = M$ defines an edge of P, and this contains a as well as b. □

Definition 2.2.2. We say that a cycle C in a planar graph G is *heavy*, if

1. it has two nodes, v_1 and v_2, such that v_i is incident with a cut edge e_i connecting v_i with a subgraph G_i of positive genus;

2. and there is a third subgraph, G_3, also of positive genus, which shares at least one node with the cycle C; cf. Figure 2.3.

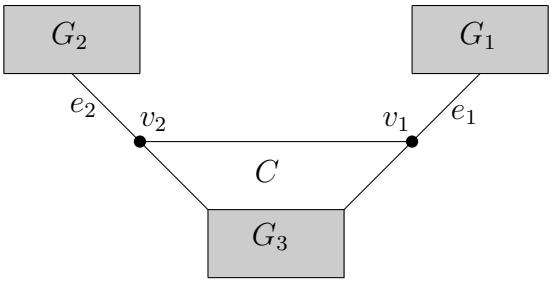

Figure 2.3: Graph with the heavy cycle C

In particular, a graph with a heavy cycle has genus at least four. From the classification of hyperelliptic graphs in [40], we infer that a graph with a heavy cycle is not hyperelliptic. Moreover, it follows from Lemma 2.1.1 that there are split lines, S_1 and S_2, dual to the edges e_1 and e_2 of G. While the split lines may not be unique we just pick some. By Lemma 2.1.4 the splits S_1 and S_2 are compatible, and thus P decomposes into a union of three lattice polygons P_1, P_2 and P' such that Δ induces triangulations of all three. In this way, we get triangulations Δ_1, Δ_2 and Δ' such that the component G_i is the skeleton of Δ_i for $i = 1, 2$, and $G_3 \cup C$ is the skeleton of Δ'. The triangles in Δ' which are dual to v_1 and v_2 are denoted T_1 and T_2, respectively. We refer to the polygon P' as the *heavy component* of P, and likewise Δ' is the *heavy component* of Δ. Expressed in the language of [16], the heavy component Δ' arises from Δ via "bridge-reduction".

The following lemma is the technical core of this chapter. Its proof is a bit cumbersome, with several cases to distinguish. However, it is rather powerful as it delineates a fine border between trivalent planar graphs which are realizable as skeleta of tropically planar curves and those which are not.

Lemma 2.2.3. *Suppose that G has a heavy cycle with cut edges e_1 and e_2 as in Figure 2.3. Then the triangles T_1 and T_2 in Δ share an edge $[z, w]$, where z is the interior lattice point dual to C, and the split lines S_1 and S_2 intersect in w, which is a vertex of P', and which lies in the boundary of P.*

Before we enter the proof, we sketch an outline. The overall strategy is indirect, i.e., we will assume that T_1 and T_2 share a vertex but not an edge. Now the split lines from Lemma 2.1.4 are either parallel or not; cf. Figure 2.4. In both cases we can exploit the convexity of the four lattice polygons P_1, P_2, P' and P to arrive at contradictions. The situation with intersecting split lines is the more difficult one, as it ramifies into sub-cases.

Proof. By Lemma 2.1.2 the triangles T_1 and T_2 share a vertex z, which is the interior lattice point in P dual to the heavy cycle C. Up to a unimodular transformation we may assume that $z = (0, 0)$, and $T_1 = \text{conv}\{z, (1, 0), (0, 1)\}$.

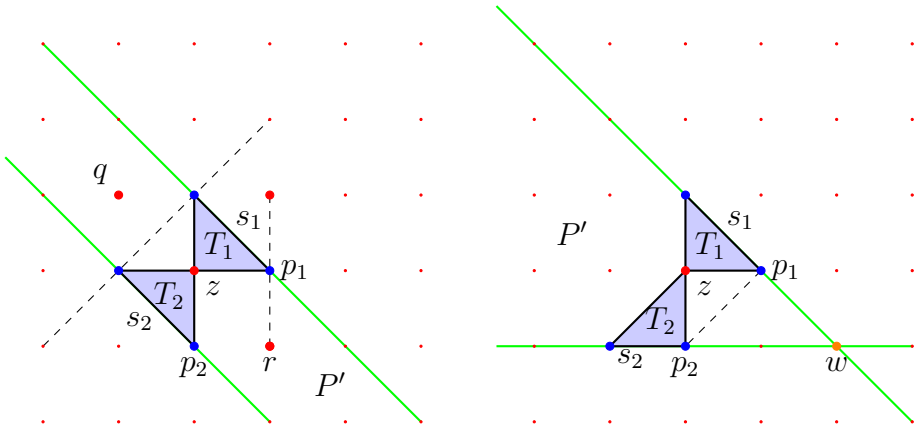

Figure 2.4: Two possibilities for S_1 and S_2, which are ruled out a posteriori in the proof of Lemma 2.2.3. Left: S_1 and S_2 are parallel. Right: S_1 and S_2 intersect in a point.

We consider the point $(1,1)$. We notice that if $(1,1) \notin P$, then by convexity of P, the positive genus component attached to the split edge $s_1 = [(1,0),(0,1)]$ is squeezed between the lines $y = 0$ and $y = 1$, which has no interior lattice points and we get a contradiction. Therefore the point $(1,1)$ lies in P. We want to show that $(1,1)$ is an interior lattice point of P_1 (and P). First, since $(1,0)$ is in the boundary and z is in the interior of P, there are no interior lattice points on the ray $(1,0) + \mathrm{pos}\{(1,0)\}$. Similarly, there are no interior lattice points on $(0,1) + \mathrm{pos}\{(0,1)\}$. However, since G_1 has positive genus at least one interior lattice point of P_1 exists, and it must lie in the translated orthant $(1,1) + \mathrm{pos}\{(1,0),(0,1)\}$. As $(1,0)$ and $(0,1)$ lie in P_1 it follows from the convexity of P_1 that $(1,1)$ must be an interior lattice point. Now consider the triangle $T_2 = \mathrm{conv}\{z,(\alpha,\beta),(\gamma,\delta)\}$ where $\alpha,\beta,\gamma,\delta \in \mathbb{Z}$ with

$$\alpha\delta - \beta\gamma \;=\; 1 \;. \tag{2.2.1}$$

Suppose T_1 and T_2 do not share an edge. We are aiming for a contradiction, which then establishes a proof of this lemma. Since $(1,1) \in \mathrm{int}\, P_1$ the horizontal line $(0,1) + \mathbb{R}(1,0)$ intersects P' only in $(0,1)$. Similarly, the vertical line $(1,0) + \mathbb{R}(0,1)$ intersects P' only in $(1,0)$. As (α,β), (γ,δ), $(1,0)$, and $(0,1)$ are pairwise distinct this yields $\alpha,\beta,\gamma,\delta \leq 0$.

First, suppose the split line S_2 is parallel to S_1. As T_2 is a unimodular triangle S_2 is the line through $(-1,0)$ and $(0,-1)$. Then, S_2 and $\alpha,\beta,\gamma,\delta \leq 0$ forces $\alpha = \delta = -1$ and $\beta = \gamma = 0$. We consider the lattice points $q = (-1,1)$ and $r = (1,-1)$. As P' has positive genus, it follows from Lemma 2.2.1 that either q or r is an interior lattice point of P'. By symmetry we may assume $r \in \mathrm{int}\, P'$. Then, the point q can either lie on the boundary of P or is not in P. Now the interval $[(1,1),(1,-1)]$ is the convex hull of two interior lattice points of P, but it contains the boundary point p_1 in its relative interior. Hence we obtain a contradiction.

We conclude that the split lines S_1 and S_2 intersect in some point $w = (\psi, \omega)$, as depicted in the Figure 2.4. Since T_1 is fixed, T_1 and T_2 do not share an edge and $\alpha, \beta, \gamma, \delta \leq 0$, we obtain $\omega \leq 0$. We use the labels from Figure 2.4 and intend to show that w lies in ∂P. Suppose the contrary. Then, due to Lemma 2.1.4, the point w must lie outside P. From our choice of w we see that distance between the point $p_1 := (1, 0)$ and w is lesser than the distance between the points $(0, 1)$ and w. From (2.2.1) it follows that the distance between $p_2 := (\gamma, \delta)$ and w is lesser than the distance between w and (α, β). Applying Lemma 2.1.3 we infer that the interior of the quadrangle $\operatorname{conv}\{z, p_1, w, p_2\}$ does not contain an interior lattice point of P. We realize that since the triangles T_1 and T_2 do not share an edge, and since $p_1, p_2 \in \partial P$ therefore in this case $[p_1, p_2]$ is a boundary edge and the triangle $\operatorname{conv}\{z, p_1, p_2\}$ belongs to Δ.

We now look at possible coordinates of the point $p_2 = (\gamma, \delta)$. Since the triangle $\operatorname{conv}\{z, p_1, p_2\}$ is unimodular and as $\delta \leq 0$ we have $\delta = -1$. Hence p_2 lies on the ray $\{(\gamma, \delta) \colon \gamma \leq 0, \delta = -1\}$. We consider some values of γ starting with the case of $\gamma = 0$. Then (2.2.1) implies that (α, β) is on the line $x = -1$, i.e., $\alpha = -1$. We explore the possible values for β.

For $\beta = -2$ the split edge on the line S_2 would be $s_2 = [(0, -1), (-1, -2)]$. This cannot be as then S_2 would contain p_1 as a third boundary point, a contradiction to Lemma 2.1.1. For $\beta = -1$ and $s_2 = [(0, -1), (-1, -1)]$, we realize that the polygon P_2 is bounded in the rectangular strip between the parallel lines $y = x$ and $y = x - 1$. Yet there is no interior lattice point between them, and this contradicts G_2 to have positive genus. Any other value of $\beta < -2$ contradicts the convexity of P at z. This rules out the possibility $\gamma = 0$.

The arguments for excluding the other values of γ are very similar. We summarize them briefly. For $\gamma = -1$ we obtain $\beta = \alpha + 1$. Then either $s_2 = [(-1, -1), (-1, 0)]$, and we obtain $\omega = 2 \geq 0$, which is absurd. Or $s_2 = [(-1, -1), (-2, -1)]$, whence P_2 is squeezed between the lines $2y = x$ and $2y = x - 1$, which does not leave space for an interior lattice point. Or $s_2 = [(-1, -1), (-3, -2)]$, which then lies on the line spanned by the boundary edge $[p_1, p_2]$. Again, any other value of β on the line $y = x + 1$, contradicts the convexity of P at z.

Similarly, when $\gamma = -2$, we obtain $2\beta = \alpha + 1$. Then either $s_2 = [(-2, -1), (-1, 0)]$, and we obtain $\omega = 1 \geq 0$, which is absurd. Or $s_2 = [(-2, -1), (-3, -1)]$, whence P_2 is squeezed between the lines $3y = x$ and $3y = x - 1$, which does not leave space for an interior lattice point. Or $s_2 = [(-2, -1), (-5, -2)]$, which then lies on the line spanned by the boundary edge $[p_1, p_2]$. Again, any other value of β on the line $2y = x + 1$, contradicts the convexity of P at z.

The case $\gamma \leq -3$ is left. Then the point (α, β) lies on the line $-\gamma y = x + 1$. The following three possibilities occur for the split edge s_2. Either $s_2 = [(-1, 0), (\gamma, -1)]$, and

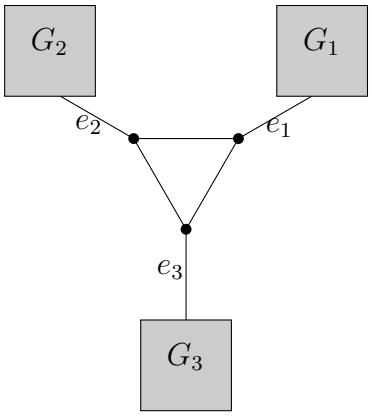

Figure 2.5: A graph with a sprawling triangle; e_1, e_2, e_3 are cut edges; G_1, G_2, G_3 are subgraphs of positive genus.

we obtain $\omega \geq 0$, forcing $\omega = 0$. In this case we see that there is no edge to join between the points $(-1, 0)$ and $(0, 1)$ such that the polygon P remains convex, which gives us a contradiction. Or $s_2 = [(\gamma - 1, -1)(\gamma, -1)]$, whence P_2 is squeezed between the lines $(1 - \gamma)y = x$ and $(1 - \gamma)y = x - 1$, which does not leave space for an interior lattice point. Or $s_2 = [(2\gamma - 1, -2), (\gamma, -1)]$, which then lies on the line spanned by the boundary edge $[p_1, p_2]$. Any other value of β on the line $-\gamma y = x + 1$, contradicts the convexity of P at z.

Therefore, finally, we conclude that there is no lattice point $p_2 = (\gamma, \delta)$ such that the triangle $\text{conv}\{z, p_1, p_2\}$ belongs to Δ. Hence, our initial assumption was wrong, and the triangles T_1 and T_2 do share the edge $[z, w]$, where $w = p_1 = p_2$ is the intersection of S_1 and S_2. Consequently, s_1 and s_2 are two distinct edges of P', and so w is a vertex of P'. □

We notice that the anti-honeycomb triangulation of genus 4 in Example 2.1.5 and Figure 2.2 is a positive example for the result in Lemma 2.2.3. For the three triangular cells containing the split edges and sharing a common vertex, each pair of them has a common edge. In fact, the specific shape of the heavy component in that example gives rise to another concept, which covers a special case of Definition 2.2.2.

Definition 2.2.4. We say that the planar graph G has a *sprawling triangle* if it has a cycle with three nodes, each of which is also incident with a unique cut edge, such that at the other end there is a subgraph of positive genus; cf. Figure 2.5.

It turns out that Example 2.1.5 is the only case where this occurs:

Theorem 2.2.5. *If G has a sprawling triangle then $g = 4$, and, up to unimodular equivalence, we have*

$$P \;=\; A_{(-2,4;\,-2,4;\,-2,4)} \quad \textit{and} \quad \Delta \;=\; \Delta_{(-2,4;\,-2,4;\,-2,4)} \;.$$

Proof. We use the notation from Figure 2.5. Let s_1, s_2 and s_3 be the split edges in Δ corresponding to the cut edges e_1, e_2 and e_3. Using Lemma 2.2.3 on these three splits, we obtain that each pair of them intersects in a point on ∂P. This gives three lattice points a, b, c in the boundary of P such that each pair is joint by one of the three edges s_1, s_2, s_3. Let $\Delta|_{abc}$ be the subcomplex of Δ restricted to the lattice triangle abc. Its skeleton is the sprawling triangle, whose genus is one. Hence there is a unique interior lattice point, z, of P contained in abc. It follows that the lattice triangle abc has normalized area three, and its unimodular triangulation into abz, acz, and bcz forms the induced subcomplex $\Delta|_{abc}$. Those maximal cells of Δ are dual to the three nodes of the sprawling triangle of G.

As in the proof of Lemma 2.2.1 we may assume that $a = (1, 0)$, $b = (0, 1)$ and $z = (0, 0)$. It then follows that $c = (-1, -1)$. Directly from Definition 2.2.4 it follows that the line ab is dual to a cut edge in G and thus induces a split of Δ. All the interior lattice points corresponding to a region of the subgraph G_1 must lie in the halfspace defined by ab which does not contain z. Since z is the only interior lattice point of P which does not correspond to a region of $G_1 \cup G_2 \cup G_3$, the lattice points a, b and c must lie in the boundary of P.

Now Definition 2.2.4 requires the subgraphs G_1, G_2 and G_3 to have positive genus. This excludes the possibility that one of the three points a, b, c is a vertex of P. Thus they must lie on pairwise distinct edges of P. Now we can apply Lemma 2.2.1 three times to learn that the three lattice points

$$\begin{aligned} (1,0) + (0,1) - (0,0) &= (1,1) \\ (1,0) + (-1,-1) - (0,0) &= (0,-1) \\ (0,1) + (-1,-1) - (0,0) &= (-1,0) \end{aligned}$$

are contained in P.

Let L, M, N be the three lines spanned by the edges of P through a, b, c, respectively. Suppose that $(1, 1)$ is a boundary point of P. Then, since P is lattice polygon, $(1, 1)$ is the intersection point of L and M and thus a vertex of P. This contradicts the fact that G_1 has positive genus, and it follows that $(1, 1)$ is an interior lattice point of P. By symmetry, also $(0, -1)$ and $(-1, 0)$ are interior lattice points of P.

Now the lattice point $(1, 2)$ is not contained in P because it would then need to lie on the line M, together with $(-1, 0)$. But this cannot happen as $(-1, 0)$ was already identified as an interior point of P. Similarly, $(2, 1)$ is not contained in P either. Yet this implies that the intersection of the lines L and M lies strictly between the two parallel lines $(1, 0) + \lambda(1, 1)$ and $(0, 1) + \lambda(1, 1)$. Thus there is at least one vertex of P, which must be a lattice point, on the line $(0, 0) + \lambda(1, 1)$. This forces $(2, 2)$ to lie in P.

Again the situation is symmetric, which is why also $(-2, 0)$ and $(0, -2)$ lie in P. The single choice left is that $(2, 2)$ as well as $(-2, 0)$ and $(0, -2)$ are vertices of P, and L, M, N

are the only facets. This establishes $P = \text{conv}\{(-2,0),(0,-2),(2,2)\}$. The claim about Δ follows as there is only one way to extend the triangulation from the triangle abc to all of P. □

Remark 2.2.6. Contracting a sprawling triangle in a planar graph yields a graph with a sprawling node, and this cannot be tropically planar. Therefore, Example 2.1.5 shows that the class of tropically planar graphs is not minor closed; this was observed before [16, Figure 6].

2.3 Graph with a heavy cycle and two loops

Graphs with a sprawling triangle form special cases of graphs with a heavy cycle. Thus our main technical result, Lemma 2.2.3, allowed us to derive decisive structural constraints for triangulations whose skeleton has a sprawling triangle in Theorem 2.2.5. Now we are looking into another special class of groups with a heavy cycle, aiming for a second structural result on unimodular triangulations of lattice polygons.

Definition 2.3.1. We say that a connected trivalent planar graph G has a *heavy cycle with two loops* if it has the form as described in Figure 2.6, where the shaded region represents a subgraph of positive genus.

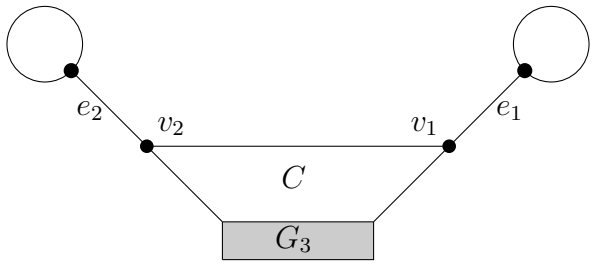

Figure 2.6: Heavy cycle with two loops

The latter is the special case of Definition 2.2.2, where $g(G_1) = 1 = g(G_2)$. This type of skeleton does actually occur.

Example 2.3.2. The quadrangle $Q_4^{(5)}$ of genus 5, cf. [10, Figure 22], admits a (regular) unimodular triangulation whose skeleton features a heavy cycle with two loops, cf. [10, Figure 23].

Our aim in this section is to establish the following,

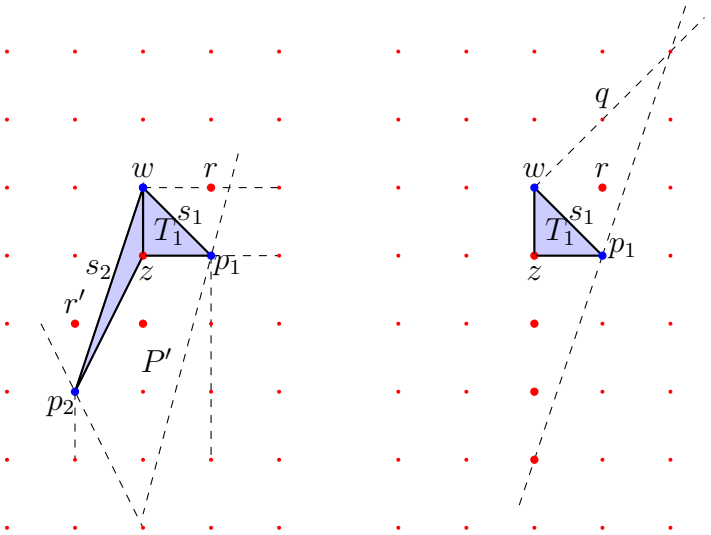

Figure 2.7: This illustrates Theorem 2.3.3: general sketch (left) and the case when $g(P') \geq 4$ (right), which is impossible

Theorem 2.3.3. *Suppose G is a graph with a heavy cycle C and two loops with cut edges, e_1 and e_2, as in Figure 2.6. Then the heavy component P' can have at most three interior lattice points, and these lie on the line spanned by the edge $[z, w] \in \Delta$, where z is the interior lattice point dual to C, and w is the intersection point of the split edges s_1 and s_2. In particular, P' is hyperelliptic and $g \leq 5$.*

Proof. It follows from Lemma 2.2.3 that the two triangles share the edge $[z, w]$, where $w \in \partial P$ is the point where the two split edges meet. We will first show that the interior lattice points of P' lie on the line spanned by $[z, w]$.

As previously, we fix $T_1 = \text{conv}\{(0,0),(0,1),(1,0)\}$ and use the labels from Figure 2.7; in particular, we may assume that $w = (0,1)$. Using Lemma 2.2.3 and the unimodularity of T_2, we realize that p_2 must lie on the line $x = -1$; so let $p_2 = (-1, -k)$ for some integer k. We use Lemma 2.2.1 on the points $z = (0,0)$, $w = (0,1)$ and $p_1 = (1,0)$ and infer that the point $r := (1,1)$ is an interior lattice point of P; moreover it is the unique interior lattice point of P_1. Similarly, we infer that the point $r' := (-1, -k+1)$ is the unique interior lattice point of P_2. By considering the lines connecting the interior point r with the boundary points p_1 and w, respectively, we see that $k \geq 0$. The same argument shows that the entire polygon P' is squeezed between the lines $x = 1$ and $x = -1$. In particular, the interior lattice points of P' lie on $x = 0$, which is the line spanned by z and w.

Next we will show that $g(P') \leq 3$. We assume the contrary, i.e., $g(P') \geq 4$ Then, since all interior lattice points of P' lie on the line $x = 0$, the point $(0, -3)$ must be an interior lattice point of P.

The vertical line $x = 1$ contains the point p_1, which is a boundary point, and r, which is an interior lattice point. It follows that there is a lattice point $(1, \lambda)$ in the boundary of P_1 for $\lambda > 1$; in particular, either $(1, 2) \in P_1$ or the boundary edge at w passes through a point in the open interval $((1, 2), (1, 1))$. Also, as $(0, -3)$ is an interior point, no point in ∂P_1 is present on the line $y = 3x - 3$. We realize that in this case P_1 is contained in the triangle $\text{conv}\{p_1, w, (1, 3)\}$. However, this triangle has no valid lattice point which could be a vertex of P_1; recall that $(1, 3)$ has been excluded; see Figure 2.7. This provides the desired contradiction, and thus $g(P') \leq 3$. □

The above result is sharp as Example 2.3.2 shows. The following summarizes the known obstructions to tropical planarity together with our new results.

Theorem 2.3.4. *A trivalent planar graph of genus $g \geq 3$ is not tropically planar if one of the following holds:*

1. *it contains a sprawling node, or*
2. *it contains a sprawling triangle and $g \geq 5$, or*
3. *it is crowded, or*
4. *it is a TIE-fighter, or*
5. *it has a heavy cycle with two loops such that the interior lattice points of the heavy component do not align with the intersection of the two split lines.*

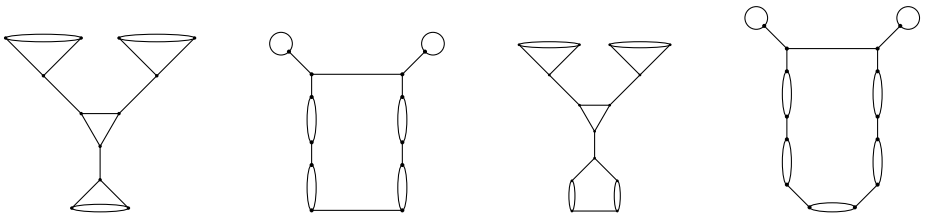

Figure 2.8: Examples of non realizable graphs of genus 7 and 8

For instance, the preceding result excludes the graphs in Figure 2.8.

2.4 Anti-honeycombs

The purpose of this section is to define a class of lattice polygons each of which admits a special triangulation. This is motivated by Theorem 2.2.5, which characterizes one of these

triangulations. These triangulations show high degree of symmetry and the entire family deserves some attention. Consider three families of parallel lines:

$$L_k = \{y{=}2x{+}k\}\,,\ M_\ell = \{2y{=}x{-}\ell\}\,,\ N_m = \{y{=}{-}x{+}m\}\ , \tag{2.4.1}$$

where $k, \ell, m \in \mathbb{Z}$. By picking a sixtuple $\pi = (k, k'; \ell, \ell'; m, m')$, with $k < k'$, $\ell < \ell'$, and $m < m'$ we obtain a polygon A_π which is defined by three pairs of inequalities, where each pair comes from one of the parallel families (2.4.1). We call A_π the *anti-honeycomb polygon of type* π; in general, this is not a lattice polygon. The following characterizes when the lines from the three families intersect at lattice points; we omit the proof, which is a direct calculation.

Lemma 2.4.1. *We have*

1. $L_k \wedge M_\ell \in \mathbb{Z}^2$ *if and only if* $k - \ell$ *is divisible by* 3*;*
2. $L_k \wedge N_m \in \mathbb{Z}^2$ *if and only if* $k - m$ *is divisible by* 3*;*
3. $M_\ell \wedge N_m \in \mathbb{Z}^2$ *if and only if* $\ell - m$ *is divisible by* 3*.*

The name comes about from the connection to the "honeycomb polygons" studied in [10, pp. 10ff]. Note that not all of the six inequalities need to be facet defining, whence A_π is a hexagon, a pentagon, a quadrangle or a triangle. For instance,

$$A_{(k,-2k;\,k,-2k;\,k,-2k)} \ = \ \operatorname{conv}\{(-k,-k),(0,k),(k,0)\} \tag{2.4.2}$$

is a triangle, and its genus equals

$$g(A_{(k,-2k;\,k,-2k;\,k,-2k)}) \ = \ \frac{3k^2 - 3k + 2}{2}\ .$$

We fix a type $\pi = (k, k'; \ell, \ell'; m, m')$, and we let $V = A_\pi \cap \mathbb{Z}^2$ be the set of lattice points in A_π. Intersecting with the shifted lattice

$$\mathcal{L} \ = \ \begin{pmatrix}-1\\-1\end{pmatrix} + \mathbb{Z}\begin{pmatrix}2\\1\end{pmatrix} + \mathbb{Z}\begin{pmatrix}1\\2\end{pmatrix}$$

of index 3 we obtain a subset $V' = V \cap \mathcal{L}$ of the lattice points in A_π. The families of lines (2.4.1) yield weakly compatible splits of the point configuration V', and they induce a triangulation Δ'_π of the lattice points in V'. Notice that all the points in $V \setminus V'$ lie in the interior $\operatorname{int} A_\pi$. Since none of these lattice points lies on any of the lines (2.4.1) it follows that each of them is contained in the interior of a unique triangle of Δ'_π. Employing stellar subdivisions at the points in $V \setminus V'$ this yields a triangulation Δ_π of V, which we call the *anti-honeycomb*

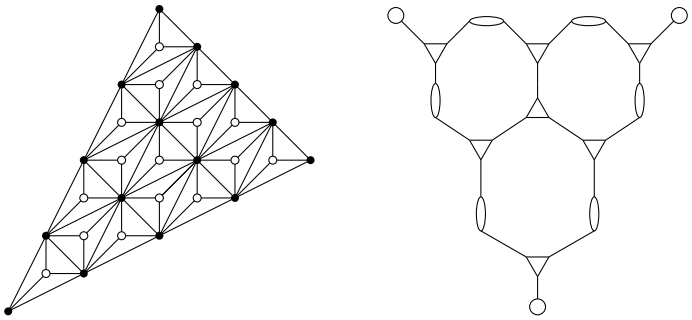

Figure 2.9: Anti-honeycomb triangulation of genus 19 on the left, and the corresponding skeleton on the right

triangulation of type π. Figure 2.2, Example 2.1.5, and Theorem 2.2.5 are concerned with the case $\pi = (-2, 4; -2, 4; -2, 4)$ of genus 4. Figure 2.9 shows a genus 19 anti-honeycomb triangulation along with its corresponding skeleton for $\pi = (4, -8; 4, -8; 4, -8)$.

The honeycomb curves yield moduli cones of maximal dimension $2g + 1$, where g is the genus, cf. [10, Theorem 1]. In contrast the anti-honeycomb curves form a large family whose moduli cones are much smaller. For instance, a direct `polymake` [23] computation shows that the moduli cone of $\Delta_{(4,-8;4,-8;4,-8)}$ is only 28-dimensional, whereas the upper bound $2g + 1$ equals 39.

Example 2.4.2. Two interesting classes of anti-honeycomb quadrangles are:

$$A_{(k,-2k;\,k,k-3;\,k,-2k)} = \operatorname{conv}\{(-k,-k),(k,0),(k{-}1,1),(1{-}k,2{-}k)\}\ ,$$
$$A_{(k,3-2k;\,k,k-3;\,k,-2k)} = \operatorname{conv}\{(-k,-k),(k{-}2,-1),(k{-}1,1),(1{-}k,2{-}k)\}\ .$$

They arise from the triangle $A_{(k,-2k;k,-2k;k,-2k)}$ in (2.4.2) by imposing M_{k-3} and L_{3-2k}, respectively, as additional facets. The quadrangle $A_{(k,-2k;k,k-3;k,-2k)}$ is a lattice trapezoid of genus $2k - 1$, while $A_{(k,3-2k;k,k-3;k,-2k)}$ is a lattice parallelogram of genus $2k - 2$. These examples provide anti-honeycomb polygons of arbitrary genus. Additionally, their skeleta are hyperelliptic, despite the fact that the interior lattice points do not lie on a line. The first few cases are shown in Figure 2.10. Because of their shapes we call them *anti-honeycomb quadrangles of zigzag type*.

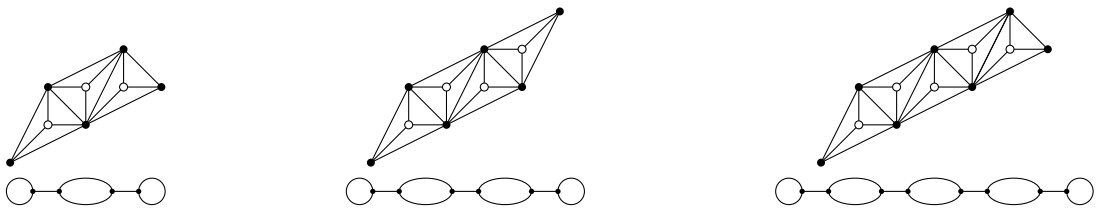

Figure 2.10: Anti-honeycomb quadrangles of zigzag type and their skeleta; genus 3, 4 and 5.

The anti-honeycomb polygons of low genus can be found by directly inspecting the possibilities of stacking copies of the elliptic "building block" $A_{(1,-2;1,-2,1,-2)}$.

Proposition 2.4.3. *The anti-honeycomb polygons of genus $g \leq 6$ are unimodularly equivalent to either quadrangles of zigzag type or to the triangle $A_{(2,-4;2,-4;2,-4)}$.*

Up to an affine transformation, which is not a lattice transformation, the three families of lines in (2.4.1) form a Coxeter hyperplane arrangement of type $\tilde{A}_2$. This generalizes to arbitrary dimensions, and so does the construction of the anti-honeycomb triangulations. The resulting anti-honeycomb polytopes are affine images of the "alcoved polytopes" of Lam and Postnikov [37].

2.5 Conclusion

We would now want to list all conclusions that we inferred with our results regarding the status of tropically planar graphs. The classification of the tropically planar graphs of genus $g \leq 5$ was obtained in [10]. Theorem 2.3.4 now allows for a combinatorial characterization:

Corollary 2.5.1. *A trivalent planar graph of genus $g \leq 5$ is tropically planar if and only if none of the obstructions in Theorem 2.3.4 occurs.*

Proof. The trivalent graphs of low genus have been classified in [4]. For $g = 3$ there are five such graphs, one of which has a sprawling node; the other four are tropically planar [10, Theorem 5.1]. For $g = 4$ there are 17 graphs: one is non-planar, three have a sprawling node, the remaining 13 are tropically planar [10, Theorem 7.1]. This was known before.

There are exactly 71 trivalent graphs of genus 5. Among them only 52 are planar without a sprawling node [10]. Of these 14 were ruled out by explicit computations [10], which leaves 38 tropically planar graphs of genus 5. One of the key contributions of [16, Figure 8] is to obtain obstructions to tropical planarity, which rules out another ten, which are crowded or TIE-fighters.

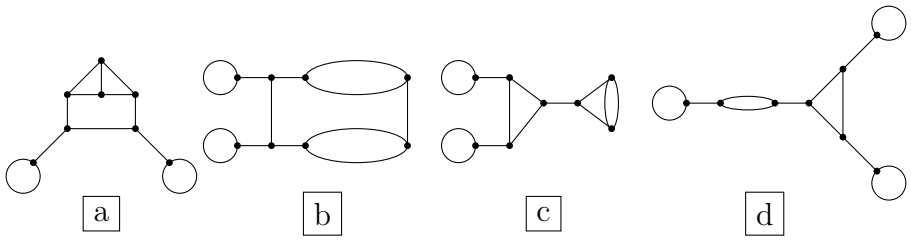

Figure 2.11: The four genus 5 graphs that are not ruled out by any prior known criteria

As our new contribution we can now discuss the remaining four graphs, which are shown in Figure 2.11. Firstly, we observe that all of these exhibit a heavy cycle. The graph labeled "a" has a heavy cycle with two loops, but the component away from the two loops is not hyperelliptic; i.e., it is ruled out by Theorem 2.3.3. The second graph, labeled "b" also has a heavy cycle with two loops, the component (of genus 3) away from the two loops is even hyperelliptic. However, we see that the interior point z dual to the heavy cycle would lie in between the other two interior lattice points in the hyperelliptic polygon dual to the genus 3 component; the latter contradicts Theorem 2.3.3, which says that the interior lattice points in the genus 3 component should lie below z on the line spanned by z and w, where w is the point of intersection of the two splits. Thus "b" is ruled out by Theorem 2.3.3, too. The graphs labeled "c" and "d" feature sprawling triangles, whence they are taken care of by Theorem 2.2.5. This completes our combinatorial characterization of the tropically planar graphs of genus at most five. □

For genus 6, there are 388 trivalent graphs altogether, 354 of which are planar [4]. In [16] it was shown that 152 tropically planar graphs of genus 6 remain. There are 28 graphs which are non-realizable and could not be ruled out using any prior known criteria; cf. [16, Figure 17]. Out of these 28 graphs, 19 have a heavy cycle with two loops and can be ruled out using Theorem 2.3.3 because the genus is too high. One of the remaining graphs has a sprawling triangle, and thus excluded by Theorem 2.2.5. We are left with eight graphs of genus 6, which are shown in Figure 2.12; for these we are not aware of any a priori obstruction. There are 672 troplanar graphs of genus 7 according to [16, Table 1]; however, the full list does not seem to be available.

We now discuss some other recent advances that were made in the study of troplanar graphs. In [16, Theorem 4.2], it is shown that as the genus g grows asymptotically large, then the number of troplanar graphs tends to 0. This helps us understand that the complete classification that we obtain in 2.3.4 for genus upto five, is something which can not be replicated for arbitrarily large genus, as the family of distinct forbidden patterns would keep getting larger, and this helps us appreciate the completeness of the result. Also, in [17], a closed formula for computing the dimension of $\mathbb{M}_\Delta$ for a non-hyperelliptic lattice polygon is obtained, which earlier could only be computed via computer-aided computations. It complements the computation we did to compute the dimension of the antihoneycomb triangulation in Figure 2.9 via `polymake`. Also, in [17], it is shown that for a non-hyperelliptic lattice polygon P the following holds,

$$\dim\left(\mathcal{M}_P\right) = \dim\left(\mathbb{M}_P\right)$$

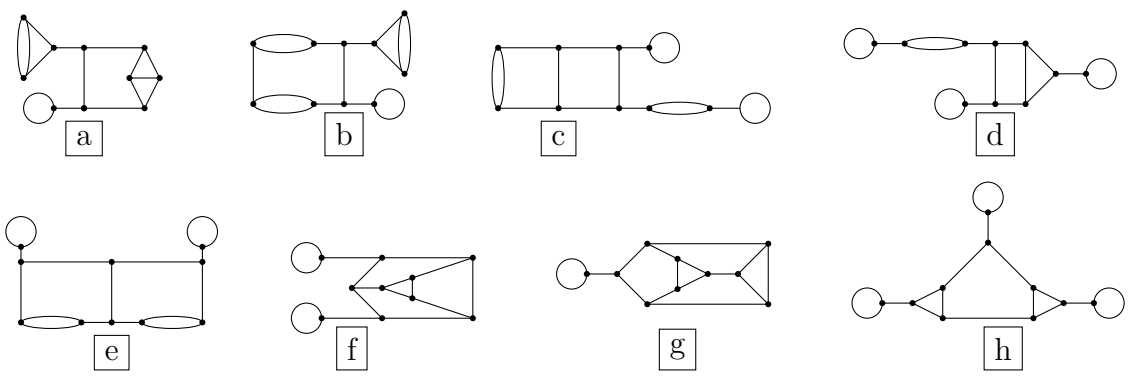

Figure 2.12: The eight trivalent planar graphs of genus 6, which are not tropically planar [16], but which are not covered by Theorem 2.3.4.

where $\mathcal{M}_P$ is the moduli space of non-degenerate curves defined over P and $\mathbb{M}_P$ denotes the closure of the set of all metric graphs that are the skeleton of a smooth tropical curve with Newton polygon P. In ongoing work, we are trying to find all the possible values of the dimension of $\mathbb{M}_P$ and to obtain a closed formula to compute the dimension of $\mathbb{M}_\Delta$ for a non-maximal hyperelliptic polygon.

Another possible avenue for further exploration could be to know how the tropically plane curves of a fixed genus fit into the moduli space of all tropical curves. For genus 3 this was recently answered in terms of modifications by Hahn et al. [26].

Results of the presented work in this chapter have been published in - Michael Joswig and Ayush Kumar Tewari. "Forbidden patterns in tropical plane curves" Beiträge zur Algebra und Geometrie / Contributions to Algebra and Geometry, Aug 2020 [34]. Licensed under a Creative Commons Attribution 4.0 International License.

Chapter 3

Lattice visibility and Panoptigons

3.1 Preliminaries

A lattice point in $\mathbb{R}^2$ is any point with integer coordinates, and a lattice polygon is any polygon whose vertices are lattice points. We say that two distinct lattice points $p = (a, b)$ and $q = (c, d)$ are visible to one another if the line segment $\overline{pq}$ contains no lattice points besides p and q, or equivalently if $\gcd(a - c, b - d) = 1$; by convention we say that any p is visible from itself. Points visible from the origin $O = (0, 0)$ are called visible points, with all other points being called invisible. The properties of visible and invisible points have been subject to a great deal of study over the past century, as surveyed in [9, §10.4]. The question of which structures can appear among visible points, invisible points, or some prescribed combination thereof was studied in [28], where it was proved that one can find a copy of any convex lattice polygon (indeed, any arrangement of finitely many lattice points) consisting entirely of invisible points.

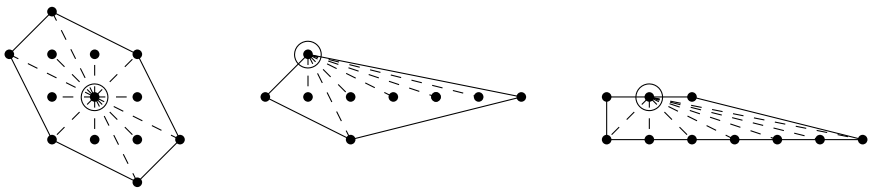

Figure 3.1: Three panoptigons, with a panoptigon point circled and lines of sight illustrated; the middle polygon has a second panoptigon point, namely the bottom vertex

In this chapter we pose and answer a somewhat complementary question: which convex lattice polygons including the origin contain only visible lattice points? We define a *panoptigon*[1] to be a convex lattice polygon P containing a lattice point p such that all other

[1]This name is modeled off of *panopticon*, an architectural design that allows for one position to observe all others. It comes from the Greek word *panoptes*, meaning "all seeing".

lattice points in P are visible from p. We call such a point p a *panoptigon point* for P. Thus up to translation, a panoptigon is a convex lattice polygon containing the origin such that every point in $P \cap \mathbb{Z}^2$ is a visible point. Three panoptigons are pictured in Figure 3.1, each with a panoptigon point and its lines of sight highlighted; note that the panoptigon point need not be unique.

One can quickly see that there exist infinitely many panoptigons; for instance, the triangles with vertices at $(0,0)$, $(1,0)$, and $(a,1)$ are panoptigons for any value of a. However, this is not an interesting family of examples since any two of these triangles are *equivalent*, the definition of which we recall below.

Definition 3.1.1. A *unimodular transformation* is an integer linear map $t : \mathbb{R}^2 \to \mathbb{R}^2$ that preserves the integer lattice $\mathbb{Z}^2$; any such map is of the form $t(p) = Ap + b$, where A is a 2×2 integer matrix with determinant ± 1 and $b \in \mathbb{Z}^2$ is a translation vector. We say that two lattice polygons P and Q are *equivalent* if there exists a unimodular triangulation t such that $t(P) = Q$.

It turns out that there are infinitely many panoptigons even up to equivalence: note that the triangle with vertices at $(0,0)$, $(0,-1)$, and $(b,-1)$ is a panoptigon for every positive integer b, and any two such triangles are pairwise inequivalent since they have different areas. We can obtain nicer results if we stratify polygons according to the *lattice width* of a polygon P, the minimum integer w such that there exists a polygon P' equivalent to P in the horizontal strip $\mathbb{R} \times [0, w]$. Although there are infinitely many panoptigons of lattice widths 1 and 2, we can still classify them completely, as presented in Lemmas 3.3.1 and 3.3.2. Once we reach lattice width 3 or more, we obtain the following powerful result.

Theorem 3.1.2. *Let P be a panoptigon with lattice width $\mathrm{lw}(P) \geq 3$. Then $|P \cap \mathbb{Z}^2| \leq 13$.*

Since there are only finitely many lattice polygons with a fixed number of lattice points up to equivalence [36, Theorem 2], it follows that there are only finitely many panoptigons P with $\mathrm{lw}(P) \geq 3$. In section 3.6 we detail computations to enumerate all such lattice polygons. This allows us to determine that there exactly 73 panoptigons of lattice width 3 or more. One is the triangle of degree 3, which has a single interior lattice point; and the other 72 are non-hyperelliptic, meaning that the convex hull of their interior lattice points is two-dimensional.

As an application of our classification of panoptigons, we prove new results about tropically planar graphs [16]. We prove a new criterion for ruling out certain graphs from being tropically planar, notable in that the graphs it applies to are 2-edge-connected, unlike those ruled out by most existing criteria; this resolves an open question posed in [16, §5]. We say that a

planar graph G is a *big face graph* if for every planar embedding of G, there is a bounded face sharing an edge with all other bounded faces.

Theorem 3.1.3. *If G is a big face graph of genus $g \geq 14$, then G is not tropically planar.*

The idea behind the proof of this theorem is as follows. If a big face graph G is tropically planar, then it is dual to a regular unimodular triangulation of a lattice polygon P. One of the interior lattice points p of P must be connected to all the other interior lattice points, so that the bounded face dual to p can share an edge with all other bounded faces. Thus, the convex hull of the interior lattice points of P must be a panoptigon. If that panoptigon has lattice width 3 or more, then it can have at most 13 lattice points, and so G cannot have $g \geq 14$.

For the case that the lattice width of the interior panoptigon is smaller, we need an understanding of which polygons of lattice width 1 or 2 can appear as the interior lattice points of another lattice polygon. We obtain this in Propositions 3.4.1 and 3.4.5, and can once again bound the genus of G. In fact, if we are willing to rely on our computational enumeration of all panoptigons with lattice width at least 3, then we can improve this result to say that big face graphs of genus $g \geq 12$ are not tropically planar. We will see that this bound is sharp.

In Section 3.2 we present background on lattice polygons, including a description of all polygons of lattice width at most 2. In Section 3.3 we classify all panoptigons. In Section 3.4 we classify all maximal polygons of lattice width 3 or 4. Finally, in Section 3.5 we prove Theorem 3.1.3. Our computational results are then summarized in section 3.6.

3.2 Properties of lattice polygons

In this section we recall important terminology and results regarding lattice polygons. This includes the notion of maximal polygons, and of lattice width. Throughout we will assume that P is a two-dimensional convex lattice polygon, unless otherwise stated.

The *genus* of a polygon P is the number of lattice points interior to P. A key fact is that for fixed $g \geq 1$, there are only finitely many lattice polygons of genus g, up to equivalence [13, Theorem 9]. We say a lattice polygon P is a *maximal polygon* if it is maximal with respect to containment among all lattice polygons containing the same set of interior lattice points.

In the case that P is non-hyperelliptic, there is a strong relationship between P and P_{int}. Let $\tau_1, \ldots, \tau_n$ be the one-dimensional faces of a (two-dimensional) lattice polygon Q. Then Q can be defined as an intersection of half-planes:

$$Q = \bigcap_{i=1}^{n} \mathcal{H}_{\tau_i},$$

where $\mathcal{H}_\tau = \{(x,y) \in \mathbb{R}^2 \,|\, a_\tau x + b_\tau y \leq c_\tau\}$ is the set of all points on the same side of the line containing τ as Q. Without loss of generality, we assume that $a_\tau, b_\tau, c_\tau \in \mathbb{Z}$ with $\gcd(a_\tau, b_\tau) = 1$. With this convention, we define

$$\mathcal{H}_\tau^{(-1)} = \{(x,y) \in \mathbb{R}^2 \,:\, a_\tau x + b_\tau y \leq c_\tau + 1\},$$

and from there we define the *relaxed polygon* of Q as

$$Q^{(-1)} := \bigcap_{i=1}^{n} \mathcal{H}_{\tau_i}^{(-1)}.$$

We can think of $Q^{(-1)}$ as the polygon we would get by "moving out" the edges of Q. It is worth remarking that $Q^{(-1)}$ need not be a lattice polygon. We denote $Q^{(-1)} \cap \mathcal{H}_{\tau_i}^{(-1)}$ as $\tau_i^{(-1)}$. It is not necessarily the case that $\tau_i^{(-1)}$ is a one-dimensional face of $Q^{(-1)}$; however, if $Q^{(-1)}$ is a lattice polygon, then $Q^{(-1)} \cap \tau_i^{(-1)}$ must contain at least one lattice point, as proved in [17, Lemma 2.2]. Examples where $Q^{(-1)}$ is not a lattice polygon, and where $Q^{(-1)}$ is a lattice polygon but an edge has collapsed, are illustrated in Figure 3.2. There is a very important case when we are guaranteed to have that $Q^{(-1)}$ is a lattice polygon, namely when $Q = P_{\text{int}}$ for some non-hyperelliptic lattice polygon P.

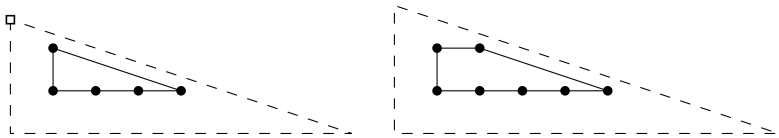

Figure 3.2: Two lattice polygons, one with a relaxed polygon with a non-lattice vertex marked; and one with a collapsed edge in the relaxed (lattice) polygon

Proposition 3.2.1 ([35], §2.2)**.** *Let P be a non-hyperelliptic lattice polygon, with interior polygon P_{int}. Then $P_{int}^{(-1)}$ is a lattice polygon containing P whose interior polygon is also P_{int}. In particular, $P_{int}^{(-1)}$ is the unique maximal polygon with interior polygon P_{int}.*

If we are given a polygon Q and we wish to know if there exists a lattice polygon P with $P_{\text{int}} = Q$, it therefore suffices to compute the relaxed polygon $Q^{(-1)}$, and to check whether its vertices have integral coordinates. This might fail because two adjacent edges τ_i and τ_{i+1} of Q are relaxed to intersect at a non-integral vertex of $Q^{(-1)}$; we also might have that some $\tau_i^{(-1)}$ is completely lost, which cannot happen when $Q^{(-1)}$ is a lattice polygon by [17, Lemma 2.2]. Careful consideration of these obstructions will be helpful in classifying the maximal polygons of lattice widths 3 and 4 in Section 3.4.

An important tool in studying lattice polygons is the notion of *lattice width*. Let P be a non-empty lattice polygon, and let $v = \langle a, b\rangle$ be a lattice direction with $\gcd(a,b) = 1$. The

width of P with respect to v is the smallest integer d for which there exists $m \in \mathbb{Z}$ such that the strip

$$m \leq ay - bx \leq m + d$$

contains P. We denote this d as $w(P, v)$. The *lattice width of P* is the minimal width over all possible choices of v:

$$\mathrm{lw}(P) = \min_{v} w(P, v).$$

Any v which achieves this minimum is called a *lattice width direction for P*. Equivalently, $\mathrm{lw}(P)$ is the smallest d such that there exists a lattice polygon P' equivalent to P with $P' \subset \mathbb{R} \times [0, d]$.

We recall the following result connecting the lattice widths of a polygon and its interior polygon. Let $T_d = \mathrm{conv}((0,0),(d,0),(0,d))$ denote the standard triangle of degree d.

Lemma 3.2.2 (Theorem 4 in [14])**.** *For a lattice polygon P we have $lw(P) = lw(P_{int}) + 2$, unless P is equivalent to T_d for some $d \geq 2$, in which case $lw(P) = lw(P_{int}) + 3 = d$.*

The following result tells us precisely which polygons have lattice width 1 or 2. It is a slight reworking of a result due to [35], also presented in [13, Theorem 10]

Theorem 3.2.3. *Let P be a two-dimensional lattice polygon. If $lw(P) = 1$, then P is equivalent to*

$$T_{a,b} := conv((0,0),(0,1),(a,1),(b,0))$$

for some $a, b \in \mathbb{Z}$ with $0 \leq a \leq b$ and $b \geq 1$.

If $lw(P) = 2$, then up to equivalence either $P = T_2$; or $g(P) = 1$ and $P \neq T_3$ (all such polygons are illustrated in Figure 3.3); or $g(P) \geq 2$. In the latter case we have $\frac{1}{6}(g+3)(2g^2+15g+16)$ polygons, sorted into three types:

- *Type 1:*

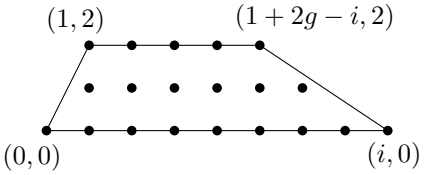

  where $g \leq i \leq 2g$.

- *Type 2:*

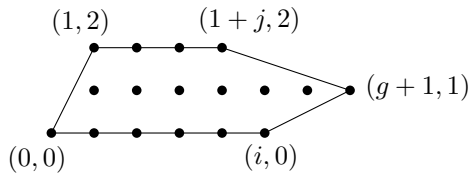

  where $0 \leq i \leq g$ and $0 \leq j \leq i$; or $g < i \leq 2g+1$ and $0 \leq j \leq 2g - i + 1$

- *Type 3:*

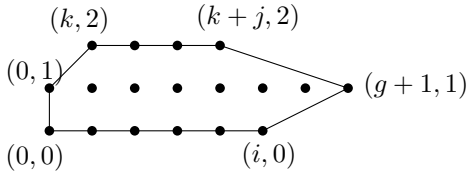

where $0 \leq k \leq g + 1$ *and* $0 \leq i \leq g + 1 - k$ *and* $0 \leq j \leq i$*; or* $0 \leq k \leq g + 1$ *and* $g + 1 - k < i \leq 2g + 2 - 2k$ *and* $0 \leq j \leq 2g - i - 2k + 1$

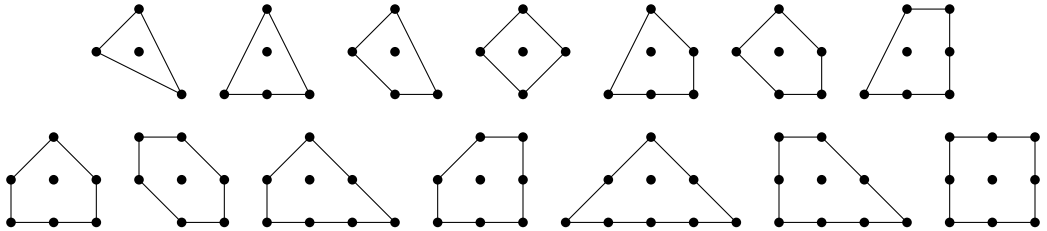

Figure 3.3: The 14 genus 1 polygons with lattice width 2

Proof. The classification proved in [35] was similar, except with polygons sorted by genus ($g = 0$, $g = 1$, and $g \geq 2$ with all interior lattice points collinear) rather than by lattice width. We can translate their work into the desired result as follows.

For $\mathrm{lw}(P) = 1$, we know P has no interior lattice points, so $g = 0$; all polygons of genus 0 besides T_2 have lattice width 1. By [35] all genus 0 polygons besides T_2 are equivalent to $T_{a,b}$ for some $a, b \in \mathbb{Z}$ with $0 \leq a \leq b$ and $b \geq 1$.

For $\mathrm{lw}(P) = 2$, we deal with the three cases of $g = 0$, $g = 1$, and $g \geq 2$. If $g = 0$, then the only polygon of lattice width 2 is T_2. If P is a polygon with genus $g = 1$, then by Lemma 3.2.2 we know that $\mathrm{lw}(P) = \mathrm{lw}(P_{\mathrm{int}}) + 2 = 0 + 2 = 2$ unless P is equivalent to T_d for some d. The only value of d such that T_d has genus 1 is $d = 3$, so every genus 1 polygon except T_3 has lattice width 2.

Finally, suppose P is a polygon of lattice width 2 and genus $g \geq 2$. Since $\mathrm{lw}(T_d) = d$ and $g(T_2) = 0$, we know $P \neq T_d$ for any d, and so $\mathrm{lw}(P_{\mathrm{int}}) = \mathrm{lw}(P) - 2 = 2 - 2 = 0$. It follows that all the g interior lattice points of P must be collinear, and so P is hyperelliptic. Conversely, if P is a hyperelliptic polygon of genus $g \geq 2$, by definition the interior polygon P_{int} has lattice width 0. Since no triangle T_d has genus $g \geq 2$ with all its interior points collinear we may apply Lemma 3.2.2 to conclude that $\mathrm{lw}(P) = \mathrm{lw}(P_{\mathrm{int}}) + 2 = 2$. This means that for polygons of genus $g \geq 2$, being hyperelliptic is equivalent to having lattice width 2. Combined with the classification of hyperelliptic polygons in [35], this completes the proof. □

A counterpart of lattice width is *lattice diameter*. Following [6], the lattice diameter $\ell(P)$ is the length of the longest lattice line segment contained in the polygon P:

$$\ell(P) = \max\{|L \cap P \cap \mathbb{Z}^2| - 1 \,:\, L \text{ is a line}\}.$$

We define a *lattice diameter direction* $\langle a, b\rangle$ to be one such that there exists a line L with slope vector $\langle a, b\rangle$ with $|L \cap P \cap \mathbb{Z}^2| - 1 = \ell(P)$. We remark that there exist other works where lattice diameter is defined as the largest number of collinear lattice points in the polygon P [1]; this is simply one more than the convention we set above. The following result relates $\ell(P)$ to $\mathrm{lw}(P)$.

Theorem 3.2.4 ([6], Theorem 3)**.** *We have* $lw(P) \leq \lfloor \frac{4}{3}\ell(P)\rfloor + 1$.

Assume for the remainder of the section that P is a lattice polygon of genus $g \geq 2$. We recall the *skeleton* G associated to a unimodular traingulation Δ of P. An example of a regular unimodular triangulation, the dual graph, and the tropically planar skeleton are pictured in Figure 3.4. Note that there is a one-to-one correspondence between the interior lattice points of P and the bounded faces of G in this embedding, where two faces of G share an edge if and only if the corresponding interior lattice points are connected by an edge in Δ.

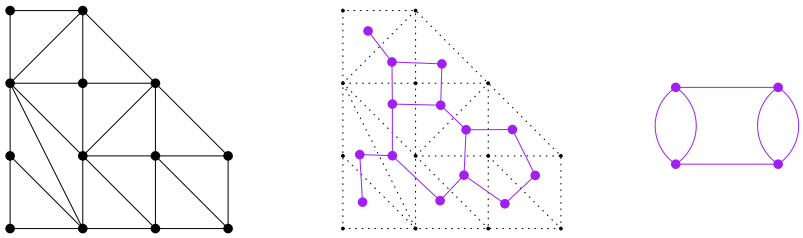

Figure 3.4: A regular unimodular triangulation of a polygon, the dual graph of the triangulation, and the corresponding tropically planar skeleton

It is worth remarking that we could still construct a graph G from a non-regular triangulation. The reason that we insist that Δ is regular is so that the graph G appears as a subset of a smooth tropical plane curve, which is a balanced 1-dimensional polyhedral complex that is dual to a regular unimodular triangulation of a lattice polygon; see [38]. (Indeed, the regularity is necessary if we wish to endow a skeleton with the structure of a *metric graph*, with lengths assigned to its edges, as explored in [10] and [17].) Most of the results that we prove in this chapter, and that we recall for the remainder of this section, also hold if we expand to graphs that arise as dual skeleta of *any* unimodular triangulation of a lattice polygon.

The first Betti number of a tropically planar graph, also known as its genus[2], is equal to the number of interior lattice points of the lattice polygon P giving rise to it. It is also equal to the number of bounded faces in any planar embedding of the graph. A systematic method of computing all tropically planar graphs of genus g was designed and implemented in [10] for $g \leq 5$. The algorithm is brute-force, and works by considering all maximal lattice polygons of genus g, finding all regular unimodular triangulations of them, and computing the dual skeleta. These computations were pushed up to $g = 7$ in [16]. In general there is no known method of checking whether an arbitrary graph is tropically planar short of this massive computation.

A fruitful direction in the study of tropically planar graphs has been finding properties or patterns that are forbidden in such graphs, an example of which is discussed in the previous chapter. Since the graph before skeletonization is dual to a unimodular triangulation of a polygon, any tropically planar graph is 3-regular, connected, and planar. Several additional constraints are summarized in the following result.

Theorem 3.2.5 ([12], Proposition 4.1; [16], Theorem 3.4; [34], Theorems 10 and 14)**.** *Suppose that G is a 3-regular graph of genus g of one of the forms illustrated in Figure 3.5, where each gray box represents a subgraph of genus at least 1. If G is tropically planar, then it must have either the third or fourth forms, with $g = 4$ for the third form and $g \leq 5$ in the fourth form. In particular, if $g \geq 6$, then G is not tropically planar.*

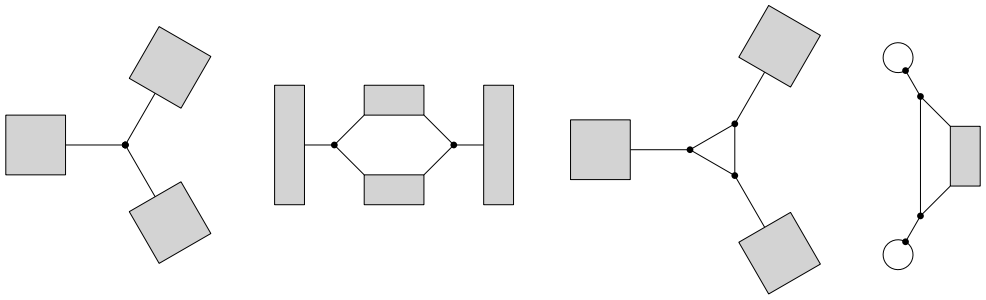

Figure 3.5: Forbidden patterns in tropically planar graphs of genus $g \geq 6$

The proofs of all these results rely on the observation that any cut-edge in a tropically planar graph must arise from a split in the dual unimodular triangulation that divides the polygon into two polygons of positive genus. For planar graphs that are 2-edge-connected and thus have no cut-edges, the only known general criterion to rule out tropical planarity is the notion of crowdedness [40]. However, crowded graphs are ones that cannot be dual to *any*

[2]This terminology comes from [3] and is motivated by algebraic geometry; it is unrelated to the notion of graph genus defined in terms of embeddings on surfaces. The first Betti number of a graph is also sometimes called its *cyclomatic number*.

triangulation of *any* point set in $\mathbb{R}^2$, regardless of whether or not the point set comes from a convex lattice polygon; thus it is not especially interesting that crowded graphs are not tropically planar. In Section 3.5 we will find a family of 2-edge-connected, 3-regular planar graphs that are not crowded but are still not tropically planar, the first known such examples.

3.3 A classification of all panoptigons

Let P be a convex lattice polygon. Recall from the introduction that P is a panoptigon if there is lattice point $p \in P \cap \mathbb{Z}^2$ such that every other point in $P \cap \mathbb{Z}^2$ is visible from p. In this section we will classify all panoptigons, stratified by a combination of genus and lattice width. We begin with the panoptigons of genus 0.

Lemma 3.3.1. *Let P be a panoptigon of genus 0. Then P is one of the following polygons, up to lattice equivalence:*

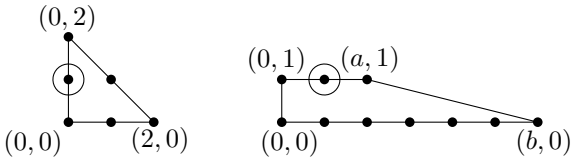

where $0 \leq a \leq \min\{2, b\}$.

Proof. By [35], any genus 0 polygon is equivalent either to the triangle T_2, or to the (possibly degenerate) trapezoid $T_{a,b}$ where $0 \leq a \leq b$ and $1 \leq b$. The triangle of degree 2 is a panoptigon, as any non-vertex lattice point can see every other lattice point. For $T_{a,b}$, we note that if $a \geq 3$ then the polygon is not a panoptigon: each lattice point p is on a row with at least 3 other lattice points, not all of which can be visible from p since the 4 (or more) points in that row are collinear. However, if $a \leq 2$, then a point p can be chosen on the top row that can see the other a points on the top row, as well as all points on the bottom row. Thus $T_{a,b}$ is a panoptigon if and only if $a \leq 2$. □

For polygons with exactly one interior lattice point, there is no obstruction to being a panoptigon.

Lemma 3.3.2. *If P is a polygon of genus 1, then P is a panoptigon.*

Proof. Let p be the unique interior lattice point of P, and let q be any other lattice point of P. Since $g(P) = 1$, the point q must be on the boundary. By convexity, the line segment $\overline{pq}$ must have its relative interior contained in the interior of the polygon, and so the line segment does not intersect ∂P outside of q. Since p is the only interior lattice point, we have

that the only lattice points of $\overline{pq}$ are its endpoints. It follows that q is visible from p for all $q \in P \cap \mathbb{Z}^2 - \{p\}$. We conclude that P is a panoptigon with panoptigon point p. $\square$

We now consider hyperelliptic polygons of genus $g \geq 2$. We will characterize precisely which of these are panoptigons based on the classification of them in Theorem 3.2.3 into Types 1, 2, and 3. Any hyperelliptic polygon can be put into one of these forms in the horizontal strip $\mathbb{R} \times [0, 2]$; thus we may say a lattice point (a, b) of such a polygon is at height b, where every point is either at height 0, height 1, or height 2.

Lemma 3.3.3. *Let P be a hyperelliptic polygon of genus $g \geq 2$, transformed so that it of one of the forms presented in Theorem 3.2.3. Then P is a panoptigon if and only if*

- *P is of Type 1, with $g \leq 3$; or*
- *P is of Type 2, either with $g \leq 2$, or with $j = 0$ and $0 \leq i \leq 1$; or*
- *P is of Type 3, either with $j = 0$ and $i \leq 2$, with k odd if $i = 0$ and k even if $i = 2$; or with $i = 0$ and $j \leq 2$, and k odd if $j = 0$ and k even if $j = 2$.*

For the reader's convenience we recall the polygons of Types 1, 2, and 3 in Figure 3.6.

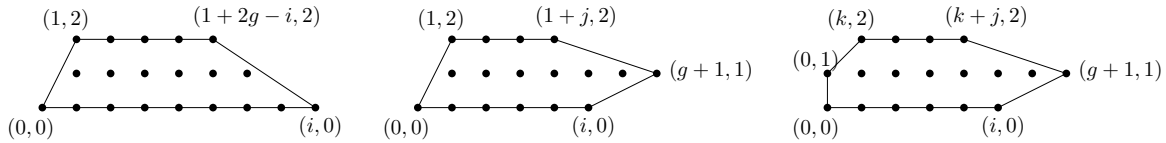

Figure 3.6: Hyperelliptic polygons of Types 1, 2, and 3

Proof. We start by making the following observations. If $p = (a, b)$ is a panoptigon point for a hyperelliptic polygon P, then there must be at most 3 points at height b; and if there are exactly 3, then p must be the middle such point. We also make several remarks in the case that $b \in \{0, 2\}$. There are no obstructions to a point at height b seeing a point at height 1, so we will not concern ourselves with this. Choose $b' \in \{0, 2\}$ distinct from b, and suppose height b' has 2 or more lattice points; then two of those points have the form $q = (a, b')$ and $q' = (a + 1, b')$. We claim that p cannot view both q and q'. Writing $p = (a, b)$, the midpoints of the line segments $\overline{pq}$ and $\overline{pq'}$ have coordinates $\left(\frac{a+a'}{2}, 1\right)$ and $\left(\frac{a+a'+1}{2}, 1\right)$, respectively. Exactly one of $\frac{a+a'}{2}$ and $\frac{a+a'+1}{2}$ is an integer, meaning that either q or q' is not visible from p. So, if $p = (a, b)$ is a panoptigon point at height $b \in \{0, 2\}$, there must be exactly one lattice point $q = (a', b')$ at height $b' \in \{0, 2\}$ with $b' \neq b$; moreover, we must have that $a - a'$ is odd.

We are ready to determine the possibilities for a hyperelliptic panoptigon P of genus $g \geq 2$, sorted by type.

- Let P be a hyperelliptic polygon of Type 1. If $g \leq 3$, then we may choose $p = (a, 1)$ that can see every other point at height 1, as well as all points at heights 0 and 2; in this case P is a panoptigon. If $g \geq 4$, then there are at least 4 points at height 1. Moreover, the number of points at height 0 is $i + 1$ where $g \leq i \leq 2g$, and we have $i + 1 \geq 5$ since $g \geq 4$. Thus it is impossible to have at most 3 points at one height and 1 at another. This means that for $g \geq 4$, P cannot be a panoptigon

- Let P be a hyperelliptic polygon of Type 2. If $g = 2$, then P has exactly three points at height 1, and we can choose the middle point as a panoptigon point. Now assume $g \geq 3$; we cannot choose a panoptigon point at height 1, since there are $g+1 \geq 4$ points at that height. To avoid having 4 points on both the top and bottom rows we need $0 \leq i \leq g$ and $0 \leq j \leq i$; and one of i and j must be 0, so we need $j = 0$ since $j \leq i$. From there we need at most 3 lattice points on the bottom row, so $0 \leq i \leq 2$. If $i = 2$, then the only possible panopticon point is the middle one on the bottom row, namely $(1, 0)$; but this point cannot see $(1, 2)$, a contradiction. Thus $0 \leq i \leq 1$; note that in either case $(0, 0)$ can serve as a panoptigon point.

- Finally, let P be a hyperelliptic polygon of Type 3. We cannot have a panoptigon point at height 1, since there are at least $g + 2 \geq 4$ points at that height. If there is a panoptigon point at height 0, then we must have at most 3 points at height 0 and exactly one point at height 2; that is, we must have $j = 0$ and $i \leq 2$. Moreover, we need to verify that way may choose a panoptigon point at height 0 that can see the unique point at height 2; this can always be done if $i = 1$, but if $j = 0$ then we need k odd (the only possible panoptigon point is then $(0, 0)$), and if $j = 2$ we need k even (the only possible panoptigon point is then $(1, 0)$). A similar argument shows that we can choose a panoptigon point at height 2 if and only if $i = 0$ and $j \leq 2$, with k odd if $j = 0$ and k even if $j = 2$.

□

As with the lattice width 1 panoptigons, we find infinitely many lattice width 2 panoptigons, namely those of Type 2 with $j = 0$ and $0 \leq i \leq 1$, and those of Type 3.

We have now classified all hyperelliptic panoptigons, and have found that there are infinitely many of lattice width 1 and infinitely many of lattice width 2. Our last step is to understand non-hyperelliptic panoptigons; with the exception of the triangle T_3, this is equivalent to panoptigons of lattice width 3 or more. We are now ready to prove that the total number of lattice points of such a panoptigon is at most 13.

Proof of Theorem 3.1.2. Let us consider the lattice diameter $\ell(P)$ of P. We know by [1, Theorem 1] that $|P \cap \mathbb{Z}^2| \leq (\ell(P)+1)^2$, so if $\ell(P) \leq 2$ we have $|P \cap \mathbb{Z}^2| \leq 9$. Thus we may assume $\ell(P) \geq 3$.

Perform an $\mathrm{SL}_2(\mathbb{Z})$ transformation so that $\langle 1, 0\rangle$ is a lattice diameter direction for P, and translate the polygon so that the origin $O = (0, 0)$ is a panoptigon point. Thus $P \cap \mathbb{Z}^2$ consists of O and a collection of visible points.

Since $\ell(P) \geq 3$ and $\langle 1, 0\rangle$ is a lattice diameter direction, we know that the polygon P must contain 4 lattice points of the form (a, b), $(a+1, b)$, $(a+2, b)$, and $(a+3, b)$. We claim that $b \in \{-1, 1\}$. Certainly $b \neq 0$, since there are only three such points allowed in P: $(0, 0)$ and $(\pm 1, 0)$. We also know that b cannot be even: any set $\mathbb{Z} \times \{2k\}$ has every second point invisible from the origin.

Suppose for the sake of contradiction that the points (a, b), $(a+1, b)$, $(a+2, b)$, and $(a+3, b)$ are in P with b odd and $b \geq 3$ (a symmetric argument will hold for $b \leq -3$). Consider the triangle $T = \mathrm{conv}(O, (a, b), \ldots, (a+3, b))$. By convexity, $T \subset P$. Consider the line segment $T \cap L$, where L is the line defined by $y = b - 1$. The length of this line segment is $3 - \frac{1}{b}$, and since $b \geq 3$ this is strictly greater than 2. Any line segment of length 2 at height $b - 1$ will intersect at least two lattice points. But since $b - 1$ is even and $b - 1 \geq 2$, at least one of these lattice points is not visible from O. Such a lattice point must be contained in T, and therefore in P, a contradiction. Thus we have that $b = \pm 1$.

Rotating our polygon 180° degrees if necessary, we may assume that $b = -1$, so that the points $(a, -1), \ldots, (a+3, -1)$ are contained in P. It is possible that the number k of lattice points on the line defined by $y = -1$ is more than 4; up to relabelling, we may assume that $(a, -1), \ldots, (a+k-1, -1)$ are lattice points in P while $(a-1, -1)$ and $(a+k, -1)$ are not, where $k \geq 4$. Applying a shearing transformation $\begin{pmatrix} 1 & a+1 \\ 0 & 1 \end{pmatrix}$, we may further assume that the points at height -1 are precisely $(-1, -1), \ldots, (k-2, -1)$.

We will now make a series of arguments that rule out many lattice points from being contained in P. The end result of these constraints is pictured in Figure 3.7, with points labelled by the argument that rules them out.

(i) The polygon P has (regular) width at least 3 at height -1, and width strictly smaller than 2 at heights 2 and -2, since it cannot contain two consecutive lattice points at those heights. It follows from convexity that the width of the polygon is strictly smaller than 1 at height -3, and that the polygon cannot have any lattice points at all at height -4. It also follows that the polygon cannot have a nonnegative width at height 8. Thus every lattice point (x, y) in the polygon satisfies $-3 \leq y \leq 7$.

(ii) We can further restrict the possible heights by showing that there can be no lattice points at height -3. Suppose there were such a point $(x, -3)$ in P. Consider the triangle $\text{conv}((x, -3), (-1, -1), (2, -1))$. This triangle has area 3, so by Pick's Theorem [44] the triangle satisfies $3 = g + \frac{b}{2} - 1$, or $4 = g + \frac{b}{2}$, where g and b are the number of interior lattice points an boundary lattice points of the triangle, respectively. The 4 lattice points at height -1 contribute 2 to this sum, and the one lattice point at height -3 contributes $\frac{1}{2}$ to this sum, meaning that the lattice points at height -2 contribute $\frac{3}{2}$ to this sum. It follows that there must be at least two lattice points at height -2; but this is a contradiction, since at least one of these points will be invisible from O. We conclude that P cannot contain a lattice point of the form $(x, -3)$, and thus $y \geq -2$ for all lattice points $(x, y) \in P$.

(iii) We know that the lattice point $(-2, 0)$ is not in P since it is not visible from O. If there is any lattice point of the form (x, y) with $y \geq 1$ and $y \leq -x - 2$, then the triangle $\text{conv}(O, (-1, -1), (x, y))$ will contain $(-2, 0)$. Thus no such lattice point (x, y) can exist in P.

(iv) No point of the form (x, y) with $x \geq 2$ and $y \geq 0$ may appear in P: this would force the point $(2, 0)$ to appear, as it would lie in the triangle $\text{conv}(O, (2, -1), (x, y))$.

(v) There are now only finitely many allowed lattice points (x, y) with $y \geq 1$, namely those with $-y - 1 \leq x \leq 2$ and $1 \leq y \leq 7$. For each such point, we consider the triangle $\text{conv}((x, y), (-1, -1), (-1, 3))$. We claim that only the 13 choices of (x, y) pictured in Figure 3.7. that do not introduce a forbidden point. To see this, we note that the points $(0, 2)$, $(-2, 2)$ and $(-2, 4)$ are all forbidden. The point $(0, 2)$ rules out (x, y) with $x = 1$ and $y \geq 5$; with $x = 0$ and $y \geq 2$; with $x = -1$ and $y \geq 4$; ant with $x = -2$ and $y \geq 5$. For $x = -2$, the points $(-2, 2)$ and $(-2, 4)$ are already ruled out. For all remaining points with $x \leq -3$, every point besides $(-3, 2)$, $(-4, 3)$, and $(-5, 3)$ introduces the point $(-2, 2)$ or $(-2, 4)$ or both. This establishes our claim.

(vi) By assumption, we know there are no lattice points of the form $(x, -1)$ where $x \leq -2$. It follows that there are also no lattice points of the form $(x, -2)$ where $x \leq -4$, since $(-1, -2)$ would lie in the convex hull of such a point with O and $(2, -1)$.

(vii) We will now use the fact that we have assumed that P satisfies $\text{lw}(P) \geq 3$. We cannot have that P is contained in the strip $-2 \leq y \leq 0$, so there must be at least one point (x, y) with $y \geq 1$. If there is a point of the form $(x', -1)$ with $x' \geq 6$, then we would have that $\text{conv}((x, y), (x', -1), (-1, -1))$ contains the point $(2, 0)$, which is invisible.

Thus we can only have points $(x', -1)$ if $-1 \leq x \leq 5$. A similar argument shows that P can only contain a point $(x, -2)$ if x is odd with $-3 \leq x \leq 9$.

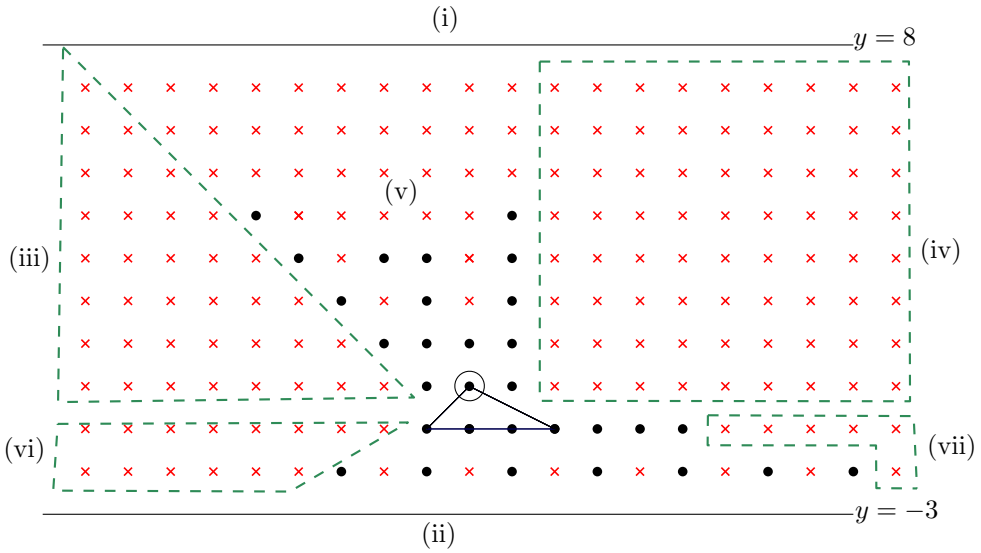

Figure 3.7: Possible lattice points in P, with impossible points labelled by the argument ruling them out

We have now narrowed the possible lattice points in our polygon down to the 30 lattice points in Figure 3.7, five of which we know appear in P. For every such point (x, y), there does indeed exist a polygon P with $\mathrm{lw}(P) \geq 3$ containing (x, y) as well as the five prescribed points such that $P \cap \mathbb{Z}^2$ is a subset of the 30 allowed points, so we cannot narrow down any further.

One way to finish the proof is by use of a computer to determine all possible subsets of the 25 points that can be added to our initial 5 points to yield a polygon of lattice width at least 3; we would then simply check the largest number of lattice points. We have carried out this computation, and present the results in section 3.6. We also present the following argument, which will complete our proof without needing to rely on a computer.

First we split into four cases, depending on the number k of lattice points at height -1: 4, 5, 6, or 7. When there are more than 4, we can eliminate more of the candidate points (x, y) with $y \geq 1$ or $y = -2$; the sets of allowable points in these four cases are illustrated in Figure 3.8. In each case we will argue that our polygon P has at most 13 lattice points.

- Suppose $k = 4$. There are 20 possible points at height -1 or above; since there is at most one point at height -2, it suffices to show that we can fit no more than 12 lattice points at height -1 or above into a lattice polygon.

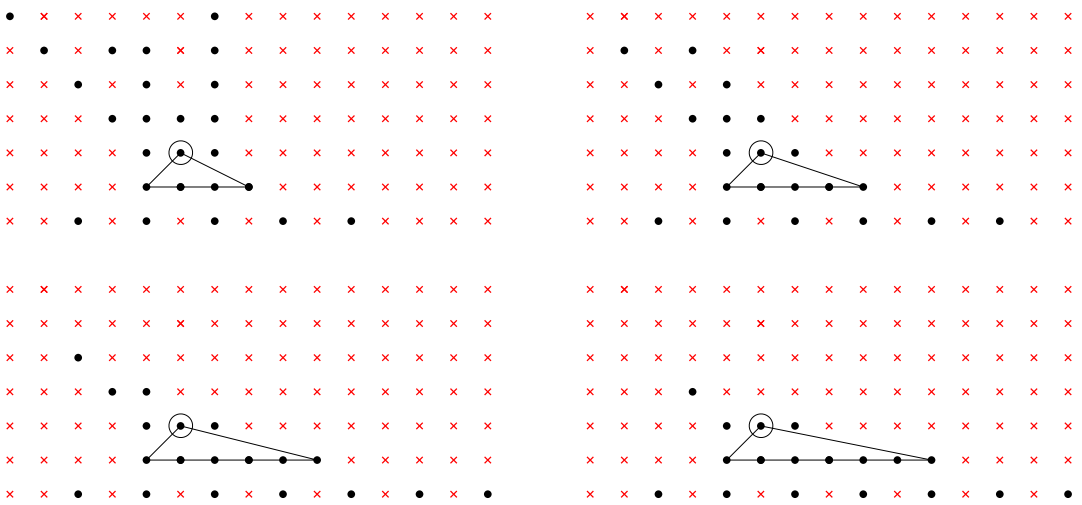

Figure 3.8: Narrowing down possible points depending on the number of points at height -1

First suppose the point $(-5, 4)$ is in P. This eliminates 9 possible points from appearing in P, yielding at most $20 - 9 + 1 = 12$ lattice points total in P. Leaving out $(-5, 4)$ but including $(-4, 3)$ similarly eliminates 9 possible points. Including $(-2, 3)$ eliminates 8; including $(-1, 3)$ and leaving out $(-2, 3)$ eliminates 8; including $(1, 4)$ eliminates 9; and including $(1, 3)$ and leaving out $(1, 4)$ eliminates 9. In all these cases, we can conclude that P has at most 13 lattice points in total.

The only remaining case is that all lattice points of P have heights between -2 and 2. The polygon can have at most one lattice point at height -2, at most one lattice point at height 2, and some assortment of the 11 total points with heights between -1 and 1. Once again, P can have at most 13 lattice points.

- Suppose $k = 5$. If P includes the point $(-4, 3)$, then it cannot include $(-2, 3)$, $(-1, 2)$, or $(0, 1)$. Combined with the fact that P can only have one lattice point at height -2, this leaves P with at most 13 total lattice points. A similar argument holds if P includes the point $(-2, 3)$. If P contains neither $(-4, 3)$ nor $(-2, 3)$, then it has at most 1 point at height 3, at most one point at height -2, and some collection of the 11 points between. Thus P has at most 13 lattice points.

- Suppose $k = 6$. Since P has at most one lattice point at height -2, and only 12 points are allowed outside of that height, P has at most 13 lattice points total.

- Suppose $k = 7$. Since P has at most one lattice point at height -2, and only 11 points are allowed outside of that height, P has at most 12 lattice points total.

We conclude that $|P \cap \mathbb{Z}^2| \leq 13$. □

As detailed in section 3.6, we enumerated all non-hyperelliptic polygons containing the five prescribed points from the previous proof, along with some subset of the other 25 permissible points. The end result was 69 non-hyperelliptic panoptigons of lattice diameter 3 or more, up to equivalence. In the same section we show that there are 3 non-hyperelliptic panoptigons with lattice diameter at most 2, yielding a grand total of 72 non-hyperelliptic panoptigons. If we instead wish to count panoptigons of lattice width at least 3, this count becomes 73 due to the inclusion of T_3.

We remark that it is possible to give a much shorter proof that there are only finitely many non-hyperelliptic panoptigons. Suppose that P is a panoptigon of lattice diameter $\ell(P) \geq 7$. By the same argument that started our previous proof, we may assume without loss of generality that P has $(0,0)$ as a panoptigon point as well as eight or more lattice points at height -1. If P contains a point of the form (x,y) where $y \geq 2$, then the line segment $P \cap L$ where L is the x-axis must have length at least $7\left(1-\frac{1}{y+1}\right) \geq 7\left(1-\frac{1}{2+1}\right) = \frac{14}{3} > 4$. As such P must contain at least 4 points at height 0, impossible since there are only 3 visible points at this height. Similarly P can have no lattice points at height 1: these would force the inclusion of either $(2,0)$ or $(-2,0)$. Finally, if P contains a point of the form (x,y) where $y \leq -3$, then the line segment $P \cap L'$ where L' is the horizontal line at height -2 must have width at least $7\left(1-\frac{1}{|y|-1}\right) \geq 7\left(1-\frac{1}{3-1}\right) = \frac{7}{2} > 3$. As such we know that P must contain at least 3 lattice points at height -2, impossible since no two consecutive points at that height are both visible. Thus we know that P only has lattice points at heights 0, -1, and -2, and so is a hyperelliptic polygon. This means that if P is a non-hyperelliptic panoptigon, it must have $\ell(P) \leq 6$. Since $|P \cap \mathbb{Z}^2| \leq (\ell(P)+1)^2$, it follows that if P is a non-hyperelliptic panoptigon then it must have at most $(6+1)^2 = 49$ lattice points; there are any finitely many such polygons. In principle one could enumerate all such polygons with at most 49 lattice points as in [13] and check which are panoptigons; this would be much less efficient than the computation led to by our longer proof.

3.4 Maximal polygons of lattice width 3 or 4

In this section we will characterize all maximal polygons of lattice width 3 or 4. By Lemma 3.2.2, this will allow us to determine which polygons of lattice width 1 or 2 can be the interior polygon of some lattice polygon. This will be helpful in Section 3.5, when we will need to know which of the infinitely many panoptigons of lattice width at most 2 can be an interior polygon.

For lattice width 3, we do have the triangle T_3 as an exceptional case; all other polygons with lattice width 3 must have an interior polygon of lattice width 1.

Proposition 3.4.1. *Let P be a maximal polygon. Then P has lattice width 3 if and only if up to equivalence we either have $P = T_3$, or $P = T_{a,b}^{(-1)}$ where $a \geq \frac{1}{2}b - 1$, $0 \leq a \leq b$, and $b \geq 1$, and where $T_{a,b} \neq T_1$.*

Proof. If P is equivalent to T_3, then it has lattice width 3 as desired. If P is equivalent to some other T_d, then P has lattice width $d \neq 3$, and so need not be considered.

Now assume P is not equivalent to T_d for any d, so that P has lattice width 3 if and only if P_{int} has lattice width 1 by Lemma 3.2.2. This is the case if and only if P_{int} is equivalent to $T_{a,b}$ for some $a, b \in \mathbb{Z}$ where $0 \leq a \leq b$ and $b \geq 1$ (where $T_{a,b} \neq T_1$) by Theorem 3.2.3. Thus to prove our claim, it suffices by Proposition 3.2.1 to show that $T_{a,b}^{(-1)}$ is a lattice polygon if and only if $a \geq \frac{1}{2}b - 1$.

We set the following notation to describe $T_{a,b}$. Starting with the face connecting $(0, 0)$ and $(0, 1)$ and moving counterclockwise, label the faces of $T_{a,b}$ as τ_1, τ_2, τ_3, and τ_4 (where τ_4 does not appear if $a = 0$).

Pushing out the faces, we find that $\tau_1^{(-1)}$ lies on the line $x = -1$, $\tau_2^{(-1)}$ on the line $y = -1$, $\tau_3^{(-1)}$ on the line $x + (b - a)y = b + 1$, and $\tau_4^{(-1)}$ on the line $y = 2$. Note that working cyclically, we have $\tau_i^{(-1)} \cap \tau_{i+1}^{(-1)}$ is a lattice point: we get the points $(-1, -1)$, $(2b - a + 1, 1)$, $(2a - b + 1, 2)$, and $(-1, 2)$. Thus if these are the vertices of $T_{a,b}^{(-1)}$, then $T_{a,b}^{(-1)}$ is a lattice polygon. Certainly $(-1, -1)$ and $(2b-a+1, 1)$ appear in $T_{a,b}^{(-1)}$. The points $(2a-b+1, 2)$ and $(-1, 2)$ will appear as (not necessarily distinct) vertices of $T_{a,b}^{(-1)}$ if and only if $2a-b+1 \geq -1$; that is, if and only if $a \geq \frac{1}{2}b - 1$. Thus in the case that $a \geq \frac{1}{2}b - 1$, we have that $T_{a,b}^{(-1)}$ is a lattice polygon with vertices at $(-1, -1)$, $(2b - a + 1, -1)$, $(2a - b + 1, 2)$, and $(-1, 2)$.

If on the other hand $a < \frac{1}{2}b-1$, then $\tau_4^{(-1)}$ is not a face of $T_{a,b}^{(-1)}$, and so one of the vertices of $T_{a,b}^{(-1)}$ is $\tau_1^{(-1)} \cap \tau_3^{(-1)}$. These faces intersect at the point $\left(\frac{b+2}{b-a}, -1\right)$, where we may divide by $b - a$ since $a < \frac{1}{2}b - 1$ and so $a \neq b$. Note that $b - a > b - \frac{1}{2}b + 1 = \frac{1}{2}(b + 2)$. It follows that that $\frac{b+2}{b-a} < 2$, and certainly $\frac{b+2}{b-a} > 1$, so $\left(\frac{b+2}{b-a}, -1\right)$ is not a lattice point. We conclude that $T_{a,b}^{(-1)}$ is a lattice polygon if and only if $a \geq \frac{1}{2}b - 1$, thus completing our proof. □

The explicitness of this result, combined with the fact that $g\left(T_{a,b}^{(-1)}\right) = a + b + 2$, allows us to count the number of maximal polygons P of genus g with lattice width 3. First, note that there are $\left\lfloor \frac{g-2}{2} \right\rfloor$ choices of $T_{a,b}$ with g lattice points: with our assumption that $a \leq b$, we can choose a to be any number from 1 up to $\left\lfloor \frac{g-2}{2} \right\rfloor$, and b is determined from there. Next, we will exclude those choices of a that yield $a < \frac{1}{2}b - 1$, or equivalently $a \leq \frac{1}{2}b - \frac{3}{2}$ since $a, b \in \mathbb{Z}$. Given that $a + b = g$, this is equivalent to $a \leq \frac{1}{2}(g - a) - \frac{3}{2}$, or $\frac{3}{2}a \leq \frac{1}{2}g - \frac{3}{2}$, or $a \leq \frac{g}{3} - 1$. Thus the number of polygons we must exclude from the total count $\left\lfloor \frac{g-2}{2} \right\rfloor$ is $\left\lfloor \frac{g}{3} \right\rfloor - 1$. We conclude that the number of maximal polygons of genus g with lattice width 3 is

$$\left\lfloor \frac{g-2}{2} \right\rfloor - \left\lfloor \frac{g}{3} \right\rfloor + 1$$

when $g \geq 4$ (which allows us to ignore T_3).

We now wish to classify maximal polygons P of lattice width 4. One possibility is that P is T_4. Other than this example, the interior polygon P_{int} must have lattice width 2. Note that if $g(P_{\text{int}}) = 0$, then $P_{\text{int}} = T_2$; this has relaxed polygon T_5, which has lattice width 5 and so is not under consideration. If $g(P_{\text{int}}) = 1$, then P_{int} is one of the polygons in Figure 3.3. It turns out that all of these can be relaxed to a lattice polygon, each of which has lattice width 4; these polygons are illustrated in Figure 3.9.

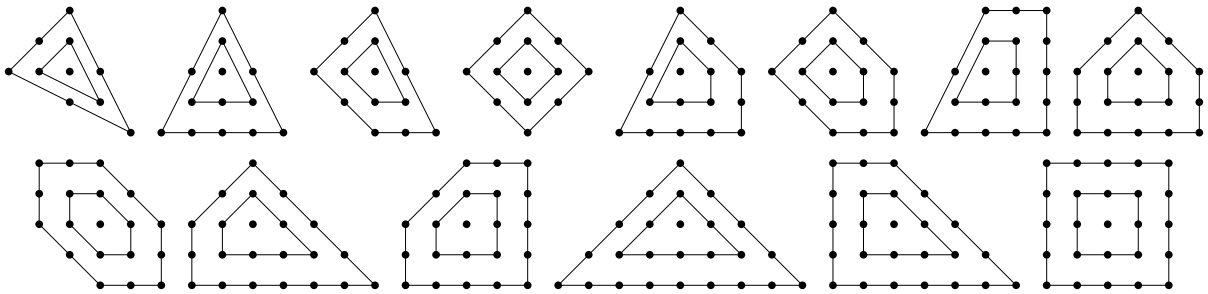

Figure 3.9: The lattice width 4 polygons with exactly one doubly interior point

Now we deal with the most general case of polygons with $\text{lw}(P) = 4$, namely those where P_{int} has lattice width 2 and genus $g' \geq 2$. Thus P_{int} must be one of the $\frac{1}{6}(g+3)(2g^2+15g+16)$ hyperelliptic polygons presented in Theorem 3.2.3. We must now determine which of these hyperelliptic polygons Q have a relaxed polygon $Q^{(-1)}$ that has lattice points for vertices. We do this over three lemmas, which consider the polygons of Type 1, Type 2, and Type 3 separately.

Lemma 3.4.2. *If Q is of Type 1, then the relaxed polygon $Q^{(-1)}$ is a lattice polygon if and only if $i \leq \frac{3g+1}{2}$.*

Proof. Let τ_1, τ_2, τ_3, and τ_4 denote the four one-dimensional faces of Q, proceeding counterclockwise starting from the face connecting $(0,0)$ and $(1,2)$ (note that τ_4 does not appear as a one-dimensional face if $i = 2g$). Consider the relaxed faces $\tau_1^{(-1)}$, $\tau_2^{(-1)}$, $\tau_3^{(-1)}$, and $\tau_4^{(-1)}$. These lie on the lines $-2x + y = 1$, $y = -1$, $2x + (2i - 2g - 1)y = 2i + 1$, and $y = 3$. Proceeding cyclically, the intersection points $\tau_i^{(-1)} \cap \tau_{i+1}^{(-1)}$ of these relaxed faces are $(-1,-1)$, $(2i-g,-1)$, $(3g-2i+2,3)$, and $(1,3)$. All these points are lattice points, so if they are indeed the vertices of P_{int} then $Q^{(-1)}$ is a lattice polygon.

The one situation in which our relaxed polygon will not have all lattice points is if $\tau_1^{(-1)}$ and $\tau_3^{(-1)}$ intersect at a height strictly below 3, cutting off the face $\tau_4^{(-1)}$ and yielding a vertex with y coordinate strictly between 2 and 3. These faces intersect at $\left(\frac{g+1}{2(i-g)}, \frac{i+1}{i-g}\right)$, which has y-coordinate strictly smaller than 3 if and only if $\frac{i+1}{i-g} < 3$, which can be rewritten as

$i+1 < 3i-3g$, or as $\frac{3g+1}{2} < i$. Thus when $i \leq \frac{3g+1}{2}$, our relaxed polygon is a lattice polygon; and when $i > \frac{3g+1}{2}$, it is not. □

Lemma 3.4.3. *If Q is of Type 2, then the relaxed polygon $Q^{(-1)}$ is a lattice polygon if and only if $i \geq \frac{g}{2}+1$ and $j \geq \frac{g-1}{2}$.*

Proof. Label the faces of Q cyclically as τ_1, τ_2, τ_3, τ_4, and τ_5. Due to the form of the slopes of these faces, the relaxed face $\tau_i^{(-1)}$ will intersect the relaxed face $\tau_{i+1}^{(-1)}$ at a lattice point; this is true for τ_1 with τ_2 and τ_5 by computation, and for any horizontal line with a face of slope $1/k$ for some integer k. Similarly, we are fine with the intersections of $\tau_3^{(-1)}$ and $\tau_4^{(-1)}$: these will always intersect at the lattice point $(g+2, 1)$. Thus the only way the relaxed polygon will fail to have lattice vertices is if certain edges are lost while pushing out. Considering the normal fan of Q, this leads to two possible cases for Q to not be integral: if the face $\tau_2^{(-1)}$ is lost, and if the face $\tau_5^{(-1)}$ is lost.

First we consider the case that $\tau_2^{(-1)}$ is lost due to $\tau_1^{(-1)}$ and $\tau_3^{(-1)}$ intersecting at a point with y-coordinate strictly between 0 and -1; note that this can only happen when $i < g$. The face $\tau_1^{(-1)}$ is on the line $-2x+y=1$, and $\tau_3^{(-1)}$ is on the line $x-(g+1-i)y = i+1$. These intersect at $\left(-\frac{g+2}{2g-2i+1}, -\frac{2i+3}{2g-2i+1}\right)$. Note that $-\frac{2i+3}{2g-2i+1} > -1$ is equivalent to $\frac{2i+3}{2g-2i+1} < 1$, which in turn is equivalent to $2i+3 < 2g-2i+1$. This simplifies to $i < \frac{g}{2}+1$. Thus we have a collapse of $\tau_2^{(-1)}$ that introduces a non-lattice vertex point if and only if $i < \frac{g}{2}+1$.

Now we consider the case that $\tau_5^{(-1)}$ is lost due to $\tau_1^{(-1)}$ and $\tau_4^{(-1)}$ intersecting at a point with y-coordinate strictly between 2 and 3. The face $\tau_4^{(-1)}$ lies on the line with equation $x+(g-j)y = 2g-j+2$. This intersects $\tau_1^{(-1)}$ at $\left(\frac{g+2}{2g-2j+1}, \frac{4g-2j+5}{2g-2j+1}\right)$. Having $\frac{4g-2j+5}{2g-2j+1} < 3$ is equivalent to $4g-2j+5 < 6g-6j+3$, which can be rewritten as $4j < 2g-2$, or $j < \frac{g-1}{2}$. Thus we have a collapse of $\tau_5^{(-1)}$ that introduces a non-lattice vertex point if and only if $j < \frac{g-1}{2}$.

We conclude that $Q^{(-1)}$ is a lattice polygon if and only if $i \geq \frac{g}{2}+1$ and $j \geq \frac{g-1}{2}$

□

Lemma 3.4.4. *If Q is of Type 3, then the relaxed polygon $Q^{(-1)}$ is a lattice polygon if and only if $i \geq g/2$ and $j \geq g/2$.*

Proof. Label the faces of Q cyclically as $\tau_1, \ldots, \tau_6$, where τ_1 is the face containing the lattice points $(k, 2)$ and $(0, 1)$ (with the understanding that some faces might not appear if one or more of i, j and k are equal to 0). If the faces $\tau_1^{(-1)}, \ldots, \tau_6^{(-1)}$ are all present in the polygon $P^{(-1)}$, then they intersect at lattice points by the arguments from the previous proof. Thus we need only be concerned with the following cases: where $\tau_3^{(-1)}$ collapses due to $\tau_2^{(-1)}$ and

$\tau_4^{(-1)}$ intersecting at a point (x, y) with $0 > y > -1$; and where $\tau_6^{(-1)}$ collapses due to $\tau_5^{(-1)}$ and $\tau_1^{(-1)}$ intersecting at a point (x, y) with $2 < y < 3$.

First we consider $\tau_2^{(-1)}$ and $\tau_4^{(-1)}$. We have that $\tau_2^{(-1)}$ lies on the line defined by $x = -1$, and that $\tau_4^{(-1)}$ lies on the line defined by $x - (g + 1 - i)y = i + 1$. These lines intersect at $(-1, -\frac{i+2}{g+1-i})$. The y-coordinate is strictly greater than -1 when $\frac{i+2}{g+1-i} < 1$, i.e. when $i + 1 < g + 1 - i$, which can be rewritten as $i < \frac{g}{2}$. Thus we lose $\tau_3^{(-1)}$ to a non-lattice vertex precisely when $i < \frac{g}{2}$.

Now we consider $\tau_5^{(-1)}$ and $\tau_1^{(-1)}$. We have that $\tau_1^{(-1)}$ lies on the line $x - ky = -k + 1$, unless $k = 0$ in which case it lies on the line $x = -1$; and that $\tau_5^{(-1)}$ lies on the line $x + (g + 1 - k - j)y = 2g + 2 - k - j$. In the event that $k \neq 0$, these intersect at $\left(\frac{gk+g-j+1}{g-j+1}, \frac{2g-j+1}{g-j+1}\right)$, which has y-coordinate strictly smaller than 3 when $\frac{2g-j+1}{g-j+1} < 3$, or equivalently if $2g - j + 1 < 3g - 3j + 1$, or equivalently if $j < \frac{g}{2}$. For the $k = 0$ case, the intersection point becomes $\left(-1, \frac{2g-j+3}{g-j+1}\right)$, which has y-coordinate strictly smaller than 3 when $\frac{2g-j+3}{g-j+1} < 3$, or equivalently when $2g - j + 3 < 3g - 3j - 3k + 3$, or equivalently when $j < \frac{g}{2}$. Thus we have a non-lattice vertex due to $\tau_5^{(-1)}$ collapsing precisely when $j < \frac{g}{2}$.

We conclude that $Q^{(-1)}$ is a lattice polygon if and only if $i \geq g/2$ and $j \geq g/2$. □

Combining Lemmas 3.4.2, 3.4.3, and 3.4.4 and the preceding discussion, we have the following classification of maximal polygons with lattice width 4.

Proposition 3.4.5. *Let P be a maximal polygon of lattice width 4. Then up to lattice equivalence, P is either T_4; one of the 14 polygons in Figure 3.9; or $Q^{(-1)}$, where Q is a hyperelliptic polygon satisfying the conditions of Lemma 3.4.2, 3.4.3, or 3.4.4.*

The most important consequence of Propositions 3.4.1 and 3.4.5 is that we can determine which panoptigons of lattice width 1 or lattice width 2 are interior polygons of some lattice polygon. We summarize this with the following result.

Corollary 3.4.6. *Let Q be a panoptigon with $\mathrm{lw}(Q) \leq 2$ such that $Q^{(-1)}$ is lattice polygon. Then $|Q \cap \mathbb{Z}^2| \leq 11$.*

Proof. If $\mathrm{lw}(Q) = 1$ with $Q^{(-1)}$ a lattice polygon, then Q must be the trapezoid $T_{a,b}$ with $0 \leq a \leq b$, $b \geq 1$, and $a \geq \frac{b}{2} - 1$ by Proposition 3.4.1. In order for $T_{a,b}$ to be a panoptigon, we need $a \leq 2$ by Lemma 3.3.1, so $2 \geq \frac{b}{2} - 1$, implying $b \leq 6$. It follows that $|Q \cap \mathbb{Z}^2| = a + b + 2 \leq 2 + 6 + 2 = 10$.

Now assume $\mathrm{lw}(Q) = 2$ with $Q^{(-1)}$ a lattice polygon. If Q has genus 0 then it is T_2, and has 6 lattice points. If Q has genus 1 then it is one of the polygons in Figure 3.3, and so has at most 9 lattice points. Outside of these situations, we know that Q is a hyperelliptic

panoptigon of genus $g \geq 2$ as characterized in Lemma 3.3.3. We deal with two cases: where Q has a panoptigon point at height 1, and where it does not.

In the first case, we either have $g = 2$ with Q of Type 1 or Type 2, or $g = 3$ with Q of Type 1. A hyperelliptic polygon of Type 1 has $(i+1)+(1+2g-i) = 2g+2$ boundary points. A hyperelliptic polygon of Type 2 has $i + j + 3$ boundary points. If Q is of Type 1, then it has in total $3g + 2 \leq 11$ lattice points. If Q is of Type 2, then $i + j \leq 2g + 1 = 2 \cdot 2 + 1 = 5$, implying that Q has a total of $i + j + 3 + g \leq 5 + 3 + 2 = 10$ lattice points.

In the second case, we know that Q must have at most 3 points at height 0 or 2, and exactly 1 point at the other height. First we claim that Q cannot be of Type 1: there are $2g + 2 \geq 6$ boundary points, all at height 0 or 2, and Q can have at most 4 points total at those heights. For Types 2 and 3, we know by Lemmas 3.4.3 and 3.4.4 that either $i \geq \frac{g}{2} + 1$ and $j \geq \frac{g-1}{2}$, or $i \geq \frac{g}{2}$ and $j \geq \frac{g}{2}$. At least one of i and j must equal 0 to allow for a single point at height 0 or height 2, so these inequalities are impossible for $g \geq 2$. Thus Q cannot have Type 2 or Type 3 either, and this case never occurs.

We conclude that if Q is a panoptigon of lattice width 1 or 2 such that $Q^{(-1)}$ is a lattice polygon, then $|Q \cap \mathbb{Z}^2| \leq 11$.

□

3.5 Big face graphs are not tropically planar

Let G be a planar graph. Recall that we say that G is a *big face graph* if for any planar embedding of G, there exists a bounded face that shares an edge with every other bounded face. Our main examples of big face graphs will come from the following construction. First we recall the construction of a *chain* of genus g from [10, §6]. Start with g cycles in a row, connected at $g - 1$ vertices which are 4-valent. We will resolve each of these 4-valent vertices to result in two 3-valent vertices in one of two ways. Let v be a vertex, incident to the edges e_1, e_2, f_1, f_2 where e_1 and e_2 are part of one cycle and f_1 and f_2 are part of another. We will remove v and replace it with two connected vertices v_1 and v_2, and we will either connect v_1 to e_1 and f_1 and v_2 to e_2 and f_2; or we will connect v_1 to e_1 and e_2 and v_2 to f_1 and f_2. Any graph obtained from making such a choice at each vertex is then called a chain. Figure 3.10 illustrates, for $g = 3$, the starting 4-regular graph; the two ways to resolve a 4-valent vertex; and the resulting chains of genus 3. We remark that although there are $2 \times 2 = 4$ ways to choose the vertex resolutions, two of them yield isomorphic graphs, giving us 3 chains of genus 3 up to isomorphism. Note that for every genus, there is exactly one chain that is bridge-less, i.e. 2-edge-connected.

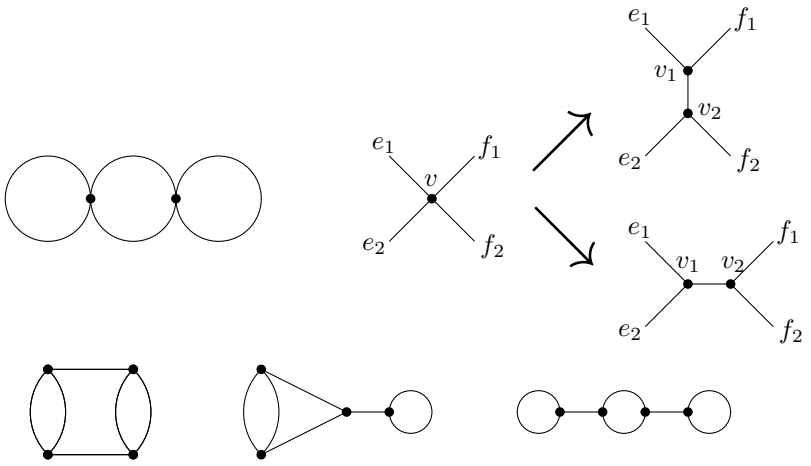

Figure 3.10: The starting 4-regular graph in the chain construction; the two choices for resolving a 4-valent vertex; and the three chains of genus 3, up to isomorphism

Given a chain of genus g, we construct a *looped chain* of genus $g+1$ by adding an edge from the first cycle to the last one. The looped chains of genus 4 corresponding to the chains of genus 3 are illustrated in Figure 3.11. For larger genus, we remark that two non-isomorphic chains can give rise to isomorphic looped chains.

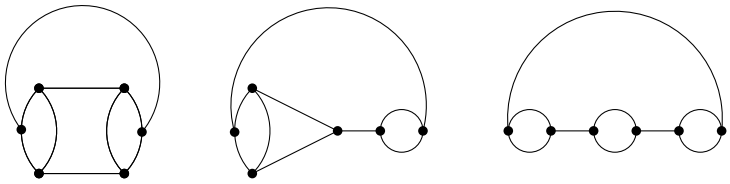

Figure 3.11: The looped chains of genus 4

In order to argue that any looped chain is a big face graph, we recall the following useful result. By a special case of Whitney's 2-switching theorem [39, Theorem 2.6.8], if G is a 2-connected graph, then any other planar embedding can be reached, up to weak equivalence[3], from the standard embedding by a sequence of *flippings*. A flipping of a planar embedding finds a cycle C with only two vertices v and w incident to edges exterior to C, and then reverses the orientation of C and all vertices and edges interior to C to obtain a new embedding. This process is illustrated in Figure 3.12, where C is the highlighted cycle $v-a-b-w-d-v$.

Lemma 3.5.1. *Any looped chain is a big face graph.*

[3]Weak equivalence means two graph embeddings have the same facial structure, although possibly with different unbounded faces.

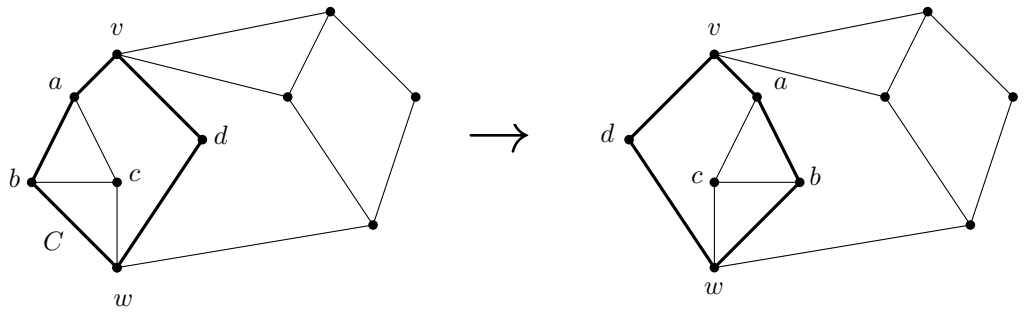

Figure 3.12: Two embeddings of a planar graph related by a flipping

Proof. In the standard embedding of a looped chain as in Figure 3.11, there are (at least) two faces that share an edge with all other faces: one bounded and one unbounded. Since any looped chain is 2-connected, any other embedding can be reached, up to weak equivalence, by a sequence of flippings. It thus suffices to show that the standard embedding of a looped chain is invariant under flipping.

Consider the standard embedding of a looped chain G, and assume that C is a cycle in G that has exactly two vertices v and w incident to edges exterior to C. Let $\overline{C}$ denote the set of all vertices in or interior to C. Since G is trivalent and C is 2-regular, we know that v and w are each incident to exactly one edge, say e for v and f for w, that is exterior to C. We now deal with two possibilities: that $\overline{C} = V(G)$, and that $\overline{C} \subsetneq V(G)$.

If $\overline{C} = V(G)$, then $e = f$, and the only possibility is that v and w are the vertices added to a chain H to build the looped chain G; that H is the bridge-less chain; and that C is the outside boundary of H in its standard embedding. Flipping with respect to C does not change the embedding of this graph.

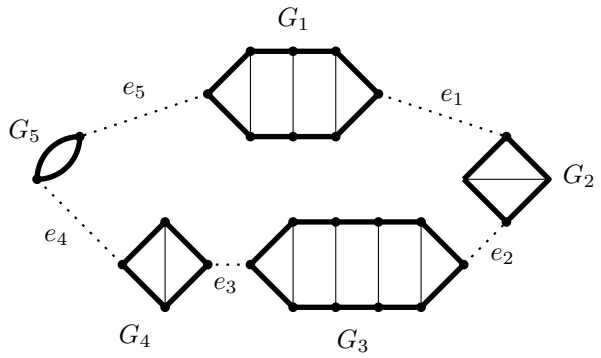

Figure 3.13: The structure of a looped chain, where the bridge-less chains G_i have solid edges and the edges e_i are dotted; the boundaries of the G_i are bold, and are the only possible choices of C for a flipping

If $\overline{C} \subsetneq V(G)$, then $\{e, f\}$ forms a 2-edge-cut for G, separating it into $\overline{C}$ and $\overline{C}^C$. Consider the structure of G: it is a collection of 2-edge-connected graphs $G_1, \ldots, G_k$, namely a collection

of bridge-less chains, connected in a loop by edges $e_1, \ldots, e_k$, where e_i connects G_i and G_{i+1}, working modulo k; see Figure 3.13 for this labelling scheme. We claim that $e, f \in \{e_1, \ldots, e_k\}$. If not, then without loss of generality e is in some bridge-less chain G_i. If $f \in E(G_j)$ for $j \neq i$, then the graph remains connected; the same is true if $f \in \{e_1, \ldots, e_k\}$. So we would need f to also be in G_i. By the structure of the looped chain, we would need the removal of e and f to disconnect G_i into multiple components, at least one of which is not incident to e_i or e_{i+1}; however, this is impossible based on the structure of a bridge-less chain. It follows that e and f must be among $e_1, \ldots, e_k$. The only way to choose a pair $\{e, f\}$ from among $e_1, \ldots, e_k$ so that they are the only exterior edges incident to the boundary of a cycle C is if they are incident to the same bridge-less chain G_i; that is, if up to relabelling we have $e = e_i$ and $f = e_{i+1}$ for some i. Thus C and its interior constitutes one of the bridge-less chains G_i. But flipping a bridge-less chain does not change the embedding of our (unlabelled) graph, completing the proof. □

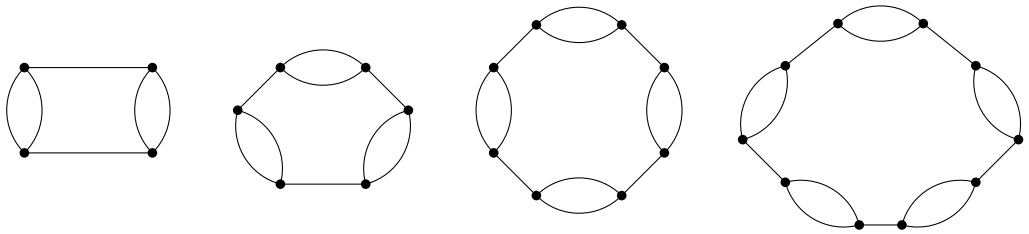

Figure 3.14: The loop of loops L_g for $3 \leq g \leq 6$

We summarize the connection between big face graphs and panoptigons in the following lemma.

Lemma 3.5.2. *Suppose that G is a tropically planar big face graph arising from a polygon P. Then P_{int} is a panoptigon.*

This is not an if-and-only-if statement, since not all triangulations of P connect a point of P_{int} to all other points of P_{int}; for instance, the chain of genus 3 with two bridges is not a big face graph, but by [10, §5] it arises from T_4 whose interior polygon is a panoptigon.

Proof. Let Δ be a regular unimodular triangulation of P such that G is the skeleton of the dual graph of Δ. The embedding of G arising from this construction must have a bounded face F bordering all other faces. By duality, we know that F corresponds to an interior lattice point p of P. Since F shares an edge with all other bounded faces, dually p is connected to each other interior point of P by a primitive edge in Δ. Thus P_{int} is a panoptigon, with p a panoptigon point for it. □

One common example of a looped chain of genus g is the *loop of loops* L_g, obtained by connecting $g-1$ bi-edges in a loop. This is illustrated in Figure 3.14 for g from 3 to 6. For low genus, the loop of loops is tropically planar. Figure 3.15 illustrates polygons of genus g for $3 \leq g \leq 10$ along with collections of edges emanating from an interior point; when completed to a regular unimodular triangulation[4], they will yield L_g as the dual tropical skeleton. Thus L_g is tropically planar for $g \leq 10$. Another example of a tropically planar looped chain, this one of genus 11, is pictured in Figure 3.16, along with a regular unimodular triangulation of a polygon giving rise to it. Since the theta graph of genus 2 is also tropically planar [10, Example 2.5] and is a big face graph, there exists at least one tropically planar big face graph of genus g for $2 \leq g \leq 11$. We are now ready to prove that this does not hold for $g \geq 14$.

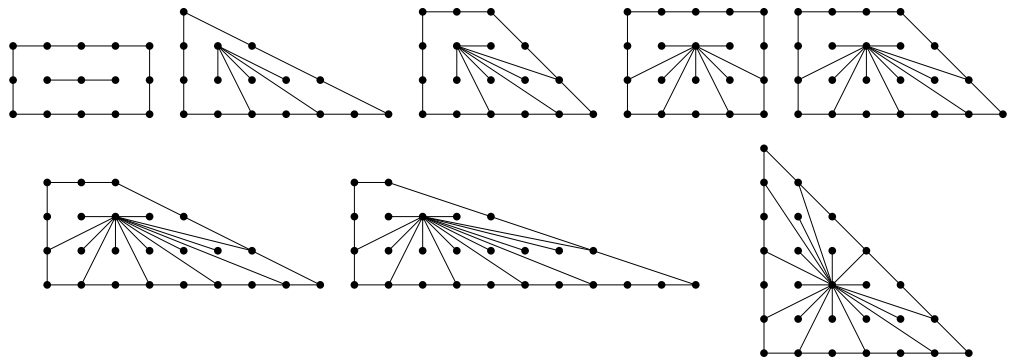

Figure 3.15: Starts of triangulations that will yield the loop of loops as the dual tropical skeleton

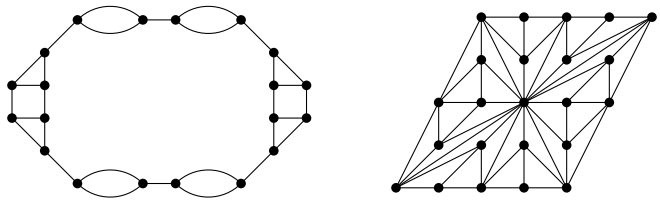

Figure 3.16: A tropically planar big face graph of genus 11, with a regular unimodular triangulation giving rise to it

Proof of Theorem 3.1.3. Let G be a tropically planar big face graph, and let P be a lattice polygon giving rise to it. By Lemma 3.5.2, P_{int} is a panoptigon. If $\text{lw}(P_{\text{int}}) \leq 2$, then $g = |P_{\text{int}} \cap \mathbb{Z}^2| \leq 11$ by Corollary 3.4.6. If $\text{lw}(P_{\text{int}}) \geq 3$, then $g = |P_{\text{int}} \cap \mathbb{Z}^2| \leq 13$ by Theorem 3.1.2. Either way, we may conclude that the genus of G is at most 13. □

[4]One way to see that this can be accomplished is to use a placing triangulation [20, §3.2.1], where the highlighted panoptigon point is placed first and the other lattice points are placed in any order.

It follows, for instance, that no looped chain of genus $g \geq 14$ is tropically planar.

If we are willing to rely on our computational enumeration of all non-hyperelliptic panoptigons, we can push this further: there does not exist a tropically planar big face graph for $g \geq 12$, and this bound is sharp. We have already seen in Figure 3.16 that there exists a tropically planar big face graph of genus 11. To see that none have higher genus, first note that if P_{int} is a panoptigon with 12 or 13 lattice points, then P_{int} must be non-hyperelliptic by Corollary 3.4.6. Thus P_{int} must be one of the 15 non-hyperelliptic panoptigons with 12 lattice points, or one of the 8 non-hyperelliptic panoptigons with 13 lattice points, as presented in section 3.6. However, for each of these polygons Q, we have verified computationally that $Q^{(-1)}$ is not a lattice polygon; see Figure 3.20. Thus no lattice polygon of genus $g \geq 12$ has an interior polygon that is also a panoptigon. It follows from Lemma 3.5.2 that no big face graph of genus larger than 11 is tropically planar.

We close with several possible directions for future research.

- For any lattice point p, let $\text{vis}(p)$ denote the set of all lattice points visible to p (including p itself). Given a convex lattice polygon P, define its *visibility number* to be the minimum number of lattice points in P needed so that we can see every lattice point from one of them:

$$V(P) = \min\left\{ |S| \,:\, S \subset P \cap \mathbb{Z}^2 \text{ and } P \cap \mathbb{Z}^2 \subset \bigcup_{p \in S} \text{vis}(p) \right\}.$$

  Thus P is a panoptigon if and only if $V(P) = 1$. Classifying polygons of fixed visibility number $V(P)$, or finding relationships between $V(P)$ and such properties as genus and lattice width, could be interesting in its own right, and could provide new criteria for determining whether graphs are tropically planar; for instance, the prism graph $P_n = K_2 \times C_n$ can only arise from a polygon P with $V(P) \leq 2$. This question is in some sense a lattice point version of the art gallery problem.

- We can generalize from two-dimensional panoptigons to n-dimensional *panoptitopes*, which we define to be convex lattice polytopes containing a lattice point p from which all the polytope's other lattice points are visible. A few of our results generalize immediately; for instance, the proof of Lemma 3.3.2 works in n-dimensions, so any polytope with exactly one interior lattice point is a panoptitope. A complete classification of n-dimensional panoptitopes for $n \geq 3$ will be more difficult than it was in two-dimensions, especially since it is no longer the case that there are finitely many polytopes with a fixed number of lattice points. Results about panoptitopes would also have applications in tropical geometry; for instance, an understanding of three-dimensional panoptitopes would have implications for the structure of tropical surfaces in $\mathbb{R}^3$.

- To any lattice polygon we can associate a toric surface [18]. An interesting question for future research would be to investigate those toric surfaces that are associated to panoptigons, or more generally toric varieties associated to panoptitopes.

3.6 Panoptigon computations

From the proof of Theorem 3.1.2, we know that any panoptigon of lattice width and lattice diameter both at least 3 must be equivalent to a polygon consisting of some subset of the thirty lattice points pictured in Figure 3.7, where the points $(0,0)$, $(-1,-1)$, $(0,-1)$, $(1,-1)$, and $(2,-1)$ must be included. Using `polymake` [23], we ran through all possible convex polygons consisting only of these 30 points. Ruling out those without interior lattice points or with all lattice points collinear, we found a total of 215 distinct polygons, some of which were equivalent under a unimodular transformation. These 215 polygons are available as the collection "Non-hyperelliptic Panoptigons" in polyDB [42] at `https://db.polymake.org`. Eliminating redundant copies, we find that there are a total of 69 non-hyperelliptic panoptigons of lattice width and lattice diameter both at least 3, up to lattice equivalence. We list all nonhyperelliptic panoptigons with lattice diameter at least 3 in Figure 3.19. The panoptigons with 12 or 13 lattice points appear in Figure 3.20, along with their relaxed polygons. Each relaxed polygon has at least one non-lattice vertex, marked by a square. The computation of these relaxed polygons verifies that no non-hyperelliptic panoptigon with 12 or 13 lattice points is the interior polygon of a lattice polygon.

To complete an enumeration of all non-hyperelliptic panoptigons of genus $g \geq 3$, it remains to find those panoptigons P that have lattice diameter smaller than 3. We accomplish this with the following proposition.

Proposition 3.6.1. *Let P be a non-hyperelliptic panoptigon of lattice diameter at most 2. Then up to lattice equivalence P is either the triangle conv$((0,1),(0,3),(4,0))$, the quadrilateral conv$((1,0),(2,0),(3,1),(0,3))$, or the quadrilateral conv$((0,1),(0,2),(2,3),(3,0))$.*

These three polygons are illustrated in Figure 3.17.

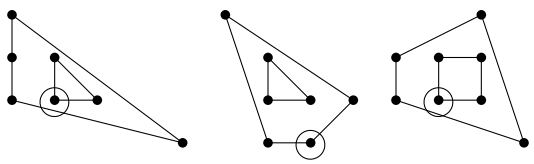

Figure 3.17: The three non-hyperelliptic panoptigons from Proposition 3.6.1

Proof. Since P is non-hyperelliptic, we know that $\mathrm{lw}(P) \geq 3$. Note that we cannot have $\ell(P) = 1$, since then we would have $\mathrm{lw}(P) \leq \lfloor \frac{4}{3}\ell(P) \rfloor + 1 = 2$. Thus $\ell(P) = 2$. It follows that $\mathrm{lw}(P) \leq \lfloor \frac{4}{3}\ell(P) \rfloor + 1 = 2+1 = 3$, so $\mathrm{lw}(P) = 3$. We know P is not T_3 since T_3 is hyperelliptic, so we know that the interior polygon P_{int} must have lattice width 1. It follows that P_{int} must be a trapezoid of height 1, and since $\ell(P) = 2$ that trapezoid must have at most 3 lattice points at each height; thus $P_{\mathrm{int}} = T_{a,b}$ where $0 \leq a \leq b \leq 2$. It follows that P must be contained in one of the polygons pictured in Figure 3.18; these are the maximal polygons associated to the candidates for P_{int}. In order to refer to the lattice points of these polygons with coordinates, we will assume that each is positioned to have the lower left corner at the origin $(0, 0)$.

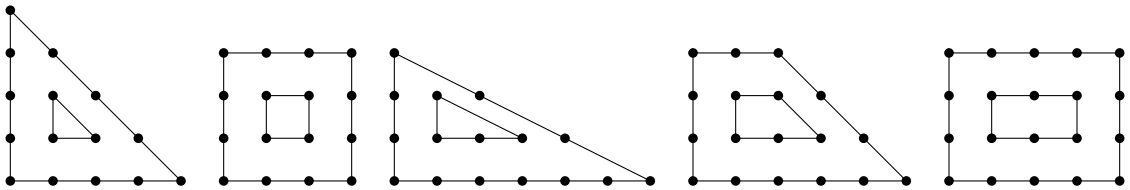

Figure 3.18: Possible interior polygons for P_{int}, and polygons that must contain P

We claim that P cannot have $T_{0,2}$ $T_{1,2}$, or $T_{2,2}$ as its interior polygon. In each of those cases, note that P automatically has 3 interior points at height 1; since $\ell(P) = 2$, there can be no boundary lattice points at height 1. In order for boundary lattice points at height 0 to connect to boundary lattice points at height greater than 1, the points $(1, 0)$ and $(4, 0)$ must be included; but then there are 4 collinear lattice points at height 0, contradicting $\ell(P) = 2$.

Now suppose $P_{\mathrm{int}} = T_{1,1}$. Note that no boundary point of the 3×3 square can see all interior points, so any panoptigon point q must be an interior point. Without loss of generality, assume that it is $q = (1, 1)$, meaning that the points $(1, 3)$, $(3, 1)$, and $(3, 3)$ cannot be included in P. Among the two points $(2, 3)$ and $(3, 2)$, at least one must be included to allow for the desired interior polygon. By symmetry we may assume that $(2, 3)$ is included. There cannot be any other points at height 3, so $(2, 3)$ must be a vertex of P and connect to a boundary point of the form $(0, b)$; the only possible such point is $(0, 2)$. It then follows that $(3, 2)$ cannot be included, since this would yield 4 collinear points at height 2. Thus P has an edge connecting $(2, 3)$ to $(3, 0)$. The point $(2, 0)$ cannot appear in P since there are already three points with x-coordinate equal to 2, so $(3, 0)$ must be connected to $(0, 1)$. At this point, we know that $P = \mathrm{conv}((0, 1), (0, 2), (2, 3), (3, 0))$. This is indeed a panoptigon of lattice width 3 and lattice diameter 2.

Finally we will deal with the case where $P_{\mathrm{int}} = T_{0,1}$. We deal with several possibilities for the (not necessarily unique) panoptigon point q of P.

- Suppose q is an interior lattice point of P. By symmetry we may assume $q = (1, 1)$, so the lattice points $(3, 1)$ and $(1, 3)$ cannot be included. Since there must at least one lattice point at height 3 or above, either $(0, 3)$ or $(0, 4)$ (or both) must be included. If it is only $(0, 4)$ and not $(0, 3)$, then the points $(1, 0)$ and $(3, 0)$ must be included, yielding the polygon $\text{conv}((1, 0), (3, 0), (0, 4))$. Otherwise, $(0, 3)$ is in P. Since $(0, 3)$, $(1, 2)$, and $(2, 1)$ are all lattice points of P, the point $(3, 0)$ cannot be included. Now, at least one lattice point from the diagonal edge must be included, namely $(4, 0)$, $(2, 2)$, or $(0, 4)$; in fact, it must be exactly one, since otherwise $(1, 3)$ or $(3, 1)$ would be introduced by convexity. If P contains $(0, 4)$ or $(2, 2)$ and no other points along that edge, then it must also contain $(3, 0)$, which we have already ruled out. Thus P contains $(4, 0)$, and as it does not contain $(3, 0)$ it must have an edge connecting $(4, 0)$ to $(0, 1)$. At this point there is a single possibility for P, namely $P = \text{conv}((0, 1), (0, 3), (4, 0))$. This polygon is equivalent to the previous one, so we need only include one. This panoptigon does indeed have lattice diameter 2.

- Now we deal with the case that the panoptigon point is a boundary point. Since the panoptigon point must see all three interior points, it must either be a vertex of T_4 or the midpoint of one of the edges. Up to symmetry, we may thus assume that q is either $(0, 0)$ or $(2, 0)$. If $q = (0, 0)$, then the point $(1, 3)$ must be included; otherwise we would need $(0, 3)$, which is not visible to $(0, 0)$. Similarly $(1, 3)$ is included, but then $(2, 2)$ is included by convexity, and this point is not visible to $(0, 0)$, a contradiction.

  If $q = (2, 0)$, then there are 1, 2, or 3 points at height 0. If there is only q, then the points $(0, 1)$ and $(3, 1)$ must be included, contradicting $\ell(P) = 2$. If there are 2 points, we will assume by symmetry that the two points are $(1, 0)$ and $(2, 0)$. The lattice point $(3, 1)$ must then be included and the point $(0, 1)$ must not be included; the only remaining point to include from the face on the line $x = 0$ is $(0, 3)$. No other lattice points can be included, so then $P = \text{conv}((1, 0), (2, 0), (3, 1), (0, 3))$. Finally, if there are 3 points at height 0 they must be $(1, 0)$, $(2, 0)$, and $(3, 0)$. But now neither $(0, 3)$ nor $(1, 3)$ may be included since $\ell(P) = 2$. Since $(0, 4)$ is not visible from q, there are no points in P with height greater than 2, a contradiction to $T_{0,1}$ being the interior polygon of P.

We conclude that the only non-hyperelliptic panoptigons P with $\ell(P) \leq 2$ are the three claimed.

□

Combined with our computation, this gives us the following count.

Corollary 3.6.2. *Up to lattice equivalence, there are* 72 *non-hyperelliptic panoptigons.*

The explicitness of our enumeration allows us to find the largest lattice width of any panoptigon: by Lemma 3.2.2, the lower right triangle in Figure 3.20 has lattice width 5, and all the other panoptigons have lattice width 4 or less.

Results of the presented work in this chapter have been published in - Ralph Morrison and Ayush Kumar Tewari. "Convex lattice polygons with all lattice points visible", Discrete Mathematics [41].

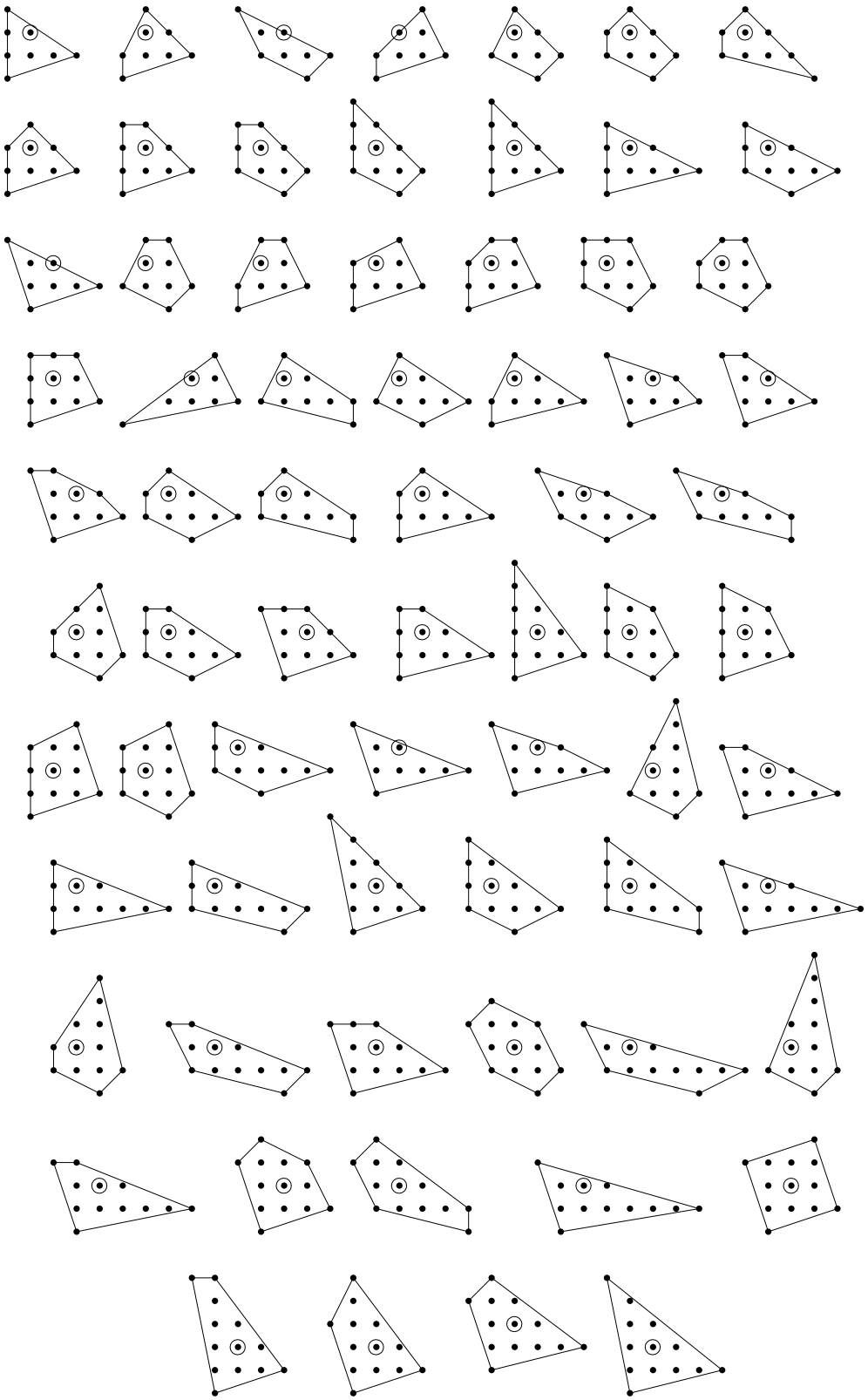

Figure 3.19: All nonhyperelliptic panoptigons with lattice diameter at least 3

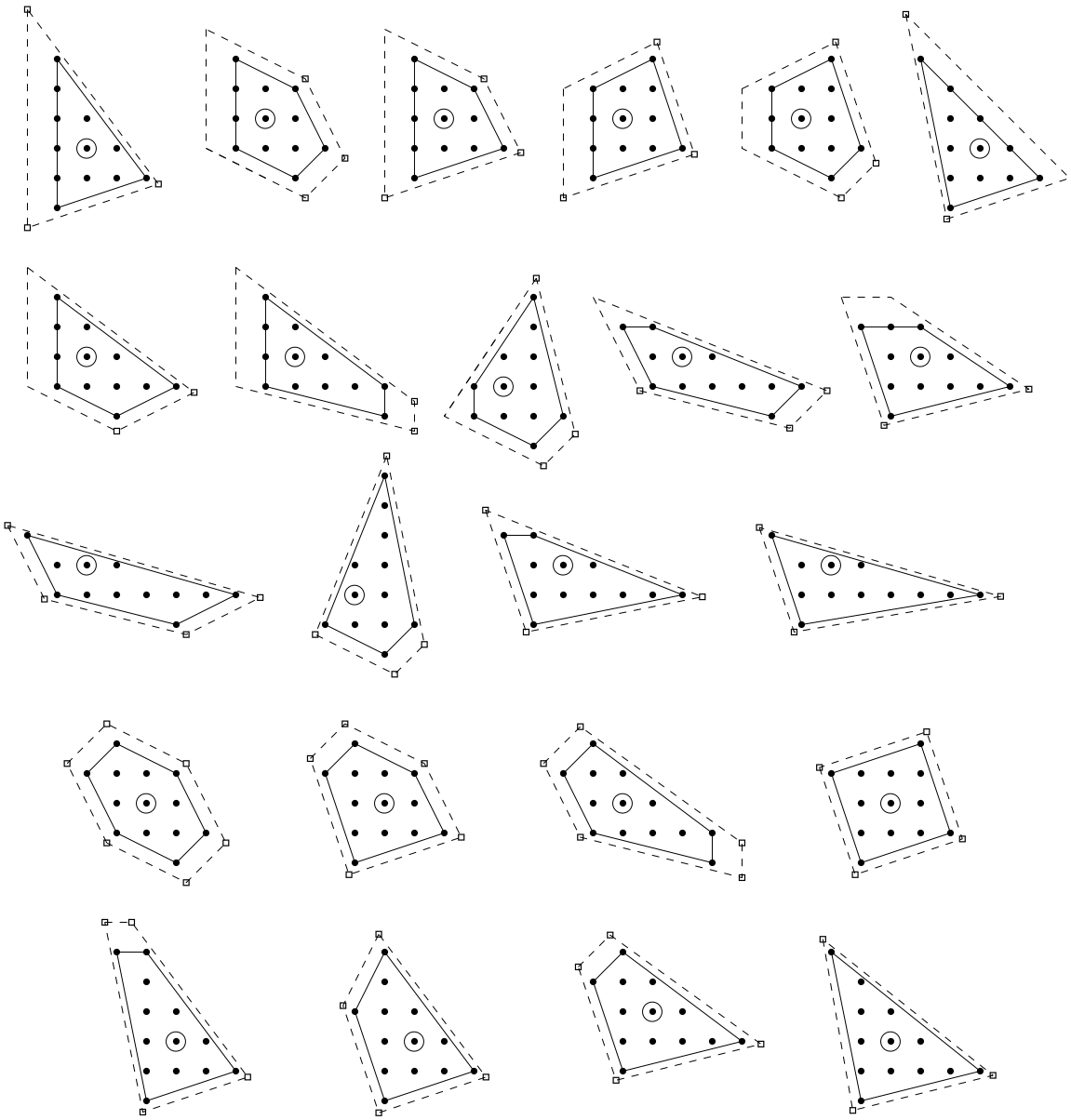

Figure 3.20: All non-hyperelliptic panoptigons with 12 or 13 lattice points, along with their relaxed polygons

Chapter 4

Point-line geometry in the tropical plane

4.1 Introduction

Point-line geometry has been studied for a long time, and it mainly deals with the question of *incidence*, i.e. when a point meets a line. There are many classical results established about the incidence of points and lines in projective and affine planes like the Sylvester-Gallai theorem, de-Bruijn Erdős theorem, Szemeredi-Trotter theorem, Beck's theorem etc. In recent times, there has been a lot of development in generalising these classical results, like [29] surveys the work done on generalizations of de-Bruijn Erdős theorem. In a recent study in [30], tropical lines present in a fixed plane are also studied.

Since tropical geometry provides a piecewise linear model of point line geometry, many incidence geometric results have also been proved in it. In [8] a tropical version of Sylvester-Gallai theorem and Motzkin-Rabin theorem is established along with the universality theorem. In [47] the term *geometric construction* is coined , in order to identify all the types of classical incidence geometric results which can have a tropical analogue. Even in [45] and [46] a tropical version of Pappus theorem is discussed along with classical point-line configurations. Another aspect is the relation to oriented matroids, and as mentioned in [8], it is elaborated in [2], in the context of hyperplane arrangements and how they correspond to tropical oriented matroids and how these matroids encode incidence information about point-line structures in the tropical plane. The fact that the tropical plane allows projective duality, facilitates much of the above mentioned results.

In this chapter, we start with some basic notions of point line geometry and specifically the point-line geometry in the tropical plane. Subsequently, using the results obtained in [8] and by introducing the notion of stable tropical lines we state a tropical counterpart to de-Bruijn-Erdős theorem. We also establish the equivalence between a much general notion

of stability for curves, in [47], and the stable lines that we define in our work. We find that tropicalization of generic lifts of points determines the stable tropical line passing through them. We establish the duality between stable lines and stable intersections and provide a full classification of the faces that they correspond to in the dual Newton subdivision. With this setup, we prove the tropical analogue of de-Bruijn-Erdős theorem,

Theorem 4.1.1 (Tropical de-Bruijn-Erdős Theorem)**.** *Let $\mathcal{S}$ denote a set of points in the tropical plane. Let v ($v \geq 4$) denote the number of points in $\mathcal{S}$, and let b denote the number of stable tropical lines determined by these points. Then,*

1. $b \geq v - 3$
2. *if $b = v - 3$, then $\mathcal{S}$ forms a* tropical near-pencil.

The definitions and the results required to state and prove Theorem 4.1.1 are elaborated in the latter parts of this chapter.

4.2 Classical incidence geometry

In classical incidence geometry a *linear space* is defined in the following manner [22],

Definition 4.2.1. A *finite linear space* is a pair $(X, \mathcal{B})$, where X is a finite set and $\mathcal{B}$ is a set of proper subsets of X, such that

1. every unordered pair of elements of X occur in a unique $B \in \mathcal{B}$.
2. Every $B \in \mathcal{B}$ has cardinality at least two.

Essentially, a linear space is a point-line incidence structure, in which any two points lie on a unique line.

Example 4.2.2. Consider $L = (X, \mathcal{B})$, where X is the set of points in the Euclidean plane and $\mathcal{B}$ is the set of lines determined by X .

Another important definition about lines is,

Definition 4.2.3. A line which passes through exactly two points is called an *ordinary* line.

Erdős and de-Bruijn, came up with a theorem about point-line arrangements in a linear space [19], which is established in [7] and stated in Theorem 4.2.4.

Theorem 4.2.4 (de-Bruijn-Erdős Theorem)**.** *Let $S = (X, \mathcal{B})$ be a linear space. Let v denote the number of points in $S(= |X|)$, and b denote the number of lines determined by these points $(= |\mathcal{B}|$, $b > 1)$. Then*

1. *$b \geq v$,*
2. *if $b = v$, any two lines have a point in common. In case (2), either one line has $v - 1$ points and all others have two points, or every line has $k + 1$ points and every point is on $k + 1$ lines, $k \geq 2$.*

For a more general treatment and recent developments, one can read [29], where enumerative results like the above have been discussed in a more general setting of geometric lattices.

Theorem 4.2.4 clearly is a very general statement, and in the case for points and lines in the Euclidean plane, the bound on the number of lines is attained when points are in a near -pencil configuration and the proof follows by induction and invoking Theorem 4.2.5.

Theorem 4.2.5 (Sylvester-Gallai Theorem)**.** *Given a finite collection of points in the Euclidean plane, such that not all of them lie on one line, then there exists a line which passes through exactly two of the points.*

4.3 A brief introduction to tropical geometry

Tropical geometry can be defined as the study of geometry over the tropical semiring $\mathbb{T} = (\mathbb{R} \cup \{-\infty\}, \max, +)$. A **tropical polynomial** $p(x_1, \ldots, x_n)$ is defined as a linear combination of tropical monomials with operations as the tropical addition and tropical multiplication.

$$p(x_1, \ldots, x_n) = a \odot {x_1}^{i_1} {x_2}^{i_2} \ldots {x_n}^{i_n} \oplus b \odot {x_1}^{j_1} {x_2}^{j_2} \ldots {x_n}^{j_n} \oplus \ldots$$

With the above definitions, we see that a tropical polynomial is a function $p : \mathbb{R}^n \longrightarrow \mathbb{R}$ given by maximum of a finite set of linear functions.

Definition 4.3.1. The **hypersurface** $V(p)$ of p is is the set of all points $w \in \mathbb{R}^n$ at which the maximum is attained at least twice. Equivalently, a point $w \in \mathbb{R}^n$ lies in $V(p)$ if and only if p is not linear at w.

The tropical polynomial defining a tropical line is given as

$$p(x, y) = a \odot x \oplus b \odot y \oplus c, \text{ where } a, b, c \in \mathbb{R},$$

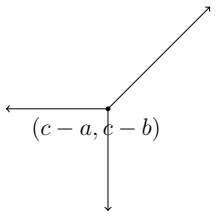

Figure 4.1: A tropical line

and the corresponding hypersurface is the corner locus defined by the above polynomial, which is a collection of three half rays emanating from the point $(c-a, c-b)$ in the primitive directions of $(-1, 0), (0, -1)$ and $(1, 1)$ (Refer [38]).

Now we look at the intersections of lines in the tropical plane. As is evident from the setup, tropical lines can intersect over a half ray. However, two tropical lines have a unique *stable intersection*, where a stable intersection is the limit of points of intersection of nearby lines which have a unique point of intersection, within a suitable ϵ, with the limit being taken as ϵ tends to 0 [38]. We refer the reader to [38] for further details about stable intersections in full generality. We also define the two types of stable intersections which we encounter in the case of tropical line arrangements,

Definition 4.3.2. A stable intersection in a tropical line arrangement is called *stable intersection of first kind* if no vertex of any line from the line arrangement is present at the point of intersection.

Definition 4.3.3. A stable intersection in a tropical line arrangement is called *stable intersection of second kind* if the vertex of a line from the line arrangement is present at the point of intersection.

An important observation is the *projective duality* which exists in the tropical plane [8], which means that given a set of points $\mathcal{P}$, there exists a incidence preserving map ϕ which maps $\mathcal{P}$ to its dual set of tropical lines $\mathcal{L}$, where for each point $P \in \mathcal{P}$, $\phi(P) = l$ with $-P$ as the vertex of the line $l \in \mathcal{L}$.

The *support* of a tropical polynomial is the collection of the exponents of the monomials which have a finite coefficient. The convex hull of the exponents in the support of a tropical polynomial defines a *Newton polytope*. We recall the definition of regular subdivisions from Chapter 1 . There exists a duality between a tropical curve T, defined by a tropical polynomial p, and the subdivision of the Newton polygon corresponding to p, induced by the coefficients of the tropical polynomial p. For further details about the description of this duality, the reader can refer to [38, Chapter 3] and [11, Proposition 2.5].

For a comprehensive study in a general setting, we analyze the underlying field K. A *valuation* on K is a map $val : K \to \mathbb{R} \cup \{\infty\}$ such that it follows the following three axioms [38],

1. $val(a) = \infty$ if and only if $a = 0$;
2. $val(ab) = val(a) + val(b)$;
3. $val(a + b) \geq min\{val(a), val(b)\}$ for all $a, b \in$ K.

An important example of a field with a non-trivial valuation is the field of *Puiseux series* over a arbitrary field k, represented as $K = k\{\{t\}\}$. The elements in this field are formal power series

$$k(t) = k_1 t^{a_1} + k_2 t^{a_2} + k_3 t^{a_3} \ldots,$$

where each $k_i \in k$, $\forall\, i$ and $a_1 < a_2 < a_3 < ....$ are rational numbers with a common denominator. This field has a natural valuation $val : k\{\{t\}\} \to \mathbb{R}$ given by taking a nonzero element $k(t) \in k\{\{t\}\}^*$, (where $k\{\{t\}\}^*$ represents the non zero element in the field $k\{\{t\}\}$) and mapping it to the lowest exponent a_1 in the series expansion of $k(t)$ [38].

It is an important observation that the valuation on the field of Puiseux series mimics the operations of a tropical semiring in essence and for further discussions one can think of the underlying field for the computations to be a Puiseux series with non-trivial valuation. So points which are considered in the plane, would have lifts residing in corresponding field of Puiseux series and the map which maps these lifts back to the points is the *tropicalization* map. For a polynomial $f = \sum_{u \in \mathbb{N}^{n+1}} c_u x^u$, where the coefficients are from the field with a non-trivial valuation, the tropicalization of f can be defined as [38],

$$\text{trop}(f)(w) = \max\{-val(c_u) + w \cdot u : u \in \mathbb{N}^{n+1} \text{ and } c_u \neq 0\}$$

We refer the reader to [38] for further details about this map.

A *tropical line arrangement* is a finite collection of distinct tropical lines in $\mathbb{R}^2$.

Definition 4.3.4. A tropical line arrangement $\mathcal{L}$ is said to be a *tropical near-pencil arrangement* if in the dual Newton subdivision, for all triangular faces present in the subdivision; at least one of the edges of the triangular face lies on the boundary of the Newton polygon.

Definition 4.3.5. A set of points $\mathcal{N}$ in the tropical plane, is said to form a *tropical near-pencil* if the dual tropical line arrangement is a tropical near pencil arrangement.

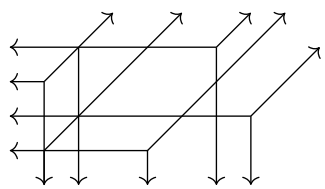

(a) A tropical near pencil arrangement

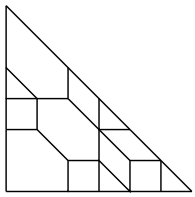

(b) The corresponding dual subdivision

Figure 4.2: An example of a tropical near pencil arrangement

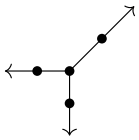

(a) Point set with stable tropical line

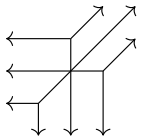

(b) Dual tropical near pencil line arrangement

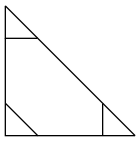

(c) Dual subdivision to the line arrangement

Figure 4.3: An example of a tropical near pencil

For a tropical line arrangement with lines $l_1, \ldots, l_n$ with corresponding tropical polynomials being $f_1, \ldots, f_n$ the tropical line arrangement, as a union of tropical hypersurfaces, is defined by the polynomial,

$$f = f_1 \cdot f_2 \ldots \cdot f_n$$

The dual Newton subdivision corresponding to the tropical line arrangement is the Newton subdivision dual to the tropical hypersurface defined by the tropical polynomial f (cf. [31]). We realize that stable intersections of first kind correspond to parallelograms and hexagons in the dual Newton subdivision and stable intersections of second kind correspond to irregular cells with four, five or six edges in the dual Newton subdivision.

For an elaborate description of dual Newton subdivisions, corresponding to tropical line arrangements, the reader is advised to refer to [8, Section 2.3].

4.4 Tropical incidence geometry

The behaviour of point-line structures in the tropical plane is distinct from the Euclidean case, specifically with the appearance of *coaxial* points.

Definition 4.4.1. Two points are said to be coaxial if they lie on the same axis of a tropical line containing them [8].

A recent result in [8] proves the tropical version of the Sylvester Gallai Theorem,

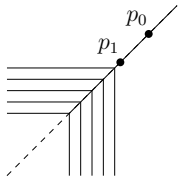

Figure 4.4: The infinite number of lines passing through the coaxial points p_0 and p_1

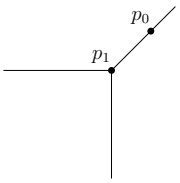

Figure 4.5: A stable tropical line (L, p_0, p_1)

Theorem 4.4.2 (Tropical Sylvester-Gallai)**.** *Any set of four or more points in the tropical plane determines at least one ordinary tropical line.*

An important observation is that if we consider a point set with no two points being coaxial, then there is a unique line passing through any two points , and therefore the point-line incidence structure in this case forms a *linear space*. Hence, we can invoke the classical de-Bruijn-Erdős theorem to conclude that such a set of n points determines at least n lines.

With the existence of a Tropical Sylvester-Gallai theorem, it is quite natural to explore the possibility of a tropical version of the de-Bruijn-Erdős theorem, i.e., a lower bound on the number of tropical lines determined by a n point set in the tropical plane. However, the number of lines determined by coaxial points are infinite in this setting. For the question of counting lines to be well posed, we would like to be in a scenario where a finite set of points determine a finite set of lines. Hence, rather than counting the number of lines as shown in Figure 4.4, we count a special class of lines, namely *stable tropical* lines.

Definition 4.4.3. Consider $(L, p_1, \ldots, p_n), (n \geq 2)$ where L is a tropical line with the points $(p_1, \ldots, p_n)$ on the line L, then $(L, p_1, \ldots, p_n)$, is called *stable* if

1. either L is the unique line passing through the p_i's, or
2. one of the points $p_1, \ldots, p_n$ is the vertex of L.

Now we show that this restriction on the counting of lines, turns out to be quite general as these stable lines turn out to be the tropicalization of the line passing through generic lifts of the points.

Figure 4.6: Newton polytope and tropicalization for $trop(P_1P_2)$

Proposition 4.4.4. *Given two coaxial points $p_1 = (-u, -v)$, $p_2 = (-u', -v') \in \mathbb{K}^2$, pick lifts $P_1 = (a_1t^u + \dots\ ,\ b_1t^v + \dots)$ and $P_2 = (a_2t^{u'} + \dots\ ,\ b_2t^v + \dots)$ over $\mathbb{K}\{\{t\}\}$. If $b_1 \neq b_2$, then $trop(P_1P_2)$ is the stable tropical line through p_1 and p_2.*

Proof. Since we assume that the two points, p_1 and p_2 are coaxial, we take $v = v'$ which would imply that the two points are coaxial in the $(-1, 0)$ primitive direction.

An equation of a line in the plane is $ax + by = c$. So if the lifts P_1 and P_2 lie on this line, then they satisfy this equation

$$a(a_1t^u + \dots) + b(b_1t^v + \dots) = c \tag{4.4.1}$$

$$a(a_2t^{u'} + \dots) + b(b_2t^v + \dots) = c \tag{4.4.2}$$

Without loss of generality we assume $u > u'$ and $a = 1$. So subtracting the two equations gives us

$$-a_2t^{u'} + O(t^{u'}) + b((b_1 - b_2)t^v + O(t^v)) = 0$$

$$\implies b = \frac{a_2t^{u'} + O(t^{u'})}{(b_1 - b_2)t^v + O(t^v)}$$

$$\implies c = a_2t^{u'} + \dots + \frac{(a_2t^u + O(t^{u'})) \cdot (b_2t^v + \dots)}{(b_1 - b_2)(t^v) + \dots)}$$

Therefore $val(c) = -u'$ and $val(b) = -u' - v$, and we get the Newton polytope and the tropicalization as shown in Figure 4.6,

which is a stable tropical line passing through $\mathrm{p}_1 = (-u', -v)$ and $\mathrm{p}_2 = (-u, -v)$.

The result for two points being coaxial in the other two primitive directions also follows with a similar computation.

□

Alternatively, in [47] in Section 2.2 a notion of a stable curve though a set of n points is introduced. The definition of a stable curve in [47] is as follows

Definition 4.4.5. The stable curve of support I passing through $\{q_1, \ldots, q_{\delta-1}\}$ is the curve defined by the polynomial $f =$ "$\sum_{i \in I} a_i x^{i_1} y^{i_2}$", where the coordinates a_i of f are the stable solutions to the linear system imposed by passing through the points q_j .

where for a curve H given by a polynomial f, the support is the set of tuples of $i \in \mathbb{Z}^n$ such that a_i appears in f, $\delta(I)$ denotes the number of elements in I and the stable solution for a set of tropical linear forms is the common solution for all the linear forms, which is also stable under small perturbations of the coefficients of the linear forms [46][45].

So let us consider the above case for tropical lines and try to see the equivalent definitions of stable lines through two points according to [47].

The linear form that represents a tropical line in the tropical plane is given by

$$a \odot x \oplus b \odot y \oplus c \tag{4.4.3}$$

So the support in this case is a set of 3-tuples of $\mathbb{Z}^3$ and $\delta(I) = 3$. We take two arbitrary points in the (-1,0) direction of a tropical line $P_1 = (-u, v)$ and $P_2 = (-u', v)$, where u and u' both are positive and $u' \leq u$. Now let us compute the stable line passing through P_1 and P_2 in the setup of [47].

The tropical linear system obtained by plugging in the points in 4.4.3 is as follows

$$\begin{cases} a \odot (-u) \oplus b \odot v \oplus c = 0 \\ a \odot (-u') \oplus b \odot v \oplus c = 0 \end{cases}$$

Now the stable solution of the above tropical linear system provides the coefficients for the linear form which defines the stable line passing through the two given points. The corresponding coefficient matrix is given as

$$C = \begin{bmatrix} -u & v & 0 \\ -u' & v & 0 \end{bmatrix}.$$

With the help of explicit computations for calculating stable solutions of tropical linear systems elaborated in [46] and [45], in the case above, we find that the stable solution is given by $(|O^1|_t : |O^2|_t : |O^3|_t) = (v : -u' : -u' + v)$ and hence the linear form representing the stable line through P_1 and P_2 is given as

$$v \odot x \oplus -u' \odot y \oplus -u' + v \tag{4.4.4}$$

This is a tropical line with vertex (α, β) satisfying

$\alpha + v = -u' + v \implies \alpha = -u'$ and $\beta - u' = -u' + v \implies \beta = v$.

Hence, we get the stable line shown in Figure 4.7.

The computation for a two point configuration in the other two primitive directions also follows in the same manner.

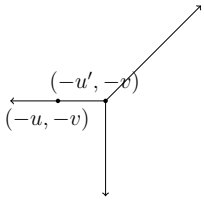

Figure 4.7: Stable line passing through two given points

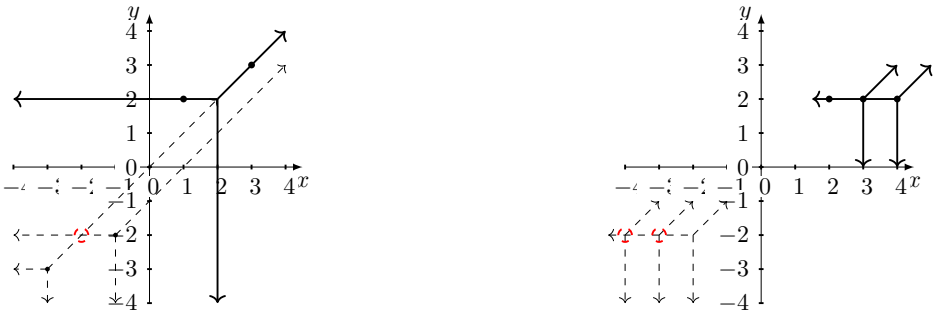

Figure 4.9: Duality between stable lines and stable intersections

So as is evident from the above discussion, taking two points on any one of the rays of a tropical line, we see that the definition of a stable line in [47] coincides with 4.4.3.

An important observation here is that the Sylvester-Gallai Theorem fails if we restrict ourselves to stable tropical lines. Figure 4.8 shows explicit examples of sets of points in the tropical plane with $n = 4$ and 5 points such that these point sets do not determine an ordinary stable tropical line.

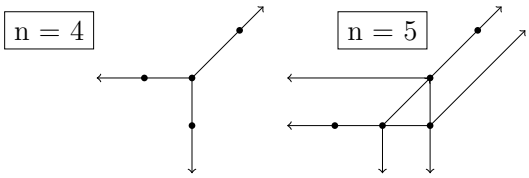

Figure 4.8: Point sets which do not determine an ordinary stable tropical line

Proposition 4.4.6. *Given a n-point set P in the tropical plane, the number of stable lines determined by P is equal to the number of stable intersections obtained in the corresponding dual line arrangement.*

Proof. Consider an arbitrary stable tropical line $(L, p_1, p_2 \dots p_n)$. By definition, either the points $p_1, p_2 \dots p_n$ uniquely determine L or one of the points amongst the $p_i's$ is the vertex of the line L. We first consider the case when the points $p_1, p_2 \dots, p_n$ determine the line uniquely, and in this case there must be at least two non coaxial points present on the line L,

and we realize that under duality, the reflection of the vertex of the line L with respect to the origin corresponds to a unique stable intersection obtained in the dual line arrangement, illustrated in the Figure 4.9. This implies a one to one correspondence between stable lines determined by such points and the stable intersections obtained in the dual line arrangement.

Also, if one of the points amongst the $p_i's$ is the vertex of the stable tropical line L, then we again oberve that the reflection of the the vertex of the line L with respect to the origin, corresponds to a unique stable intersection in the dual line arrangement, illustrated in the Figure 4.9. Hence, we see a one to one correspondence between stable tropical lines and the number of stable intersections in the dual line arrangement.

We realize that this duality between stable intersections and stable lines is a bit stronger; if the stable line is the unique line passing through the points on it, then the vertex of the line corresponds to a stable intersection of first kind and if the stable line has one of the points as a vertex, then the vertex corresponds to a stable intersection of second kind.

□

Proposition 4.4.6 illustrates the fact that stable tropical lines are in fact dual to stable intersections of tropical lines.

Proposition 4.4.6 leads on to the following corollary.

Corollary 4.4.7. *For a given tropical line arrangement $\mathcal{L}$ in the tropical plane, the number of stable intersections equals the number of non-triangular faces in the dual Newton subdivision corresponding to the tropical line arrangement.*

Proof. Since all stable intersections are obtained as intersections of two or more rays, each point of intersection has at least four or more rays emanating from it in the primitive directions. This corresponds through duality to faces with at least four edges or more and the only other faces which contribute in the dual Newton subdivision are triangular faces which are not dual to stable intersections. Hence, the number of stable intersections in the line arrangement is equal to the number of non-triangular faces in the dual Newton subdivision. □

With this duality established, let us look at the total number of faces, which we denote as t, present in a dual Newton subdivision of a tropical line arrangement of n tropical lines, where n remains fixed for our discussion. Firstly, there is a trivial lower bound of n on t, since the n vertices of the tropical lines contribute at least n faces in the corresponding Newton subdivision. Also t is bounded above by the number $\binom{n}{2} + n$, which is the number of faces when any two lines in the line arrangement intersect transversally at a unique point [8]. Therefore, t satisfies the following inequality

$$n \leq t \leq \binom{n}{2} + n$$

We recall that stable intersection of first kind correspond to parallelograms and hexagons in the dual Newton subdivision and stable intersections of second kind correspond to irregular cells with four, five or six edges in the dual Newton subdivision. A common description of all the faces appearing in a dual Newton subdivision is described in the Figure 4.10 also present in [8],

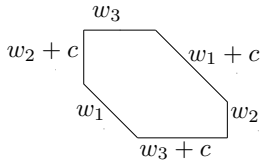

Figure 4.10: A cell in the Newton Subdivision, which is dual to a tropical line arrangement [8]

where w_1, w_2 and w_3 are the number of lines, which are coaxial in the three primitive directions, and c represents the number of lines centered at the point dual to the face in the tropical line arrangement. A Newton subdivision with faces of the shape described in Figure 4.10, is called a *linear Newton subdivision* and if the only faces occurring in a linear Newton subdivision are triangles, parallelograms and hexagons, then such a subdivision is called a *semiuniform subdivision* [8].

We refer to faces in the shapes of parallelograms and hexagons as *semiuniform* faces and faces dual to stable intersections of second kind as *non-uniform* faces.

Figure 4.11 shows all the possible shapes of cells present in the dual Newton subdivision of a tropical line arrangement; in the figure for all semiuniform faces, for each edge length parameter we consider $w_i = 1$ and for all non-uniform faces we take $c = 1$. For higher values of $w_i's$ and c the shapes remain the same however the edge lengths corresponding to each parameter get elongated according to the values described in Figure 4.10.

We move on to discuss one of the extremal cases for the values of t, which is the case when $t = n$.

Lemma 4.4.8. *Let $\mathcal{L}$ be a tropical line arrangement of n lines, having exactly n faces in the corresponding dual Newton subdivision, then $\mathcal{L}$ has no stable intersections of first kind in the tropical line arrangement.*

Proof. We start with a tropical line arrangement $\mathcal{L}$ of n tropical lines, such that it has exactly n faces. We continue by contradiction, assuming that there does exist a stable intersection of

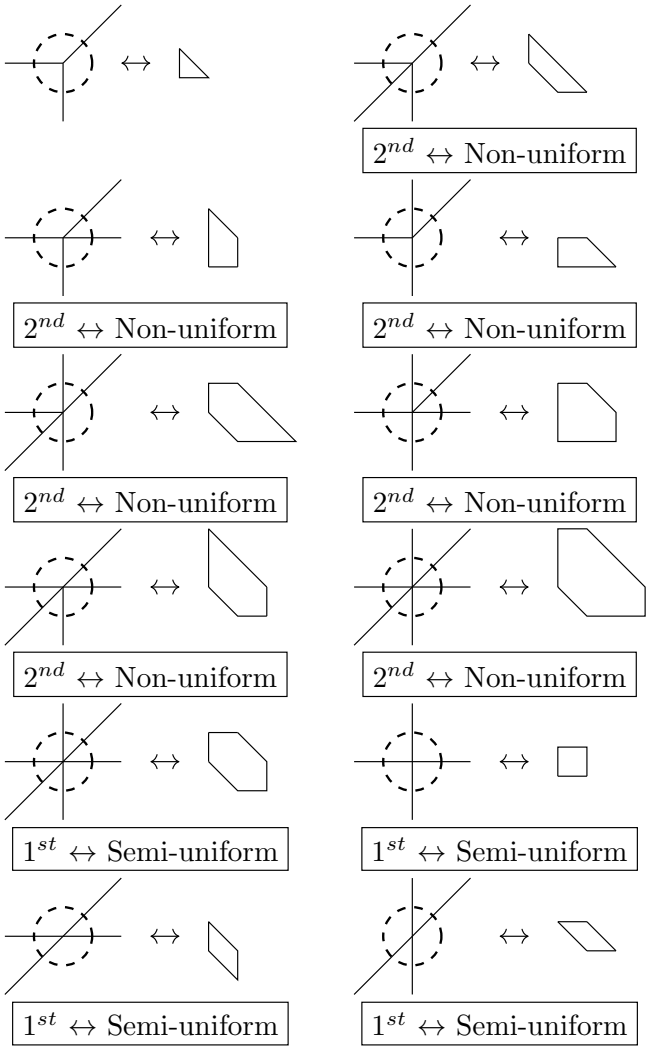

Figure 4.11: All possible shapes of faces present in the Newton subdivision of a tropical line arrangement; with the labelings having type of stable intersections on the left along with the type of face that corresponds to it on the right

first kind in the line arrangement $\mathcal{L}$. However, since there are at least n faces contributed by the n vertices of the n tropical lines, and the face corresponding to a stable intersection of first kind is not one of them, therefore this would imply that the total number of faces in the dual Newton subdivision corresponding to $\mathcal{L}$ has at least $n+1$ faces, which is a contradiction to the fact that $\mathcal{L}$ has n faces in the dual Newton subdivision. Hence, the proof. □

We look at an example of a n line arrangement with exactly n faces.

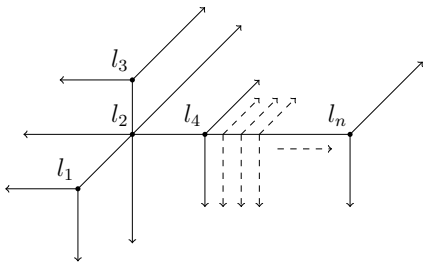

Figure 4.12: An example of a line arrangement with exactly n faces and three triangular faces

The example depicted in Figure 4.12 shows a tropical line arrangement of n tropical lines $\{l_1, l_2, l_3, l_4, \ldots, l_n\}$, such that the total number of faces in the corresponding Newton subdivision is n, and it has exactly three triangular faces located at the corners of the Newton polygon.

We use $(v^{max})_t$ to represent the maximum number of triangular faces present in a Newton subdivision corresponding to a tropical line arrangement with total number of faces in the Newton subdivision being equal to t.

Lemma 4.4.9. *Let $\mathcal{L}$ be a tropical line arrangement of n tropical lines such that the dual Newton subdivision $\mathcal{N}$ has exactly n faces, then the maximum number of triangular faces in $\mathcal{N}$ is 3, i.e., $(v^{max})_n = 3$.*

Proof. As can be seen from Figure 4.12, there are explicit tropical line arrangements of n tropical lines with n faces in the dual Newton subdivision with exactly 3 triangular faces. We proceed by contradiction, and assume that $(v^{max})_n > 3$. With $(v^{max})_n > 3$, we can conclude that there does exist at least one triangular face T in the interior of the Newton polygon, i.e., when no edges of T lie on the boundary of the Newton polygon or exactly one edge of T lies on the boundary of the Newton polygon. We first consider the case when T is in the relative interior of the Newton polygon, i.e., when no edges of T lie on the boundary of the Newton polygon .

Let us consider the three faces C_1, C_2 and C_3 that share an edge with the triangular face T and we consider an example of the local line arrangement around T as depicted in the Figure 4.13.

Figure 4.13: Positions of cells in the Newton subdivision and the local line arrangement dual to it

In the figure we see that the points D, E and F represent the vertices of the tropical lines l_1, l_2 and l_3 which are present at the stable intersections of second kind at these points, dual to the cells C_1, C_2 and C_3 in $\mathcal{N}$. Also l_0 represents the line dual to the triangular face T. Also, by Lemma 4.4.8 we know that no stable intersections of first kind are present in the line arrangement.

In the local picture, we obtain three stable intersections of first kind at the points A, B and C. Since these points are stable intersections and by Lemma 4.4.8 we know we can not have any stable intersections of first kind therefore there must exist a line with its vertex at these points. Let us consider one of these intersections, A. The points D, A and F are represented as $(x_1, y_1), (x_2, y_2)$ and (x_3, y_3), then it is easy to see that

$$x_1 < x_2 < x_3$$

This helps to conclude that if there is a tropical line present with vertex at A, then it would either intersect the lines l_0 and l_3 at two points, or meet the vertex of the line l_0. There cannot be a line with vertex at A meeting the vertex of the line l_0 as that would contradict the fact that the face corresponding to l_0 is a triangular face T in $\mathcal{N}$. So we continue with the other case when the line has the vertex at A and intersects the lines l_0 and l_3 at two points. But there cannot be a tropical line present at A with two points of intersection with the lines l_0 and l_3, as that would contradict the fact that the cells C_1, C_2 and C_3 corresponding to the stable intersections at D, E and F, share an edge with the triangular face T. Hence, there cannot be a tropical line with a vertex at A, and therefore A has to be a stable intersection of first kind, which contradicts Lemma 4.4.8. The same argument follows for the other two points of intersections, B and C. However, this is a contradiction to the Lemma 4.4.8. Another observation is that for all possibilities of non-uniform faces (arising from stable intersections of second kind) surrounding T, we obtain points of intersections in similar positions as A, B and C which establishes the existence of at least three stable intersections of first kind, and hence gives a contradiction. Therefore, this shows that it is not possible to place a triangular face in the relative interior of the Newton polygon.

Figure 4.14: Positions of cell in the Newton subdivision and the local line arrangement dual to it

The other possible case is when the triangular face intersects the boundary of the Newton polygon in exactly one edge. Without loss of generality, we take the triangular face to be intersecting with one of the edges of the Newton polygon as depicted in the Figure 4.14 and we look at the local line arrangement around the triangular face T.

We argue in the same way as we did in the previous case, and realize that by Lemma 4.4.8, C_1 and C_2 in Figure 4.14 are non-uniform faces. Also, we see that in Figure 4.14 the points B and C represent the vertices of the tropical lines l_1 and l_2 which are present at the stable intersection of second kind at these points, dual to the cells C_1 and C_2 in $\mathcal{N}$. Here l_0 represents the line dual to the triangular face T.

In the local picture, we obtain a stable intersection of first kind at the point A. If the points B, A and C are represented as $(x_1, y_1), (x_2, y_2)$ and (x_3, y_3), then it is easy to see that

$$x_1 < x_2 < x_3$$

This helps to conclude that if there is a tropical line present with vertex at A, then it would either intersect the line l_0, or meet the vertex of the line l_0. There cannot be a line with vertex at A meeting the vertex of the line l_0 as that would contradict the fact that the face corresponding to l_0 is a triangular face T in $\mathcal{N}$. So we continue with the other case when the line has the vertex at A and intersects the lines l_0. But there cannot be a tropical line present at this intersection as that would contradict the fact that the cells C_1 and C_2 corresponding to the stable intersections of second kind at B and C share an edge with the triangular face T. Hence, there cannot be a tropical line with a vertex at A, and therefore A has to be a stable intersection of first kind, which contradicts Lemma 4.4.8. It is easy to verify that this contradiction occurs for all possibilities of non-uniform faces (arising from stable intersections of second kind), which can be adjacent to T.

Therefore, the only places left to place a triangular face in the Newton polygon, are the three corners, and hence the maximum number of triangular faces that can be obtained is three, i.e., $(v^{max})_n = 3$.

□

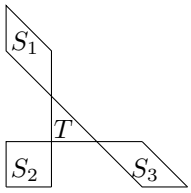

Figure 4.15: The non-adjacent semiuniform faces determined by a triangular face T

Using Lemma 4.4.9 we obtain Corollary 4.4.10,

Corollary 4.4.10. *Let $\mathcal{L}$ be a tropical line arrangement of n lines, such that $t = n$ and let v denote the number of triangular faces present in the dual Newton subdivision $\mathcal{N}$. Then*

$$n - v \geq n - 3$$

Remark 4.4.11. An important inference is that for tropical line arrangements of n lines, with n faces in the dual Newton subdivision, they occur in four distinct classes. Each class is represented by the number of triangular faces at the corners, which varies between $0, 1, 2$ and 3.

With Lemma 4.4.9, we know the bound on the number of stable intersections of an n line arrangement with exactly n faces in the corresponding dual Newton subdivision. We now move on to the more general situation.

We now define what it means for a semiuniform face to be *determined* by a triangular face T.

Definition 4.4.12. A semiuniform face S in a dual Newton subdivision is said to be *determined* by a triangular face T if,

1. S is adjacent to T, i.e., T and S share an edge, or
2. S is located as the faces S_1, S_2 or S_3 depicted in the Figure 4.15

Here the shapes and location of these three semiuniform faces has to be exactly the same as shown in the figure in order for the faces to be determined by the triangular face T. We also note that edge lengths of these faces need not be unit length, and they could be elongated depending on the lattice length parameters w_i and c of the adjacent faces to T. We also note that a triangular face determines at most six semiuniform faces; at most three adjacent to it and at most three non adjacent to it.

We note that as a consequence of the definition, the determined faces S_1, S_2 or S_3 cannot be hexagonal faces. Also, as a consequence of the definition, two triangular faces cannot have common non-adjacent determined faces.

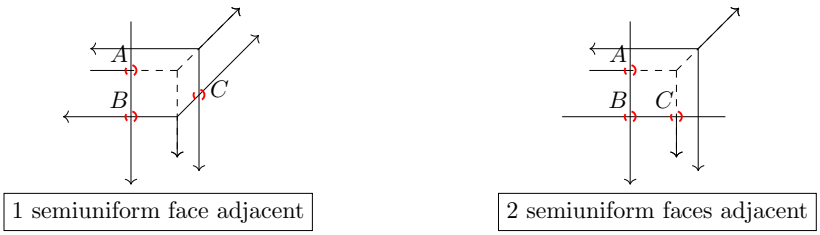

Figure 4.16: Examples depicting local line arranagements dual to a triangular face with 1 or 2 semiuniform faces adjacent to it.

With the above definitions, we look at the number of semiuniform faces determined by a triangular face depending on the location of the triangular face in the dual Newton subdivision.

Theorem 4.4.13. *Let $\mathcal{L}$ be a tropical line arrangement of n lines and let $\mathcal{N}$ be its dual Newton subdivision. If T is a triangular face in $\mathcal{N}$ (excluding the corners), then*

1. *T determines at least three seminuniform faces if T is in the relative interior of the Newton polygon; i.e., when no edges of T lie on the boundary of the Newton polygon.*

2. *T determines at least one seminuniform face if T is at the boundary of the Newton polygon; i.e, when one of the edges of T lie on the boundary of the Newton polygon.*

Proof. We continue with the discussion in the Lemma 4.4.9. As we see in Figure 4.13, it is shown that a triangular face T, which is not adjacent to a semiuniform face, determines at least three semiuniform faces if T is in the interior and at least one semiuniform face if T is located at the boundary. However, semiuniform faces might also occur as faces adjacent to the triangular face. Therefore, when we consider the triangular face T in the interior, then T can be adjacent to either one, two or at most three semiuniform faces. We know that if T is adjacent to semiuniform faces at all edges, then there are at least three semiuniform faces determined by T in the subdivision, trivially. Now we consider the case, when the triangular face is adjacent to two semiuniform faces. In this case, the location of the triangular face, implies existence of at least one non-adjacent semiuniform faces. Similarly, in the case when the triangular face is adjacent to one semiuniform face, at least two non-adjacent semiuniform faces are obtained. Both these cases are illustrated through an example in the Figure 4.16. Hence if a triangular face is in the interior of the Newton polygon, then it implies the existence of at least three semiuniform faces.

Similarly, if we consider the case when the triangular face T is located at the boundary, then if there are semiuniform faces adjacent to T at one or two edges, then there exists at least one semiuniform face in the subdivision, trivially. If T is not adjacent to any semiuniform

Figure 4.17: An example to illustrate the rearrangement when T is adjacent to semiuniform faces.

faces, then we see in Figure 4.14, that T determines at least one semiuniform face. Hence, we can conclude that if a triangular face is at the boundary then it determines at least one semiuniform face. □

We now move on to count the total number of semiuniform face determined by the triangular faces. Since two or more triangular faces can determine common semiuniform faces, therefore the total count need not be a direct sum of determined faces of all triangular faces.

With an abuse of notation we denote T to be a triangular face and $n(T)$ represent the number of semiuniform faces determined by the triangular face T. Hence, $n(T_1 \cup ... \cup T_m)$ denotes the total number of semiuniform faces determined by the triangular faces $T_1, ..., T_m$.

Theorem 4.4.14. *Let $\mathcal{L}$ be a tropical line arrangement of n lines and $\mathcal{N}$ be its dual Newton subdivision, with $T_1 \dots T_m$ being the triangular faces in $\mathcal{N}$ (excluding the corners) and k be the number of stable intersections of first kind. Then,*

$$k \geq n(T_1 \cup T_2 \dots \cup T_m) \geq m$$

Proof. We proceed with induction on m, with the base case being $m = 1$. We see that in this case, by Theorem 4.4.13, we know that the unique triangle present in the interior of $\mathcal{N}$ determines at least one semiuniform face, therefore

$$k \geq n(T) \geq 1$$

Firstly, we consider a subdivision $\mathcal{N}$ with m triangular faces in the interior. We now show that for any such subdivision $\mathcal{N}$, we can always construct a subdivision $\mathcal{N}'$, such that $\mathcal{N}'$ has exactly $m-1$ triangular faces, via a rearrangement of $\mathcal{L}$ to $\mathcal{L}'$. We consider a triangular face T in $\mathcal{N}$, dual to l' in $\mathcal{L}$, which we rearrange to obtain a stable intersection in order to construct the subdivision $\mathcal{N}'$. We go through the following cases based on the types of faces adjacent to T in $\mathcal{N}$,

1. If T has at least one semiuniform face adjacent to it, dual to a stable intersection of first kind P.

We move the vertex of the line l', dual to T, along with coaxial lines towards P, such that the vertex of l' is superimposed on the point P, illustrated in the Figure 4.17. If during the rearrangement, any rays of the lines coaxial to l' meet the vertex of another line, which might result in a reduction in the total number of triangular faces, we can consider a local perturbation of the vertex of such a line, along the half ray, and in this way we can prevent such a situation. In this way we obtain a subdivision $\mathcal{N}'$ with exactly $m-1$ triangular faces, via a local rearrangement. We also notice that the determined semiuniform face dual to the point P in $\mathcal{N}$, ceases to exist in $\mathcal{N}'$, since the vertex of l' gets superimposed on P.

2. If T is adjacent only to non-uniform faces, with at least one of the adjacent non-uniform faces being five or six edged.

If T is adjacent to non-uniform faces in $\mathcal{N}$, then by the definition of determined faces from the Figure 4.15, we realize that T determines uniquely at least one non-adjacent semiuniform face dual to a stable intersection of first kind P, in $\mathcal{N}$. We move the vertex of the line l' dual to T (along with any coaxial lines to l' if there exist any), illustrated in Figure 4.18, such that it meets the half ray of another line in $\mathcal{L}$ and there is an effective decrease in the number of triangular faces by 1 (in our example we assume P_2 to be the face which has to be a five or six edged face). We show the location of lines coaxial to l' (if present) by a dotted arrow along the ray of coaxiality in the rearrangement. If during the rearrangement, any rays of the lines coaxial to l' meet the vertex of another line, which might result in the reduction in the total number of triangular faces, we can consider a local perturbation of the vertex of such a line, along the half ray, and in this way we can prevent such a situation. Hence in this way we construct a subdivision $\mathcal{N}'$ with exactly $m-1$ triangular faces, via a local rearrangement. We also observe that the determined semiuniform face dual to P in $\mathcal{N}$ no more remains a determined semiuniform face in $\mathcal{N}'$, because firstly by the definition of determined faces, the face dual to P cannot be a hexagon. Additionally, out of the four edges of the face dual to P, only at two edges can it be adjacent to triangular faces, and we realize that in $\mathcal{N}'$ at both these edges, the face is adjacent to non-triangular faces. Hence, the face dual to P cannot be a determined face by virtue of being adjacent to a triangular face in $\mathcal{N}'$. Also, it can neither be a non-adjacent determined face, since the face dual to P was the unique non-adjacent determined face with respect to T, and the triangular face T no longer exists in $\mathcal{N}'$.

3. If T is adjacent to only four-edged non-uniform faces.

Figure 4.18: An example to illustrate the rearrangement when T is adjacent to five or six edged non-uniform faces.

Firstly, by the definition of determined faces from the Figure 4.15, we realize that T determines uniquely at least one non-adjacent semiuniform face dual to a stable intersection of first kind P in $\mathcal{N}$. We notice that in this case, we cannot obtain $\mathcal{N}'$ by the movement of just l' and its coaxial lines since it results in an increase in the number of triangular faces. However, we observe that with a local rearrangement of l' along with its neighbouring lines which are coaxial to l', we can obtain $\mathcal{N}'$. When T is adjacent to three or two such four edged faces, the local rearrangement is illustrated in Figure 4.19. In the first case we see that no lines can be present inside the hexagon $Pl_1Ql_3Rl_2$, where we abuse the notation to denote l_i as the vertex of the line $l_i, i \in \{1, 2, 3\}$, because that would contradict the adjacency of the faces dual to vertices of l_1, l_2,l_3 and T. Also other lines coaxial to any of the l_i's (if present) are depicted by dotted arrows in the figure.

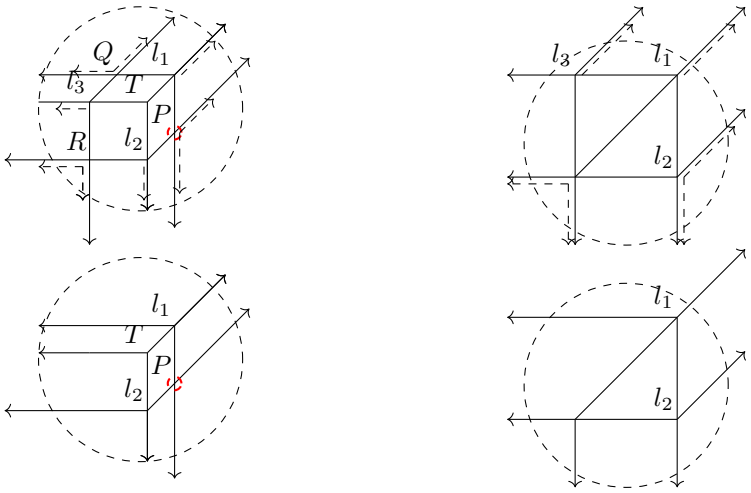

Figure 4.19: All cases where T is adjacent to two or three four edged non uniform faces along with the corresponding rearrangement $\mathcal{L}'$.

Essentially, one can think of this rearrangement as moving the line l_3 and l_2 along with the coaxial lines (if present) on the half rays not shared with l', such that the vertices of l_2 and l_3 lie on the segments Ql_1 and Pl_1 respectively and one of the rays from each l_3 and l_2 meets the vertex of l'. In this way we obtain a subdivision $\mathcal{N}'$ with one less triangular face.

Once again if during the rearrangement, any rays of the lines coaxial to l' meet the vertex of another line, which might result in the reduction in the total number of triangular faces, we can consider a local perturbation of the vertex of such a line, along the half ray, and in this way we can prevent such a situation. A similar argument works for the remaining case in Figure 4.19. Also, we realize that the face dual to P ceases to exist as we go from $\mathcal{N}$ to $\mathcal{N}'$, and this is illustrated in the Figure 4.19.

Hence, we see that in all cases for any subdivision $\mathcal{N}$ we can perform a rearrangement of $\mathcal{L}$ to $\mathcal{L}'$, to obtain a subdivision $\mathcal{N}'$ with exactly $m-1$ triangular faces. Also, we notice that as we change from $\mathcal{N}$ to $\mathcal{N}'$, there always exists a determined semiuniform face, dual to a stable intersection of first kind (P), which either ceases to exist in $\mathcal{N}'$ (Case (1) and (3)) or does not remain a determined semiuniform face in $\mathcal{N}'$ (Case (2)). Hence, there exists a determined semiuniform face in $\mathcal{N}$, which can never contribute to the total count of determined semiuniform faces in $\mathcal{N}'$. We now invoke the induction hypothesis for $\mathcal{N}'$ with $m-1$ triangular faces and we obtain,

$$k \geq n(T_1 \cup T_2 \ldots \cup T_{m-1}) \geq m-1$$

Since, the face dual to P cannot contribute to the $m-1$ faces determined by triangular faces present in $\mathcal{N}'$. Hence for $\mathcal{N}$, we have

$$n(T_1 \cup T_2 \ldots \cup T_m) \geq n(T_1 \cup T_2 \ldots \cup T_{m-1}) + 1 \geq m-1+1 \geq m$$

Therefore, we realize that for all cases, given a subdivision $\mathcal{N}$ with m triangular faces,

$$k \geq n(T_1 \cup T_2 \ldots \cup T_m) \geq m$$

Hence, the proof. □

Theorem 4.4.15. *If $\mathcal{L}$ is a tropical line arrangement of n tropical lines, then it determines at least $n-3$ stable intersections.*

Proof. We try to look at all possible places where triangular faces occur in a Newton subdivision. If v is the number of triangular faces present in a subdivision, then we can write v as

$$v = p + q$$

where p be the number of triangular faces present in the interior of the Newton polygon, i.e., triangular faces which are adjacent to at least two or more faces in the subdivision and q be the number of triangular faces present at the corners of the Newton polygon, i.e.,

triangular faces which are adjacent to exactly one other face in the subdivision. It is easy to see that $q \in \{0, 1, 2, 3\}$. Then the lower bound on the number of semiuniform faces, which are determined by these triangular faces, is p (by Theorem 4.4.14). Therefore if k is the total number of faces corresponding to stable intersections of first kind, then

$$k \geq p$$

Also, the number of stable intersections of second kind $h = n - v$ (since triangular faces and faces corresponding to stable intersections of second kind are contributed by vertices of lines, hence their sum is equal to n).

Therefore, the total number of stable intersections b is given as

$$b = n - v + k \geq n - p - q + p = n - q \geq n - 3$$

Hence, $b \geq n - 3$. □

Theorem 4.4.16. *Let $\mathcal{L}$ be a tropical line arrangement of n tropical lines and let $\mathcal{N}$ be its dual Newton subdivision. If $\mathcal{L}$ determines $n - 3$ stable intersections, then there are three triangular faces present at the corners of the Newton polygon and $\mathcal{N}$ can not have any triangular faces in the relative interior of the Newton polygon.*

Proof. If $\mathcal{L}$ determines $n-3$ stable intersections, it is the case when the bound from Theorem 4.4.15 is sharp, which happens when the following equalities hold true

$$q = 3 \tag{4.4.5}$$

and

$$k = n(T_1 \cup T_2 \ldots \cup T_m) = m \tag{4.4.6}$$

The first equality implies that there must be three triangular faces present at the corners of the Newton polygon.

We now assume to the contrary, that triangular faces do exist in the relative interior. We consider one such triangular face T in the relative interior of the Newton polygon. We consider all possible cases for T, where it can share faces with other triangular faces in $\mathcal{N}$,

1. If T does not share any semiuniform faces with any other triangular face in $\mathcal{N}$.

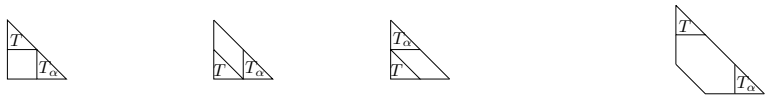

Figure 4.20: All possibilities for T, when it shares a semiuniform face with another triangular face

By theorem 4.4.13 we know that any triangular face in the relative interior determines at least three semiuniform face. Then

$$k = n((T_1 \cup T_2 \ldots \cup T_{m-1}) \cup T) = n(T_1 \cup T_2 \ldots \cup T_{m-1}) + n(T) \geq m - 1 + 3 = m + 2$$

which gives a contradiction to the equation 4.4.6.

2. If T shares a semiuniform face with exactly one other triangular face T_α in $\mathcal{N}$.

All possible cases for T, upto symmetry, are listed in Figure 4.20.

We realize that in all such cases, when we consider all possible adjacent faces to T, for all of them $n(T) = 4$, and none of the $m - 2$ triangular faces apart from T and T_α, can determine the four faces determined by T, because that would contradict the fact that T can share faces with exactly one other triangular face. Also, by Theorem 4.4.14, for the $m - 2$ triangular faces apart from T and T_α,

$$n(T_1 \cup T_2 \ldots \cup T_{m-2}) \geq m - 2$$

therefore,

$$k = n(T_1 \cup T_2 \ldots \cup T_m) \geq n(T_1 \cup T_2 \ldots \cup T_{m-2}) + n(T) \geq m - 2 + 4 = m + 2$$

which again gives a contradiction to the equation 4.4.6.

We also remark that for this case and all subsequent cases, semiuniform faces which are parallelograms, and are determined by two different triangular faces, can not have edge lengths greater than one, since they share one edge, per pair of parallel edges, with a triangular face, whose edges always have unit lattice length. Hence, for all cases, the parallelogram faces are of unit lattice length. However, for hexagonal faces, edges not adjacent with triangular faces, can be of lattice length greater than one, although this does not change the count of determined faces for T, i.e., $n(T)$, rather it only enlarges the lengths of the edges adjacent to the hexagonal face. Hence, in our considerations, we would consider all hexagonal faces having unit lattice length.

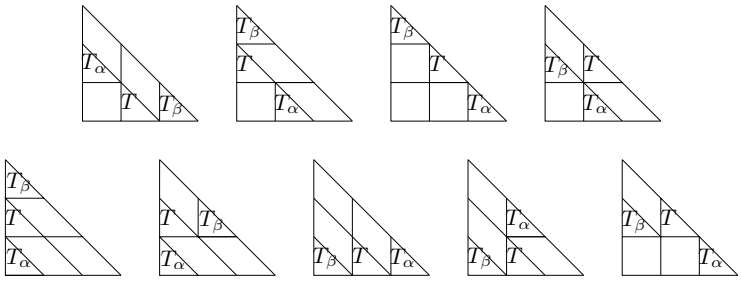

Figure 4.21: Possibilities for T, when it shares semiuniform faces with exactly two other triangular faces

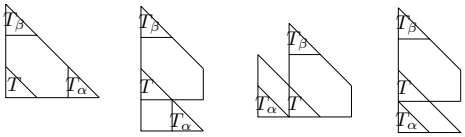

Figure 4.22: The case when T shares semiuniform with two other triangular faces, with one of the determined faces being a hexagon

3. If T shares a semiuniform face with exactly two other triangular faces T_α and T_β in $\mathcal{N}$.

All possible cases for T, upto symmetry, are listed in Figure 4.21 and Figure 4.22.

We realize that in all cases in Figure 4.21, when we consider all possible adjacent faces for T, $n(T) = 5$, and for the first case in Figure 4.22, $n(T) = 4$, while for all others in Figure 4.22, $n(T) = 5$. Also none of the $m-3$ triangular faces apart from T, T_α and T_β, can determine the faces determined by T, because that would contradict the fact that T can share faces with only two other triangular faces. By Theorem 4.4.14, for the $m-3$ triangular faces apart from T, T_α and T_β, we have

$$n(T_1 \cup T_2 \ldots \cup T_{m-3}) \geq m-3$$

therefore,

$$k = n(T_1 \cup T_2 \ldots \cup T_m) \geq n(T_1 \cup T_2 \ldots \cup T_{m-3}) + n(T) \geq m-3+4 = m+1$$

which again gives a contradiction to the equation 4.4.6.

4. If T shares a semiuniform face with exactly three other triangular faces T_α, T_β and T_γ in $\mathcal{N}$.

All possible cases for T, upto symmetry, are listed in Figure 4.23, Figure 4.24 and Figure 4.25.

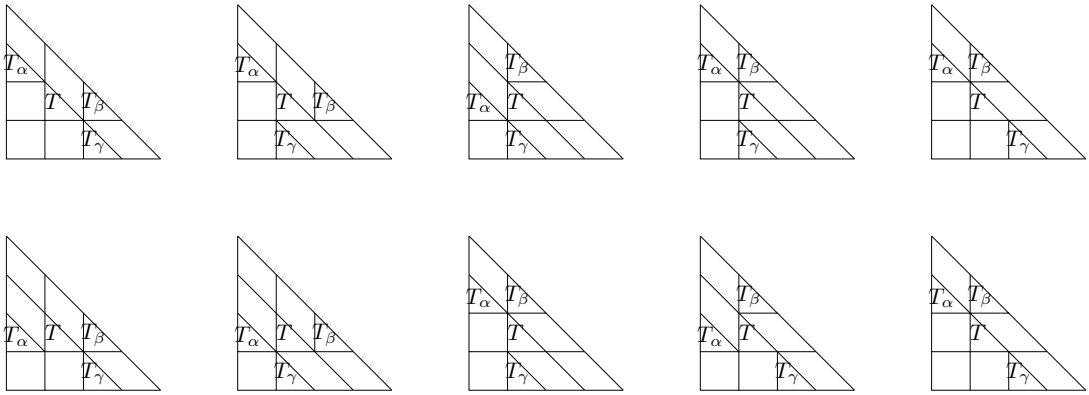

Figure 4.23: Possibilities for T, when it shares semiuniform faces with three other triangular faces

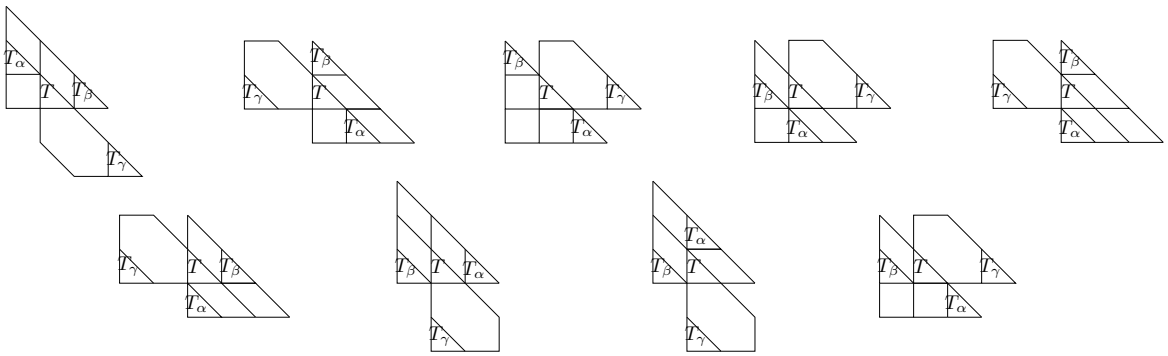

Figure 4.24: Possibilities for T, when it shares semiuniform faces with three other triangular faces, involving a hexagonal face which T shares with one other triangular face

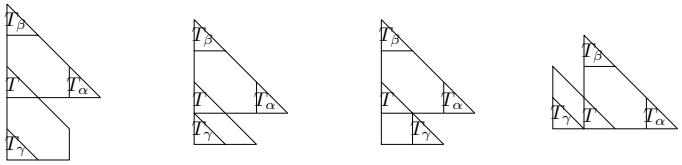

Figure 4.25: Possibilities for T, when it shares semiuniform faces with three other triangular faces, involving a hexagonal face which T shares with two other triangular face

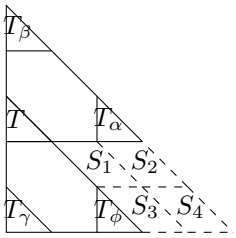

Figure 4.26: The case for T, when it shares two hexagonal faces with four other triangular faces

We realize that in all cases in Figure 4.23 and 4.24, $n(T) = 6$, and for all the cases in Figure 4.25, $n(T) = 5$. Also, none of the $m-4$ triangular faces apart from T, T_α, T_β and T_γ, can determine the faces determined by T, because that would contradict the fact that T can share faces with only three other triangular faces. By Theorem 4.4.14, for the $m-4$ triangular faces apart from T, T_α, T_β and T_γ,

$$n(T_1 \cup T_2 \ldots \cup T_{m-4}) \geq m-4$$

therefore,

$$k = n(T_1 \cup T_2 \ldots \cup T_m) \geq n(T_1 \cup T_2 \ldots \cup T_{m-4}) + n(T) \geq m-4+5 = m+1$$

which again gives a contradiction to the equation 4.4.6.

5. If T shares a semiuniform face with exactly four other triangular faces T_α, T_β, T_γ and T_ϕ in $\mathcal{N}$.

All possible cases for T, upto symmetry, are listed in Figure 4.26 and Figure 4.27.

We realize that for the case in Figure 4.26, $n(T) = 5$. However, due to the arrangements of the faces, some of the faces are fixed and are bound to appear in the subdivision, which we show as S_1, S_2, S_3 and S_4 in the Figure 4.26. Amongst these faces, S_4 is a face which can not be determined by $T, T_\alpha, T_\beta, T_\phi$ and T_γ. Additionally, we observe that it can also not be determined by any of the remaining $m-5$ triangular faces in $\mathcal{N}$ since it has no free edges which could be adjacent to a triangular face. This implies that the dual point to S_4 contributes to the count of stable intersections of first kind k, although it is not determined by any triangular face in $\mathcal{N}$. This gives a contradiction to the following equality

$$k = n(T_1 \cup T_2 \ldots \cup T_m)$$

in 4.4.6.

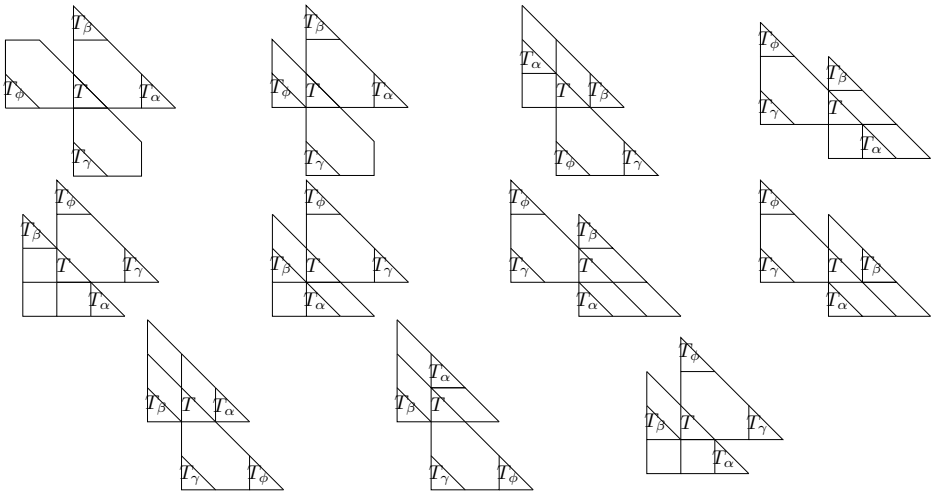

Figure 4.27: Possibilities for T, when it shares semiuniform faces with four other triangular faces

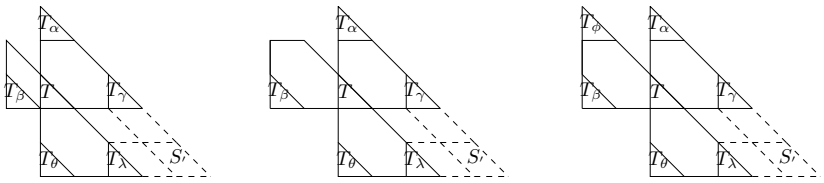

Figure 4.28: The cases where T shares faces with five or six other triangular faces

For the other cases in Figure 4.27, $n(T) = 6$. None of the $m-5$ triangular faces apart from T, T_α, T_β, T_γ and T_ϕ, can determine the faces determined by T, because that would contradict the fact that T can share faces with only four other triangular faces. By Theorem 4.4.14, for the $m-5$ triangular faces apart from T, T_α, T_β and T_γ,

$$n(T_1 \cup T_2 \ldots \cup T_{m-5}) \geq m-5$$

therefore,

$$k = n(T_1 \cup T_2 \ldots \cup T_m) \geq n(T_1 \cup T_2 \ldots \cup T_{m-5}) + n(T) \geq m-5+6 = m+1$$

which again gives a contradiction to the equation 4.4.6.

The remaining three cases illustrated in Figure 4.28 can also be eliminated by a similar argument, since in all these cases we obtain a semiuniform face S', which cannot be determined by a triangular face, which gives a contradiction to the equation 4.4.6.

Hence, we completed all cases and we infer that the presence of a triangular face in the relative interior contradicts the sharpness of the bound. Hence, the proof.

□

Remark 4.4.17. We note that the converse of Theorem 4.4.16 does not hold true, meaning that if $\mathcal{L}$ is a tropical near-pencil arrangement, then it does not imply that the number of stable intersections equals $n-3$, an example of which is illustrated in Figure 4.2.

Now we have established the required setup to state the tropical versions of the de-Bruijn Erdős Theorem,

Theorem 4.4.18 (Dual Tropical de Bruijn-Erdős Theorem)**.** *Let $\mathcal{L}$ be a tropical line arrangement of n ($n \geq 4$) tropical lines in the plane. Let b denote the number of stable intersections determined by $\mathcal{L}$. Then,*

1. $b \geq n-3$
2. *if $b = n-3$, then $\mathcal{L}$ is a* tropical near-pencil arrangement.

With the duality elaborated in 4.4.6, we can now state the main theorem,

Theorem 4.4.19 (Tropical de Bruijn-Erdős Theorem)**.** *Let $\mathcal{S}$ denote a set of points in the tropical plane. Let v ($v \geq 4$) denote the number of points in $\mathcal{S}$, and let b denote the number of stable tropical lines determined by these points. Then,*

1. $b \geq v-3$
2. *if $b = v-3$, then $\mathcal{S}$ forms a* tropical near-pencil.

4.5 Further Perspectives

In [2] a *type* of a point is defined as follows,

Definition 4.5.1. A (n,d) *type* is a n tuple $A = (A_1, \ldots, A_n)$ of nonempty subsets of $[d] := \{1, 2, \ldots, d\}$. The A_i's are called *coordinates* of A, $1, \ldots, n$ are called the *positions* and $1, \ldots, d$ are called the *directions*.

which assigns a tuple to each point in the plane based on its location with respect to a collection of hyperplanes, which in our case are lines and so $d = 3$ in this case. It might be interesting to look into the derivation of our results in terms of these types. Figure 4.29, depicts the types corresponding to all the various faces that are present in a linear Newton subdivision. The $'*'$ in the tuples represents a singleton, while the coordinates which have multiple elements may not occur consecutively, but they can be made consecutive, by rearranging the way we count the lines in the arrangement. We can obtain the type for a face P with edge lengths greater than one, by assigning copies of the directions $12, 13$ or 23

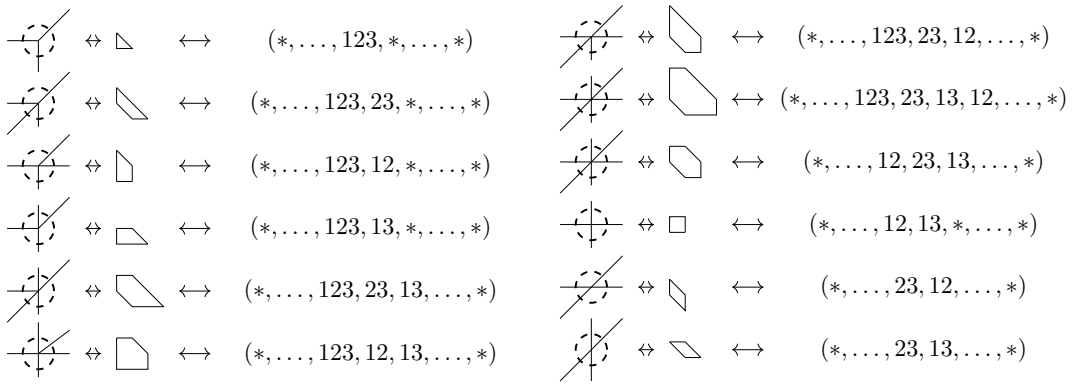

Figure 4.29: All possible shapes of faces present in the Newton subdivision of a tropical line arrangement; with the corresponding type in the tropical oriented matroid on the right

depending on the direction of coaxiality of other lines with the vertex of the line dual to P. Such an analysis could help in trying to look for generalizations of our results in higher dimensions.

Also there has been a lot of interest in the study of tropical lines present in tropical cubic surfaces owing to the existence of classical results such as the famous 27 lines on a cubic surface, which has provided detailed analysis about lines embedded in surfaces and is explored widely in [43] and [32], and one can try to generalize our results to higher dimensions using techniques from their work.

Results of the presented work in this chapter have been published in - Ayush Kumar Tewari. "Point-line geometry in the tropical plane", arXiv preprint. Submitted for further publication [48].

Bibliography

[1] Eberth Alarcon. An extremal result on convex lattice polygons. *Discrete Math.*, 190(1-3):227–234, 1998.

[2] Federico Ardila and Mike Develin. Tropical hyperplane arrangements and oriented matroids. *Mathematische Zeitschrift*, 262(4):795–816, 2009.

[3] Matthew Baker and Serguei Norine. Riemann-Roch and Abel-Jacobi theory on a finite graph. *Adv. Math.*, 215(2):766–788, 2007.

[4] Alexandru T Balaban. *Chemical applications of graph theory*. Academic Press, 1976.

[5] Elizabeth Baldwin and Paul Klemperer. Understanding preferences:"demand types", and the existence of equilibrium with indivisibilities. *Econometrica*, 87(3):867–932, 2019.

[6] Imre Bárány and Zoltán Füredi. On the lattice diameter of a convex polygon. *Discrete Math.*, 241(1-3):41–50, 2001. Selected papers in honor of Helge Tverberg.

[7] Lynn M Batten and Lynn Margaret Batten. *Combinatorics of finite geometries*. Cambridge University Press, 1997.

[8] Milo Brandt, Michelle Jones, Catherine Lee, and Dhruv Ranganathan. Incidence geometry and universality in the tropical plane. *Journal of Combinatorial Theory, Series A*, 159:26–53, 2018.

[9] Peter Brass, William OJ Moser, and János Pach. *Research problems in discrete geometry*. Springer Science & Business Media, 2006.

[10] Sarah Brodsky, Michael Joswig, Ralph Morrison, and Bernd Sturmfels. Moduli of tropical plane curves. *Res. Math. Sci.*, 2(4), 2015.

[11] Erwan Brugallé, Ilia Itenberg, Grigory Mikhalkin, and Kristin Shaw. Brief introduction to tropical geometry, 2015. Preprint `arXiv:1502.05950`.

[12] Dustin Cartwright, Andrew Dudzik, Madhusudan Manjunath, and Yuan Yao. Embeddings and immersions of tropical curves. *Collect. Math.*, 67(1):1–19, 2016.

[13] Wouter Castryck. Moving out the edges of a lattice polygon. *Discrete & Computational Geometry*, 47(3):496–518, Apr 2012.

[14] Wouter Castryck and Filip Cools. Newton polygons and curve gonalities. *J. Algebraic Combin.*, 35(3):345–366, 2012.

[15] Melody Chan, Søren Galatius, and Sam Payne. Tropical curves, graph complexes, and top weight cohomology of $\mathcal{M}_g$, 2018. Preprint `arXiv:1805.10186`.

[16] Desmond Coles, Neelav Dutta, Sifan Jiang, Ralph Morrison, and Andrew Scharf. Tropically planar graphs, 2019. Preprint `arXiv:1908.04320v3`.

[17] Desmond Coles, Neelav Dutta, Sifan Jiang, Ralph Morrison, and Andrew Scharf. The moduli space of tropical curves with fixed Newton polygon, 2020. Preprint `arXiv:2002.10874`.

[18] David A. Cox, John B. Little, and Henry K. Schenck. *Toric varieties*, volume 124 of *Graduate Studies in Mathematics*. American Mathematical Society, Providence, RI, 2011.

[19] Nicolaas G de Bruijn and Paul Erdös. On a combinatorial problem. *Proceedings of the Section of Sciences of the Koninklijke Nederlandse Akademie van Wetenschappen te Amsterdam*, 51(10):1277–1279, 1948.

[20] Jesús A. De Loera, Jörg Rambau, and Francisco Santos. *Triangulations*, volume 25 of *Algorithms and Computation in Mathematics*. Springer-Verlag, Berlin, 2010. Structures for algorithms and applications.

[21] Mike Develin and Bernd Sturmfels. Tropical convexity. *Documenta Mathematica*, 9:1–27, 2004.

[22] Paul Erdös, Ronald C Mullin, Vera T Sós, and Douglas R Stinson. Finite linear spaces and projective planes. *Discrete Mathematics*, 47:49–62, 1983.

[23] Ewgenij Gawrilow and Michael Joswig. `polymake`: a framework for analyzing convex polytopes. In *Polytopes—combinatorics and computation (Oberwolfach, 1997)*, volume 29 of *DMV Sem.*, pages 43–73. Birkhäuser, Basel, 2000.

[24] Gary Gordon and Jennifer McNulty. *Matroids: a geometric introduction*. Cambridge University Press, 2012.

[25] Mark Gross. *Tropical geometry and mirror symmetry.* Number 114. American Mathematical Soc., 2011.

[26] Marvin Anas Hahn, Hannah Markwig, Yue Ren, and Ilya Tyomkin. Tropicalized quartics and canonical embeddings for tropical curves of genus 3. *International Mathematics Research Notices*, 2019. Published online, doi:10.1093/imrn/rnz084.

[27] Sven Herrmann and Michael Joswig. Splitting polytopes. *Münster J. Math*, 1:109–141, 2008.

[28] Fritz Herzog and B. M. Stewart. Patterns of visible and nonvisible lattice points. *Amer. Math. Monthly*, 78:487–496, 1971.

[29] June Huh, Botong Wang, et al. Enumeration of points, lines, planes, etc. *Acta Mathematica*, 218(2):297–317, 2017.

[30] Philipp Jell, Hannah Markwig, Felipe Rincón, and Benjamin Schröter. Tropical lines in planes and beyond, 2020. Preprint arXiv:2003.02660.

[31] Michael Joswig. *Essentials of Tropical Combinatorics.* Online Draft, 2020. Web Draft.

[32] Michael Joswig, Marta Panizzut, and Bernd Sturmfels. The schläfli fan. *Discrete & Computational Geometry*, 64(2):355–381, Sep 2020.

[33] Michael Joswig and Benjamin Schröter. The tropical geometry of shortest paths, 2019. Preprint arXiv:1904.01082.

[34] Michael Joswig and Ayush Kumar Tewari. Forbidden patterns in tropical plane curves. *Beiträge zur Algebra und Geometrie / Contributions to Algebra and Geometry*, Aug 2020. Postprint/Accepted manuscript, doi:10.1007/s13366-020-00523-6.

[35] R. Koelman. *The number of moduli of families of curves on a toric surface.* PhD thesis, Katholieke Universiteit de Nijmegen, 1991.

[36] Jeffrey C. Lagarias and Günter M. Ziegler. Bounds for lattice polytopes containing a fixed number of interior points in a sublattice. *Canad. J. Math.*, 43(5):1022–1035, 1991.

[37] Thomas Lam and Alexander Postnikov. Alcoved polytopes. I. *Discrete Comput. Geom.*, 38(3):453–478, 2007.

[38] Diane Maclagan and Bernd Sturmfels. *Introduction to tropical geometry*, volume 161. American Mathematical Soc., 2015.

[39] Bojan Mohar and Carsten Thomassen. *Graphs on Surfaces.* Johns Hopkins series in the mathematical sciences. Johns Hopkins University Press, 2001.

[40] Ralph Morrison. Tropical hyperelliptic curves in the plane. *Journal of Algebraic Combinatorics*, 2020. Published online, doi:10.1007/s10801-019-00933-3.

[41] Ralph Morrison and Ayush Kumar Tewari. Convex lattice polygons with all lattice points visible. *Discrete Mathematics*, 344(1):112161, 2021. Postprint/Accepted manuscript, doi:10.1016/j.disc.2020.112161.

[42] Andreas Paffenholz. polydb: a database for polytopes and related objects. In *Algorithmic and experimental methods in algebra, geometry, and number theory*, pages 533–547. Springer, Cham, 2017.

[43] Marta Panizzut and Magnus Dehli Vigeland. Tropical lines on cubic surfaces, 2007. Preprint arXiv:0708.3847.

[44] Georg Pick. Geometrisches zur zahlenlehre. *Sitzungsberichte des deutschen naturwissenschaftlich-medicinischen Vereines für Böhmen Lotos in Prag (Neue Folge)*, 19:311–319, 1899.

[45] Jurgen Richter-Gebert, Bernd Sturmfels, and Thorsten Theobald. First steps in tropical geometry. *Contemporary Mathematics*, 377:289–318, 2005.

[46] Luis Felipe Tabera. Tropical constructive pappus' theorem. *International Mathematics Research Notices*, 2005(39):2373–2389, 2005.

[47] Luis Felipe Tabera et al. Tropical plane geometric constructions: a transfer technique in tropical geometry. *Revista Matemática Iberoamericana*, 27(1):181–232, 2011.

[48] Ayush Kumar Tewari. Point-line geometry in the tropical plane, 2020. Preprint arXiv:2006.04425.